2016

Chikungunya Virus Infection-Associated Bone and Joint Disease

Brad A. Goupil
Louisiana State University and Agricultural and Mechanical College

CHIKUNGUNYA VIRUS INFECTION-ASSOCIATED BONE AND JOINT DISEASE

A Dissertation

Submitted to the Graduate Faculty of the
Louisiana State University and
Agricultural and Mechanical College
in partial fulfillment of the
requirements for the degree of
Doctor of Philosophy

in

The Department of Pathobiological Sciences

by
Brad A. Goupil
B.S., University of Connecticut, 2004
M.S., University of Connecticut, 2005
D.V.M., University of Minnesota, 2010
December 2016

ACKNOWLEDGEMENTS

I dedicate this dissertation to my wife, Dr. Margaret McNulty, who has supported and put up with me for many years while I've been pursuing my seemingly never-ending education; and to my daughter Olivia who can make me smile and laugh with the simplest expression or action, no matter how stressful things get. Without their unending support and understanding, I wouldn't have been able to do this. I also have to acknowledge our furry children, past and present: Ronnie, Duncan, Curious, Sherlock, Dax, Gopher, Annie, Mikie, Flash, Chester, and Gizmo, who have always provided some much needed entertainment and recreation. I would like to thank my parents, Dr. Michael Goupil and Ms. Pegi Goupil, who have always supported me through all the ups and downs without fail, and have encouraged me to achieve any and all of my goals; my brother, Dr. Stephan Goupil, whom I have always looked up to and has subsequently helped me strive to always be better and achieve more; my sister, Mrs. Kristina Pinto, who has been a friend and confidant whenever needed, without judgment; my nephew, Zachary Goupil, who helps me blow off a little steam and have some fun during evening Xbox sessions; and my nieces, Nicole and Victoria Goupil, whom I don't get to see as often as I'd like, but put a smile on my face every time that I do.

I owe a great deal to my mentor, Dr. Christopher Mores, who has given me the freedom and independence to pursue my interests in research, make my own mistakes, and find my own way, while still providing guidance, support and insight whenever needed. To my unofficial mentor, Dr. Rebecca Christofferson (v2.0), I will be forever grateful, as she has always been available for support and guidance, and injected the necessary levity into my daily life when things got too stressful.

A special thanks to my mentors during my pathology residency at the University of Minnesota as well, particularly Drs. Cathy Carlson and Erik Olson, whose unending enthusiasm for pathology was infectious, and who showed me the fun and excitement of bones and joints, even if I fought it at the time…

To my committee members, Drs. Juan Martinez, Ingeborg Langohr, Britton Grasperge, and my Dean's Representative, Dr. Cornelis de Hoop, thank you for the support, constructive criticism and

advice. Your insights and suggestions have greatly helped improve my project and my time here at LSU.

I would also like to thank my colleagues, former Mores Lab members, Dr. Michael McCracken and Mr. Daniel Chisenhall, and current Christofferson Lab members, Ms. Anna Kawiecki and Ms. Handly Mayton; your support and humor has been much needed and appreciated.

TABLE OF CONTENTS

LIST OF FIGURES

ABSTRACT

Chikungunya virus (CHIKV) is a mosquito-borne alphavirus that circulates predominantly in tropical and subtropical regions. Infection results in severe debilitating polyarthralgia during the acute phase of disease, and reports suggest that chronic arthralgia lasting months to years after the initial infection can occur. More severe and prolonged disease has been associated with pre-existing joint disease, though this has not been experimentally examined. In the research presented herein, two established mouse models (adult IRF 3/7 $^{-/-\ -/-}$ and wild-type C57BL/6J mice) were utilized to characterize CHIKV-associated bone and joint disease and evaluate its impact on the progression of pre-existing osteoarthritis (OA) utilizing histopathology, μCT, and serology. During acute stages of the disease, CHIKV infection resulted in synovitis, cartilage necrosis, and periosteal necrosis or periostitis. Additionally, IRF mice had severe ischemic bone marrow necrosis, and C57BL/6J mice developed periosteal new bone proliferation. During chronic stages of disease (90 DPI), there was ongoing and progressive synovitis, tendonitis, enthesitis, and cartilage damage, though periostitis and periosteal bone proliferation had resolved. Infection with CHIKV in mice with pre-existing OA had no significant impact on total synovitis scores or chondrocyte cell death, but caused a decrease in volume of osteophytes and subchondral bone, as compared to OA alone. Serology results in both the footpad and intra-articular C57BL/6J models indicated there were alterations in RANKL and OPG associated with CHIKV infection, demonstrating potential changes in bone dynamics. The current experiments demonstrated novel lesions of CHIKV-associated bone and joint disease that have important ramifications for the treatment and prevention of disease. Periosteal bone proliferation associated with CHIKV is a potentially painful but reversible process, whereas articular cartilage damage is progressive and represents a potential mechanism for chronic CHIKV-associated joint disease. Additionally, the alterations in bone associated with CHIKV infection and pre-existing OA, in conjunction with changes in the RANKL-OPG pathways, could have significance in clinical monitoring of OA and treatment choices in individuals with concurrent diseases. Future studies would help

determine if RANKL and OPG levels could be useful for tracking disease progression in people and establish the long-term effects of CHIKV infection on OA progression.

CHAPTER 1: INTRODUCTION AND REVIEW OF CHIKUNGUNYA VIRUS-INDUCED ARTHRALGIA: CLINICAL MANIFESTATIONS, THERAPEUTICS, AND PATHOGENESIS

1.1 INTRODUCTION

1.1.1 Background

Chikungunya virus (CHIKV) is an arbovirus spread predominantly by *Aedes aegypti* and *Ae. albopictus* mosquitoes[99,159,184]. It belongs to the *Alphavirus* genus along with other arthritogenic viruses such as Ross River, Sindbis, O'nyong-nyong, Mayaro, Semliki forest, and Barmah forest viruses[50,99,111,178]. There are 3 genotypes of CHIKV, named for the regions in which they generally circulate: West African, East/Central/South African, and Southeast Asian[23,99,125]. CHIKV is considered a neglected tropical disease, because it circulates within these subtropical and tropical regions, has the potential to affect more than 1 billion people, and many at-risk people live in poverty stricken regions[182]. Recently, CHIKV-induced disease was named a nationally notifiable condition in the United States, because of a severe ongoing outbreak in the western hemisphere[31]. The outbreak initially began in October of 2013 and has since spread throughout the western hemisphere, affecting 45 countries and territories and causing approximately 1.8 million reported suspected cases as of March 2016[124]. In 2014, 2,811 cases of CHIKV-induced disease were reported in the United States, which included 12 locally acquired cases in Florida[29]. While no locally acquired cases were reported in the US in 2015, there is a significant risk of outbreak because of the ongoing epidemic in the Americas and the widespread presence of competent mosquito vectors[99].

Though there have been millions of people affected by CHIKV within the last decade, methods of prevention and treatment are still lacking. Preventive measures focus on the mosquito vector and include recommendations such as wearing long sleeves, making use of mosquito nets, elimination of mosquito breeding sites and use of insecticides[6]. Several vaccines are in various stages of development, though none are yet commercially available[1,3,24,27,62,102,168]. Treatments are non-specific and predominantly focus on the alleviation of symptoms utilizing analgesics, antipyretics and non-

steroidal anti-inflammatory drugs (NSAIDS)[93]. Additional medications such as disease modifying anti-rheumatic drugs (DMARDs) utilized in cases of rheumatoid arthritis, and drugs that target specific pathways of CHIKV pathogenesis are currently being investigated, but their efficacies are still unknown[53]. Some of these specific drugs will be discussed in more detail later.

1.1.2 Disease Manifestations

Following infection with CHIKV, and an incubation period of 2-7 days, approximately 95% of people will develop symptoms of disease[6,153]. The general symptoms consist of high fever, headaches, rash, myalgia and severe joint pain, for which the virus was named: “chikungunya” is a Makonde word in Tanzania meaning “to walk bent over” or “that which bends up”[37]. In most cases these acute symptoms will resolve in approximately 2 weeks[6]. However, as many as 88% of people can have arthralgia and/or arthritis persisting 1 month after the initial symptoms[25], and in some outbreaks, 50% of people reported chronic arthritis 1 year after the initial infection[52].

Additionally, while less common, severe diseases affecting other body systems have been reported. These can include gastrointestinal disease, neurologic complications including meningoencephalitis and seizures, cardiovascular disease, hemorrhagic manifestations, and death[6,70,77,87,93]. Reportedly, these severe disease manifestations are more frequent in children, the elderly, and people that have underlying comorbidities[41,93,116]. Recently, maternal-fetal transmission has also been reported, resulting in some neonatal mortality[70,153]. Research has indicated that these neonatal infections occur in cases of mothers who are viremic at the time of parturition, and result from perinatal exposure due to direct contact with maternal blood, rather than via placental transfer of virus[41,153]. These neonatal cases occurred in approximately 3 out of 1,000 births during the La Reunion outbreak[93] and often resulted in severe manifestation in infants, including seizures, hemorrhagic disease, and abnormalities in cardiac function[87,153].

1.1.3 Risk Factors for Disease Severity

Numerous risk factors for development of severe disease in adult patients have been reported. The patient’s age at the time of initial infection is one of the more consistently reported factors

associated with development of prolonged arthritis and other more severe disease manifestations[6]. Disease is often considered to be more severe in adults than in children, though adults younger than 35 years appear to be protected[151,160]. In one report that had a particularly low prevalence of chronic arthritis, the authors speculated that this may have been due to the high number of patients that were less than 17 years old in that cohort[160]. Conversely, being 45 years old or older is considered to be a risk factor for development of more severe disease[56,160]. However, it should be noted that some studies have found no correlation between age and disease severity[6]. Similarly, while some studies have reported an increased risk of severe disease in women[6,39,133], others have demonstrated no significant difference associated with gender[13,151]. Therefore, the role of age and sex in CHIKV-associated disease manifestations is still unclear.

An association between some of the more unusual disease manifestations described above and presence of underlying comorbidities at the time of initial infection have been described in up to 71.6% of patients[13]. Some of the more commonly reported comorbities include hypertension and respiratory or cardiovascular disease[6,160]. In regard to persistent joint disease in particular, ischemic heart disease and diabetes have been implicated as risk factors[13,151]. Pre-existing joint disease has also often been associated with an increased susceptibility to development of chronic CHIKV-associated arthritis[77]. Borgherini et al. reported that 44.3% of people who developed prolonged arthritis had a history of chronic arthralgia, often as a result of osteoarthritis or gout[13]. Other studies have similarly associated pre-existing arthritis, particularly osteoarthritis and rheumatoid arthritis, with development of chronic CHIKV-associated arthralgia[6,34,160]. This has also been reported in other arthritogenic alphaviruses such as Ross River virus and Sindbis-related (Pogosta) virus[23]. In fact, in one multivariate model, the 3 variables that were independently associated with chronic CHIKV-associated joint disease were being 45 years old or older, the initial severity of joint pain, and underlying osteoarthritis[160]. Although the association between existing joint disease and development of chronic CHIKV-associated arthritis have been reported, it is unclear if persistent CHIKV-associated disease is occurring, if CHIKV infection has a role in progression of existing joint disease, or if these

cases may just represent normal progression of pre-existing disease. However, in a cohort of patients that developed chronic arthralgia following the La Reunion outbreak, only 2.8% had pre-existing joint pain, indicating that there are likely other, as yet unidentified factors involved in the development of this manifestation[151]. An additional confounding factor is that presence or absence of pre-existing joint disease is often ascertained via self-reporting questionnaires, while thorough orthopedic evaluations at the time of or prior to initial infection are rarely performed[79,104,105,160,163]. Therefore, association between pre-existing joint disease and the risk of development of prolonged chronic CHIKV-associated disease is still unclear.

In addition to the existence of underlying joint disease at the time of infection, the severity of the acute disease has also been linked to risk of development of persistent arthralgia and/or arthritis. The parameters of initial disease severity that have been correlated with chronic disease include presence of joint swelling, severity of joint pain, and a stronger Th1 immune response with concurrent weak Th2 response during the acute phase of disease[52,160,185]. Other measures of initial disease severity during acute disease were not associated with development of chronic disease, including the initial viral load, number of joints affected, and duration of hospitalization[151].

1.2 JOINT DISEASE

1.2.1 Clinical Presentation

1.2.1.a Symptoms

As mentioned, one of the most consistent and debilitating manifestations of CHIKV-induced disease in people consists of an often widespread severe and incapacitating arthralgia and/or arthritis, occurring in 85-100% of people with symptomatic infection[70,91,151,160,181]. In fact, this disease manifestation is so common in CHIKV-induced disease, it has been reported that the presence of concurrent high fever and arthralgia has a specificity of 99.6% and positive predictive value of 84.6% for the diagnosis of CHIKV infection[64]. However, it should be noted that other arboviruses such as dengue, Zika, and the other alphaviruses mentioned previously can all have similar clinical presentations, including fever and arthralgia. Additionally, some of these, such as dengue, Zika, and

CHIKV are currently co-circulating in the western hemisphere[144,175], thus care should be taken to definitively identify the cause in any case with this presentation.

In most cases of CHIKV infection, patients develop symmetric oligo- or polyarthralgia[15], developing within minutes to days following the initial onset of fever[6,15,53,143]. While any joint can be affected, those that are most commonly reported are the distal extremities such as wrists, metacarpal and interphalangeal joints, as well as the ankles and metatarsophalangeal joints[15,37,44,53,98,103,105], though, some studies have indicated that the knee is also commonly affected[6,36,39,105]. Though the majority of cases have this distribution of arthralgia, it is important to recognize that patient presentation can vary and include asymmetric arthritis, monoarthralgia, and involvement of less commonly affected joints, such as the elbow, hip, shoulder, and vertebral pain in sacroiliac, lumbosacral, and cervical regions[6,91,98]. Arthralgia associated with CHIKV infection is often considered to be the result of tenosynovitis and enthesopathy[6,103,181] and can be associated with paresthesia of the overlying skin[77]. Additionally, patients often complain of joint stiffness and have variably apparent swelling of affected joints[6,39,44,77]. In many cases, these manifestations of arthralgia will resolve within 1 to 4 weeks after the initial onset[37,44,52,70].

However, in a wide range of cases (1.6-89.7%), patients can have chronic joint disease lasting months to years after the initial disease onset, which can present as either an ongoing persistent arthralgia, or relapsing arthralgia[13,15,25,36,44,52,91,104,116,133,140,141,151,160,181,188]. Some reports have indicated that patients can have continued symptoms as long as 8 years after the initial infection[181]. The distribution of joint manifestations in the chronic form is similar to the acute, including symmetrical involvement of joints of the distal extremities, knee, shoulders, and rarely the back[13,37,104,160,181]. In many instances, in a given individual, the same joints that were affected in the acute phase are involved in the chronic phase[44]. Grossly apparent joint swelling is reported in 16.1-58.5% of chronic cases, and warmth and redness are usually not observed[13,25,104]. Again, these symptoms are often associated with the presence of synovitis and/or tenosynovitis, and articular

destruction has been rarely reported[103,116]. As many as 15% of patients develop Raynaud's syndrome, consisting of feelings of cold and numbness in response to cold and stress[87,181].

While transient joint pain is not uncommon in the weeks to months following the resolution of other disease manifestations such as fever and rash, the development of the chronic or relapsing form of CHIKV-associated joint disease is poorly understood. Incidences of chronic CHIKV-associated joint disease have been fairly commonly reported since the La Reunion outbreak, though it should be noted that in most reports, concurrent underlying joint abnormalities present prior to or at the time of infection have not been ruled out[104,116,151,160]. Additionally, it is possible that some patients develop joint disease such as osteoarthritis or rheumatoid arthritis, completely unrelated to the previous CHIKV infection. Ambiguities in the pathogenesis of CHIKV-associated joint disease and the potential continued or permanent damage that may occur during acute infection make proper classification of chronic CHIKV-associated joint disease difficult. The potential mechanisms associated with chronic CHIKV-associated joint disease are unknown, and no animal model currently replicates this aspect of disease. Therefore, the association between CHIKV infection and chronic joint pain is still unclear.

1.2.1.b Diagnosis

As discussed, the clinical presentation of CHIKV-associated arthralgia during the acute stages can be quite similar to other arthritogenic alphaviruses and other tropical arboviruses such as dengue and Zika[144,175]. Therefore, definitive diagnosis is required. Serological assays for detection of anti-CHIKV IgM or IgG can be performed during the first few weeks or months, respectively, though false negative results can occur depending on the stage of disease[152]. It should also be noted that false positives have been reported as a result of cross-reactivity with other arboviruses[27]. However, this cross-reactivity was likely more of a historical problem due to inferior assays and current serological assays are considered to be able to distinguish CHIKV from flaviviruses and other alphaviruses, with the exception of O'nyong nyong virus[24]. Various serological tests exist, including enzyme-linked immunosorbent assay (ELISA), immunofluorescence, inhibition of haemagglutination, and

complement fixation[27]. Because of the high viremia associated with disease (see Laboratory Results below), reverse-transcriptase polymerase chain reaction (RT-PCR) or virus isolation utilizing cell culture or animal inoculation can be performed during the acute stage, but is only useful at 1 to 2 weeks post-infection during the viremia period[24,27,152].

1.2.1.c Laboratory Results

In the acute stages of the disease, results of a complete blood cell count can be variable, though leukopenia, often as a result of lymphopenia, is one of the most common presentations[6,70,153]. This will often persist for the first week of infection, and is occasionally accompanied by thrombocytopenia and an increased hematocrit[6,153]. In most instances, these parameters will return to normal in the second week of infection[70], though a persistent lymphopenia 36 months after the initial infection has been rarely reported[151]. Alternatively, in some cases an increased CD4+ T cell count has been described in chronic stages of disease[103]. Blood chemistry results are often normal throughout the disease course, though increased liver enzymes including ALT and AST occasionally occur[6,70].

A high viremia is common in infected patients, frequently ranging from 10^8 to 10^{12} viral RNA copies/mL, and lasting up to 12 days after the initial onset of clinical symptoms[39,70,77,93]. In many cases, patients with higher viremias had more severe alterations in the above-mentioned CBC and chemistry results[39]. Persistent viremias are not apparent during the chronic stage of disease[103,151].

Infected patients will often seroconvert and have measurable IgG levels within the first week, sometimes as early as 2 days post infection[77], and lasting for years after the initial infection[103]. Additionally, many studies have demonstrated persistent IgM levels in patients occasionally lasting 18 months or longer[13,77,103,105,151]. Neutralizing IgM antibodies can also be found in the synovial fluid of patients 3 months after the initial infection[116]. An increased CHIKV IgG titer has been associated with more severe and persistent joint disease[22,56], though virus could not be detected in the blood or synovial fluid[22]. Specifically, levels of IgG at 6 months post infection have been associated with

increased symptom severity[86]. These findings suggest that continued immune stimulation could play a role in some cases of prolonged CHIKV-associated arthritis.

In fact, several studies have suggested that chronic CHIKV-associated arthritis is similar to rheumatoid arthritis (RA)[6,15], in part due to similarities in clinical laboratory results. Many patients even meet the requirements established by the American College of Rheumatology to be diagnosed as having RA[15,104]. In one small study of 5 patients with chronic CHIKV-associated arthritis, all patients were positive for rheumatoid factor (RF)[181]. In other studies, 13.6% to 57.1% of patients with CHIKV-associated arthritis were RF positive[15,37,181], though others reported no RF positivity in any patients[104]. However, it should be noted that RF positivity is not a requirement for a diagnosis of RA.

Other similarities in laboratory results shared by CHIKV and RA include variably elevated erythrocyte sedimentation rates, elevated C-reactive protein, and presence of anti-citrullinated protein antibodies[6,15,26,37,39,64,104]. However, none of these are consistent findings in patients with acute or chronic CHIKV-associated arthralgia. While in some cases patients with chronic CHIKV-associated arthritis can be diagnosed as having RA[6,105], many patients do not meet the criteria[116]. Thus the association between CHIKV infection and development of autoimmune diseases such as RA remains unclear[23]. In at least some of these cases, it is possible the development of RA is completely unrelated to previous CHIKV infection. As current research has not determined a definitive link between CHIKV infection and development of RA, a causal relationship should not be inferred at this time.

1.2.1.d Cytokines

There has been abundant work performed analyzing cytokines in people infected with CHIKV at various stages of disease. During acute stages (4-7 days post infection [DPI]), numerous cytokines have been shown to be elevated including IFN-α, IL-1RA, IL-2, IL-4, IL-6, IL-7, IL-8, IL-12, IL-15, MIG/CXCL-9, MIP-1α/CCL-3, HGF, bFGF, G-CSF, GM-CSF, and eotaxin/CCL-11[39,52,180]. Some cytokines, such as IL-1β, IL-6, and RANTES have been correlated with disease severity[39,127], though increased levels of others are correlated specifically with higher viral load, such as IFN-α, IL-6, IL-16,

IL-17, IL-1RA, MCP-1, IL-12, IP-10/CXCL-10, IL-18, IL-18bp[39,52]. At later timepoints in acute disease (10-15 DPI), a shift towards Th2 cytokines such as IL-4 and eotaxin has been reported[39], though elevations in Th1 cytokines such as IL-12 have also been demonstrated[52]. Unfortunately most of these studies do not specifically correlate cytokine profiles with joint manifestations, though Rulli et al. reported that patients experiencing polyarthralgia had higher levels of MCP-1, TNF-α and IFN-γ[147].

During later stages, various elevated cytokines have been associated with ongoing disease and persistent arthralgia, such as IL-1RA, IL-17, IL-6, MCP-1, MIP-1α, MIP-1β, IL-8, GM-CSF, IFN-α, and IL-12[32,39,52,122,127,142]. Increased levels of CXCL10 and CXCL9 have been associated with more severe disease at 6 months post-infection[86]. While the majority of these studies focused on serological analyses, cytokines such as IFN-α, IL-6, MCP-1, IL-8, and MMP2 have been demonstrated within the synovium of a patient with chronic arthralgia, although not present in two fully recovered patients[52]. Additionally, expression of IL-6 has been demonstrated in affected joints[122]. Interestingly, it has also been report that patients who recovered from disease had higher levels of HGF and eotaxin during the recovery period, than patients with continuing disease manifestations[52] Unfortunately, many of the reports on cytokine profiles in patients report conflicting results[52,122,180], so the significances of these findings and their role in disease pathogenesis remains unclear. These differences may reflect disparities in post-infection timepoints and/or differing techniques for analyzing cytokine levels. Therefore their role or support in assessment of a clinical patient is also still unknown.

1.2.1.e Advanced Imaging

Much of the current literature focuses on the use of standard radiography for evaluation of joints in CHIKV-infected patients[6,15,77,103,104]. While there is certainly some utility for this modality, radiographs lack the sensitivity for more subtle changes that might occur early in the course of disease, and are less useful for evaluating some of the associated soft tissues, as compared to other imaging techniques such as magnetic resonance imaging (MRI) or ultrasonography.

The results of radiography are often variable in cases of CHIKV-associated disease. Some significant bony changes, such as obvious bone erosions, can be seen by 10-18 months post

infection (p.i.), involving the subchondral bone of the hands and wrists, including the interphalangeal joints[103,104]; however, many patients have completely normal radiographs during this same time period[15]. In some cases, patients who had normal radiographs at 10 months p.i. showed evidence of joint space narrowing and bone erosions years after the initial infection[15], indicating that radiography may not be sensitive enough to be used in early evaluation of CHIKV-associated joint disease. In this study, 42.9% of patients had normal radiographs at the time of diagnosis of chronic CHIKV arthritis, while 57.1% had evidence of joint space narrowing and 23.8% had visible erosions[15]. However, at the follow-up 24 months later, only 19% of patients had normal radiographs, and the percentages of patients demonstrating joint space narrowing and erosions had both increased to 81%[15].

Additionally, in some of these individuals with normal radiographs, MRI identified bone erosions in the hands of 5 of 6 patients at the 24 month post-diagnosis timepoint[15], indicating MRI may be a more sensitive technique for early identification of joint disease. In fact, CHIKV-induced arthritis has been compared to RA in regard to some of the pathologic changes, and studies have indicated that radiographs of RA patients are often normal for 6-12 months after the initial symptoms arise, though erosions can be demonstrated by MRI less than 6 months after symptom onset[115].

MRI has also been shown to be able to identify significant bilateral periosteal inflammation, carpal edema, and synovitis, which might not have been apparent on radiographs[103]. Other lesions described on MRI of patients with CHIKV include joint effusion, synovitis/tendonitis/tenosynovitis, bone marrow edema, and bone erosions affecting various regions including hands, wrists, knees, and shoulders[6,103,104]. Additionally, while radiography has been shown to be useful predominantly at the later timepoints as discussed above, in a report utilizing MRI, Mizuno et al. described bone erosions, tenosynovitis, and joint effusions at 2 months p.i., indicating the utility of this modality at earlier timepoints[116]. Simon et al. also demonstrated evidence of tenosynovitis by MRI involving multiple tendons during the first month of disease manifestations, though boney erosions were not described[159]. In one study, 80% of patients demonstrated significant lesions in CHIKV-associated

chronic arthritis by 10 months post infection[104] and in severe cases, tearing of menisci and cruciate ligaments have also been described[104].

Another benefit of MRI, as compared to other advanced imaging modalities, is that it can be utilized to evaluate all soft and hard tissues, including tendons/ligaments, articular cartilage, and bone, as well as for visualization of fluids, as in the case of joint effusion and soft tissue edema. In fact, since the presence of fluid in and around joints is one of the earliest pathologic changes associated with joint disease, the utility of MRI to identify acute changes associated with CHIKV arthralgia is apparent. Because there are fewer restrictions on tissue types and pathologic changes that can be evaluated by MRI, a wider spectrum of disease manifestations associated with CHIKV infection can be assessed. For example, bone marrow edema was not a recognized component of RA in people until MRI had been used to evaluate patients[115]. In fact, it has now been demonstrated that sites of subsequent bone erosions are highly correlated with the locations of initially observed bone marrow edema in patients suffering from RA[115]. This indicates a potential clinical utility in CHIKV patients, in which it may be possible to identify locations at potentially higher risk for development of subsequent bone erosions[115]. Similarly, synovitis adjacent to carpal bones was highly associated with risk of development of erosions at that site[115]. Therefore, MRI scanning of CHIKV patients during the acute phase of infection may be useful in predicting the outcome of disease at later timepoints. Though the utility of MRI in clinical evaluations is clear, it should be noted that baseline MRI results are not available for most CHIKV patients reported in the literature. Therefore, it is possible that some lesions being associated with CHIKV infection may actually represent progression of disease already present at the time of initial infection.

Ultrasonography has shown some utility for diagnosis of soft tissue disease associated with CHIKV-induced arthralgia. Chopra et al. described substantial tenosynovitis and enthesopathy in patients suffering from recurrent musculoskeletal discomfort in the months following CHIKV infection[37] and Mathew et al. have similarly described tenosynovitis and bursitis[105]. However, due to the lack of literature on ultrasonographic evaluation of patients with CHIKV, the consistency and reliability of this

imaging technique for evaluation of manifestations of this disease is currently unknown. Additionally, because ultrasound cannot image through bone due to the requirements of an acoustic window for ultrasound visualization, deeper evaluation of joints including assessment of the articular cartilage and some ligaments and tendons (e.g. cruciate ligaments) is not possible[72]. Another limitation of this technique is that evaluation of the soft tissues associated with joints can be very challenging via ultrasonography and requires a great deal of experience to obtain reliable and repeatable results. It is likely that one would need to evaluate a large number of joints and in particular those of CHIKV-infected individuals before being able to make full use of this modality. Therefore, the utility of ultrasonography in a clinical or research setting is unclear at this time.

1.2.1.f Histopathology/Pathology

Little histopathology has been performed on joint samples from CHIKV-infected human patients. However, those that have been reported describe vascular proliferation, perivascular macrophages, and synovial hyperplasia[181]. Macrophages also can extend into surrounding soft tissues, including connective and peritendinous tissues and muscle[35,52]. In acute stages of disease, CD4+ T helper cells are essential in the inflammatory process[34], and intense activation of these cells during this stage, in addition to dendritic cells (DC), natural killer cells (NK), and CD8+ T cells have been associated with development of chronic arthralgia[8]. While synovitis is often assumed to be a major component of disease in chronic CHIKV-associated arthritis, Jaffar-Bandjee et al. reported that tenosynovitis, enthesopathy and periosteal inflammation are more common[77]. However, due to the paucity of histopathological data associated with human disease, it is difficult to draw conclusions regarding pathogenesis of disease manifestations.

The use of various animal models of CHIKV-associated joint disease has expanded the knowledge regarding pathogenesis. Juvenile 3 to 4 week old C57BL/6 mice have demonstrated synovitis, myositis and tendonitis peaking at around 7 DPI and generally completely resolving by 12 weeks p.i., with inflammatory cells consisting predominantly of macrophages and lymphocytes[65]. In this study, the importance of CD4+ T cells in severity of acute disease was demonstrated by utilizing

a Rag1$^{-/-}$ mouse lacking T and B cells, which developed more severe and prolonged inflammation than a wild-type control[65].

Models utilizing adult C57BL/6 mice have demonstrated development of mononuclear synovitis, fibrinous exudate in joint spaces, and severe inflammation associated with skeletal muscle adjacent to joints, with most of the inflammation resolving two weeks after infection[55,129] and almost complete resolution in all tissues by 30 DPI[55]. Immunohistochemistry/histochemistry in this model demonstrated that there are large numbers of macrophages within these inflammatory infiltrates[55,129], and FACS confirmed the presence of monocytes/macrophages, NK cells, small numbers of B and T cells, and dendritic cells, similar to what has been demonstrated in the previously described human cases[55].

Alterations in trabecular and cortical bone as evaluated by micro-computed tomography (μCT) have also been demonstrated by 3 DPI utilizing a juvenile, 25-day-old C57BL/6 mouse model[35]. These alterations were associated with an increase in TRAP+ cells within the bone marrow space, potentially indicating a role for osteoclastic bone resorption in CHIKV-associated arthritis. However, it should be noted that the authors also described a reduced growth plate width in this study. This, in conjunction with the skeletal immaturity of this mouse model likely indicates that infection impacts bone growth, development and modeling. This may indicate this model is more appropriate for what may occur in neonates and children infected with CHIKV, rather than mechanisms associated with disease in adults.

Nonhuman primate (NHP) models have been less successful for demonstration of arthritogenic disease. The few existing published studies have variably reported no joint or muscle pathology[70] or fibrinous arthritis similar to that seen at early timepoints in mice at 7 DPI, only in animals receiving high intravenous doses (10^7 pfu)[93]. These animals also often developed meningoencephalitis[93]. However, NHPs receiving intermediate doses did not develop synovitis or meningoencepahlitis[93], thus the utility for use of NHPs in studying CHIKV-associated arthritis is currently unknown. However, in-depth evaluation of joints has not been reported and NHP studies have confirmed the importance

of macrophages in various other aspects of the disease, similar to that seen in humans and mouse models[52,93].

1.2.1.g Virus in Tissues

Again, data in regard to natural human infections, viral tropisms and persistence is limited, though viral persistence in tissues is considered to be a potential mechanism of chronic disease. In acute stages of disease, CHIKV antigen has been demonstrated within skeletal muscle progenitor cells of infected patients and associated with muscle necrosis and inflammation[8]. Additionally, persistent CHIKV infection in these muscle satellite cells has been demonstrated 3 months after the resolution of the acute phase of disease[105]. During the acute phase, CHIKV can also be detected in circulating monocytes[68]. Interestingly, persistent infection has also been demonstrated in synovial macrophages as long as 18 months after the initial infection, demonstrating that viral persistence may play a role in chronic disease[34,35]. Other articles have reported the presence of CHIKV antigen and/or virus within fibroblasts of the joint capsule, skin, muscle fascia and dermis, though the timeline in terms of infection in these is unclear[41,93].

Again, numerous studies utilizing animal models have greatly added to our understanding of CHIKV cell tropisms and viral persistence. Initially, viral replication occurs in the liver and then disseminates to muscle, joints and dermis, similar to what has been shown in human biopsy samples[41]. Between 3 and 5 DPI in wild-type C57BL/6 and IRF 3/7$^{-/-}$ mice, *in situ hybridization* (ISH) has demonstrated the presence of CHIKV RNA in the cytoplasm of numerous cell types including, skeletal myocytes, cells within the synovium and periosteum, endothelial cells, and cells morphologically resembling fibroblasts and macrophages within the dermis[145]. Additionally, at 5 DPI, virus has been demonstrated in the epidermis of IRF 3/7$^{-/-}$ mice[145]. In IFN α/β$^{-/-}$ mice, virus has been demonstrated in fibroblasts within the synovium at 3 DPI, though infection of chondrocytes, osteocytes and osteoblasts has not been demonstrated[41]. ISH in the IRF 3/7$^{-/-}$ mice showed equivocal infection of chondrocytes[145]. Viral tropism for fibroblasts has been consistently

demonstrated both in mouse models and *in vitro* and is believed to be one of the preferred cell types for CHIKV[41].

In cases of severe disease, virus has also been shown to disseminate to the CNS, specifically the choroid plexus and leptomeninges, although parenchymal involvement has not been demonstrated[41]. Various mouse strains including adult and neonatal C57BL/6, IFN $\alpha/\beta^{-/-}$ and IRF $3/7^{-/-}$ mice have shown similar and consistent viral tropisms at early timepoints of disease[41,145].

The presence and location of virus at later timepoints post inoculation (p.i.) is less clear. In juvenile wild-type C57BL/6 mice, CHIKV RNA has been demonstrated in joint-associated tissues at 16 weeks p.i., while there was no presence of virus in any other tissues detectable after 14 DPI.[65]. Interestingly, juvenile $Rag1^{-/-}$ mice demonstrated CHIKV RNA in joint associated tissues and muscles at similar timepoints, suggesting that although T and B cells are able to clear virus from muscle, they are ineffective at clearance from joint tissues[65]. These studies have utilized RT-PCR to demonstrate viral presence, so exact localization of virus is unknown.

Nonhuman primate models have demonstrated similar results during acute stages of disease. Reported viral tropisms included lymphoid tissues, liver, CNS, joint, and muscle, predominantly infecting macrophages, dendritic cells and endothelial cells[93]. NHP models also showed a viral tropism for the choroid plexus and leptomeninges, but spared the microvessels and parenchyma[41]. Viral persistence at 19 DPI has been demonstrated by ISH in macrophages in the spleen, and antigen persistence by IFA at 90 DPI within macrophages[93]. These studies involving NHP models have suggested that macrophages act as the main cellular reservoir during chronic stages of infection in various organs and tissues including the joints, muscle, lymphoid organs and the liver[35,93]. Additionally, CHIKV RNA has been demonstrated within synovial tissues at 1.5 months p.i.[93]. All studies involving animal models have shown a broad tropism for CHIKV, though fibroblasts and macrophages in particular have been suggested as the preferred cell type and potential locations for viral persistence.

1.2.2 Treatment

Currently, specific treatment modalities for acute and chronic CHIKV-induced disease do not exist, and the majority of treatment plans consist of supportive and symptomatic care. In acute stages of the disease, this consists predominantly of rest, antipyretics and analgesics[6]. Unfortunately, solid efficacy data for most treatment regimens are lacking[87]. Most regimens rely on non-steroidal anti-inflammatory drugs (NSAIDs), whose efficacy can be quite variable, and resolution of acute arthralgia can occur with or without their use[64,116]. Similarly, NSAIDs can have variable effects in chronic cases. In one study in Bangladesh, 2 of 6 patients treated acutely with NSAIDs had persistent pain at 2-3 months[64]. In some cases joint pain may resolve, but stiffness remains[178], perhaps suggesting permanent alterations in articular or peri-articular tissues resulting in decreased mobility.

In cases refractory to NSAID treatment, short-term courses of corticosteroids have been attempted with variable success. In some cases, steroids helped resolve symptoms of arthralgia, tenosynovitis, entrapment syndromes and Raynaud's syndrome[181], while in other cases, these had no effect[53]. In 1 case, there was initial improvement of symptoms, but synovitis persisted in the metatarsal phalangeal joints[26]. Although corticosteroid treatments are usually not recommended due to the potential for a severe rebound of arthritis and tenosynovitis after therapy is ended, in severe cases of inflammatory polyarthritis refractory to NSAID treatment, the benefits may outweigh the risks, and corticosteroid can be utilized[158].

Because of the similarities between chronic CHIKV-associated arthralgia and RA, some disease modifying antirheumatic drugs (DMARDs) such as methotrexate, sulfasalazine, leflunomide and hydroxychloroquine have been utilized[15]. Again, the efficacies of these drugs are unclear[53]. In some patients, 6 month treatments with methotrexate and hydroxychloroquine appeared to be of benefit[105], including clear improvement in severity of joint swelling, pain and tendon involvement continuing for 15 months after initiation, as confirmed by MRI[103]. Other cases have demonstrated almost complete resolution of symptoms in 4-6 months using methotrexate, sulfasalazine and hydroxyochloroquine[181]. However, Bouquillard et al. reported that all patients in their cohort treated

with DMARDs had demonstrated progression of disease evidenced by more severe radiographic lesions at followup[15].

A randomized trial on Reunion Island utilizing chloroquine demonstrated no difference in duration of febrile arthralgia or severity of viremia[153]. Interestingly, in this study, patients receiving chloroquine actually complained about their arthralgia more than the placebo group. Additionally, a randomized trial in India comparing the efficacy of chloroquine compared to meloxicam demonstrated no significant difference in pain reported in either group over the 24 week study period[38]. Although patients in this study improved overall, the authors concluded that there was no advantage to use of chloroquine as compared to NSAIDs or steroids. Additionally, there were elevated pro-inflammatory cytokines (e.g. IL-6 and TNF-a) in patients that did not improve with treatment[38]. Another case demonstrated no resolution of symptoms 16 months after initial infection, though no erosions had developed by that timepoint[26]. Waymouth et al. reported that while chloroquine may be helpful in more chronic stages, when given during the acute phase there was no benefit and patients were more likely to report joint symptoms at 200 DPI[181]. Therefore, the efficacy and utility of chloroquine in cases of CHIKV-induced disease remain unclear.

Neutralizing antibodies have also been tested as treatment modalities. If received prior to infection, viremia and virus levels in ankles were decreased to below the level of detection in a mouse model, however, when administered after infection, though viremia decreased, there were no effects on the levels of viral RNA in the inoculated foot[65]. Whereas the utility of passive immunization using monoclonal and polyclonal neutralizing antibodies *in vitro* and in mouse models have demonstrated prophylactic protection from CHIKV infection, the utility in human patients either as a prophylaxis or as a treatment during acute disease is unknown[43,168]. Similarly, although IFN-α treatment has been shown to be able to prevent development of CHIKV-associated arthritis in a mouse model, this efficacy only occurs when it is administered prior to infection[48,168]. Therefore, utility in a clinical setting is unclear.

The efficacies of specific antiviral medications are unknown, though ribavirin has shown some potential. *In vitro* studies have demonstrated potential utility of ribavirin against alphaviruses[24]. *In vivo*, in a small cohort of ten patients, decreased pain and swelling were reported in most patients[135]. However, larger scale, controlled efficacy studies have not been performed to assess the true utility of ribavirin in treating CHIKV-induced disease.

1.3 DISCUSSION

Extensive work focusing on the acute stages of CHIKV infection and utilizing animal models has enhanced our current understanding of these early timepoints of disease. Although our knowledge in this area has greatly increased in recent years, the role of CHIKV in development of more chronic stages of disease has yet to be elucidated. As previously discussed, while numerous reports describing chronic CHIKV-associated joint disease can be found in the literature, pre-existing joint disease present at the time of initial infection have not been ruled out in these cases. Although some reports utilized questionnaires to assess for presence of pre-existing joint disease, none performed thorough orthopedic evaluations to definitively rule out existing joint disease[79,104,105,160,163]. It is possible that subclinical joint disease existed in a subset of patients diagnosed with chronic CHIKV disease and that infection had little to no impact on the subsequent progression. However, it is also possible that CHIKV infection may exacerbate pre-existing subclinical joint disease and lead to more rapid progression.

Additionally, even in the absence of identifiable pre-existing disease, it is possible that some of the chronic CHIKV cases are a result of development of joint disease such as OA or RA, completely unrelated to CHIKV infection. None of the current reports compare the incidence of OA or RA in a subset of the population not infected with CHIKV. It is essential that thorough clinical workups of patients during acute stages of disease be performed to evaluate for existing disease. Additionally, more animal studies focusing on the effects of CHIKV infection on pre-existing disease would help elucidate the relationships between these diseases.

Viral persistence has also been suggested as a mechanism of chronic CHIKV disease. Some animal models have demonstrated persistence as long as 16 weeks post-infection, often accompanied by continued synovitis[65]. Even in humans, virus has been demonstrated within muscle satellite cells 3 months after resolution of the acute phase of disease and in synovial tissues 18 months after initial infection[24,105]. Therefore, it is possible that this persistence could be responsible for symptoms occurring within the weeks to months following initial infection.

Alternatively, induction of autoimmune disease following CHIKV infection has been put forth as a possible mechanism of chronic joint disease[23]. This hypothesis has been mainly based on the fact that some patients have been diagnosed with RA in the months to years following the initial infection[15,163]. It is believed that infectious diseases can result in auto-immunity or exacerbation of autoimmune diseases through mechanisms such as molecular mimicry, bystander activation, and epitope spreading[51]. In fact, another alphavirus, Semliki Forest virus, has been linked to development of an autoimmune demyelinating disease in a mouse model of experimental autoimmune encephalomyelitis[117]. It has also been suggested that viral infection may play a role in the pathogenesis of RA, as exposure to herpes-related Epstein-Barr virus and cytomegalovirus has been associated with the development of RA[6]. Additionally, some microbial infections of the gastrointestinal or urogenital systems have been associated with development of autoimmune reactions resulting in reactive arthritis (ReA) and ankylosing spondylitis[2,155,173].

However, the potential role of CHIKV and induction of autoimmunity is unknown. While mechanisms for induction of autoimmune disease exist, it is possible that development of RA is completely unrelated to previous CHIKV infection. More research is necessary, including prospective analysis of acute and chronic clinical cases, to help determine the potential role of previous CHIKV infection in chronic disease.

In particular, a more thorough focus on clinical workups of patients could add tremendously to knowledge regarding CHIKV arthralgia and arthritis. A thorough evaluation for any pre-existing joint disease at the time of initial presentation with CHIKV fever, coupled with multiple follow-up

examinations at later timepoints of disease would greatly add to the understanding of CHIKV-induced disease. Because of the variability in the clinical workups available in the literature, it is likely that patients that are currently classified as having chronic CHIKV-associated arthritis actually represent a heterogeneous group of conditions. In fact, a retrospective study examining patient outcome after the Reunion Outbreak demonstrated that patients with chronic post-CHIKV joint disease could be variably diagnosed with RA, spondyloarthropathies, undifferentiated polyarthritis or other musculoskeletal disorders[79].

Currently, the extent of the clinical evaluation performed on cases of chronic CHIKV-associated arthralgia/arthritis is highly variable, sometimes with only minimal diagnostics performed. Results of laboratory tests including CBC, clinical chemistry, serology, synovial fluid analysis, and advanced imaging diagnostics are highly variable and synovial biopsies for definitive characterization and diagnosis are only very rarely performed[41,71,103,105,116,151].

While more invasive methods such as synovial fluid samples and synovial biopsies could undoubtedly add significant information to the growing body of knowledge on CHIKV pathogenesis, these procedures are not without risk to the patients and therefore may require more substantial justification. Additionally, these techniques can cause some level of discomfort and anxiety for patients, thus obtaining volunteers for the initial procedures and ensuring their participation at additional follow-up timepoints can be difficult. Because MRI is a non-invasive procedure and minimal discomfort for the patient is expected, volunteer participation in clinical studies utilizing this modality would likely be higher.

By utilizing advanced imaging techniques, particularly MRI, it would be possible to perform a more thorough evaluation of potentially affected joints and associated soft tissues in CHIKV patients with acute disease. Assessment of the extent of the acute lesions such as joint effusion, synovitis, tendonitis, enthesopathy or bone marrow edema may make it possible to identify people with more severe disease, potentially aiding in the choice of treatment strategies for those at greater risk for developing chronic/relapsing disease. Additionally, the comparison of these early MRI analyses with

later evaluations in patients who subsequently develop chronic or recurrent disease, may help to further characterize disease pathogenesis.

While the data in the current literature in regard to MRI analyses of CHIKV patients with chronic disease is interesting and informative, the lack of baseline scans on these individuals makes the interpretation of results more challenging. In some cases, it might not be possible to differentiate between pathologic changes that are direct results of previous CHIKV infection and subsequent disease, and those that are associated with other, potentially unrelated comorbidities present at the time of initial infection, such as OA or RA. By performing baseline scans at early timepoints in infected patients, not only can the acute manifestations of disease be better characterized, but the presence of any pre-existing disease can be determined, and the progression of CHIKV disease can be further evaluated by comparing the initial scans to follow-up scans in patients with chronic disease. Furthermore, by obtaining these evaluations of CHIKV patients, and pairing them with current ongoing research using animal models, a more thorough understanding of the pathogenesis of CHIKV-induced arthralgia and/or arthritis can be elucidated, and thus novel methods of treatment and prevention may be discovered.

However, the value of the more traditional and invasive methods of sampling including synovial fluid collection and synovial biopsy should still be recognized. Because the acute presentation of CHIKV-associated disease as visualized by MRI is currently unknown, it is possible that scans performed at early timepoints will provide only minimal information in regard to disease status, or that the acute presentation will be variable among patients and therefore the interpretation of results might be challenging. Therefore, the pairing of MRI scan results and synovial fluid samples or biopsies obtained during the acute phase would be ideal. Should this prove to be too difficult or impossible for clinical studies, these early scans may still provide valuable information, and can certainly be extremely useful when paired with follow-up scans during the chronic phase. By including a minimum database of clinical information such as patient gender and age, basic clinical parameters, and evaluation of absence or presence and extent of clinical symptoms such as arthralgia, joint stiffness,

and myalgia, the utility of MRI results can be maximized, even in the absence of data associated with more invasive procedures.

These initial assessments might also be useful for guiding treatment options in patients. In many instances of less severe manifestations of joint disease associated with CHIKV infection, symptomatic treatment with antipyretics, NSAIDs, analgesics, and/or corticosteroids have been shown to be effective in alleviating symptoms[116,178,181]. However, in some more severe cases, the arthralgia and/or arthritis has proven to be resistant to these treatments, and additional more specific therapies, such as antivirals (e.g. acyclovir, ribavirin), cytokine-directed therapies (e.g. anti-IL-6 antibodies, TNF antagonists), and disease modifying anti-rheumatic drugs (DMARDs) have been attempted, with variable results[15,26,38,53,64,87,103,105]. Visualization of more severe joint manifestations of disease via MRI may help identify patients that would benefit from more aggressive therapies and/or be candidates for more frequent clinical follow-up evaluations.

As previously mentioned, treatment of CHIKV arthralgia and/or arthritis is difficult and no proven regimens currently exist. Generally, non-specific treatments such as NSAIDs and analgesics are utilized, with varying success. Additionally, immunosuppressive therapies that are utilized for RA have variable efficacies. Because of the ambiguities in mechanisms associated with both acute and chronic stages of CHIKV associated arthralgia, it is difficult to determine an appropriate treatment plan. Even in arthritides that have been better studied, such as OA and RA, treatment regimens may not offer substantial improvement in clinical signs or significantly slow the progression of disease. Even if similar mechanisms are at work in acute and chronic stages of CHIKV, treatments will likely still be variably successful. Additional research is required focusing on these pathogenic mechanisms and testing treatment modalities to clear up some of these ambiguities.

1.4 CONCLUSIONS

Though it has become commonplace to state that CHIKV can result in chronic arthralgia and/or arthritis, the evidence for this is lacking and potential pathogeneses are unknown. It seems clear that joint pain could persist for weeks to a couple of months in some cases, but care should be taken to

assume that there is a connection between initial CHIKV infection and chronic joint pain lasting months to years. Currently, in all available reports, pre-existing joint disease, or development of an unrelated joint disease such as OA or RA cannot be ruled out. The use of advanced imaging techniques, in conjunction with currently accepted methods of detection and evaluation of CHIKV-infected patients, could fill a significant gap in regard to early identification of patients at risk for developing ongoing joint disease associated with infection, and the characterization of the pathogenesis of arthralgia/arthritis.

There is currently no definitive evidence that treatments beyond conservative NSAID therapy in more severe cases have any efficacy. It should also be noted that aspirin is not recommended due to bleeding risk[168]. In cases refractory to pain alleviation by NSAIDS, weak opioids such as tramadol or codeine can be added[158]. Although investigations into alternative treatments such as inhibitors of viral replication, anti-cytokine therapies, and siRNA have occurred, their efficacies and utilities in a clinical setting are still unknown[32,168].

While animal models have been useful to study acute joint disease demonstrating evidence for viral persistence, no model exists for development of chronic joint disease associated with CHIKV infection. Therefore, to further elucidate the potential role of CHIKV in chronic cases and to establish the efficacy of alternative therapies, clinical studies are required. There is a great need for reporting clinical information associated with both acute and chronic cases.

CHAPTER 2: NOVEL LESIONS OF BONES AND JOINTS ASSOCIATED WITH CHIKUNGUNYA VIRUS INFECTION IN TWO MOUSE MODELS OF DISEASE: NEW INSIGHTS INTO DISEASE PATHOGENESIS[1]

2.1 INTRODUCTION

Chikungunya virus (CHIKV) is an alphavirus in the *Togaviridae* family. The word 'chikungunya' is roughly translated to "that which bends up" or "to walk bent over" from the Makonde language in Tanzania and is so named because of the severe incapacitating arthralgia that occurs with infection[6,116]. CHIKV is an enveloped, positive sense RNA arbovirus spread predominantly by *Aedes aegypti* and *Ae. albopictus* mosquitoes[39,41,127].

Historically, the geographical distribution of CHIKV has been restricted to tropical and subtropical regions throughout Africa and Asia, particularly the Indian subcontinent. There are three currently recognized genotypes of virus endemic in these areas, defined as the Eastern/Central/South African, West African, and Asian genotypes[177]. Due to the expanding range of the vector *Ae. albopictus* and the continually increasing ease of international travel and commerce, CHIKV has recently extended into temperate regions[9,27,63,116,170]. Most recently, beginning in October of 2013, the virus has emerged and rapidly spread throughout the Caribbean and the Americas, resulting in more than 1.6 million suspected cases and 270 deaths as of October 15, 2015[123]. It has been determined that the strain circulating in this region belongs to the Asian genotype[53].

Approximately 95% of people that are infected with CHIKV will become symptomatic, which consists predominantly of high fever, rash, and debilitating arthralgia[6,15,37,181]. While in the majority of cases symptoms resolve approximately two weeks after onset, some patients can develop ongoing symptoms of arthralgia lasting months to years after the initial infection[13,25,52,116,141,143,160,181]. Most commonly, there is symmetrical involvement of distal joints including those of the ankles, wrists, and digits, though any joint can be affected[6,37,104,160]. Although there are numerous reports of clinical

[1] This chapter previously appeared as Goupil, B. A. *et al*. Novel Lesions of Bones and Joints Associated with Chikungunya Virus Infection in Two Mouse Models of Disease: New Insights into Disease Pathogenesis. *PloS one* **11**, e0155243, doi:10.1371/journal.pone.0155243 (2016). It is reprinted by permission of "PLOS Publications"

workups on patients suffering from chronic CHIKV-associated arthralgia, the mechanisms involved in the development of disease and their association with initial viral infection are unclear[6,53,79,103,104,158,160,181]. However, some reports suggests that chronic CHIKV-associated arthritis is an erosive and inflammatory arthritis with similarities to rheumatoid arthritis[104,120]. Diagnostic imaging techniques such as radiography and MRI have demonstrated evidence of loss of articular cartilage and bony erosions in affected joints of patients with histories of CHIKV infection[15,104,116,158]. However, it should be noted that in these cases, these chronic joint manifestations cannot be unequivocally attributed to previous infection with CHIKV, as other concurrent joint diseases such as rheumatoid arthritis or osteoarthritis cannot be ruled out.

The arthralgia and/or arthritis associated with CHIKV infection represents a significant component of the clinical picture of both acute and chronic disease, though there are still gaps in knowledge regarding the pathogenesis of these manifestations. Current hypotheses for chronic disease include viral or antigen persistence within tissues of the joint (e.g. synovium) resulting in ongoing direct damage from viral infection, replication and/or immune-mediated tissue destruction, or induction of a post-infection autoimmune condition[8,39,51,67,103]. The challenge in elucidating these mechanisms of bone and joint disease is that animal models of chronic CHIKV-associated arthralgia and/or arthritis are lacking, and existing models of acute disease do not necessarily replicate all aspects of human disease manifestations[41,93,167]. While existing models can recapitulate some aspects of disease, involvement of the articular cartilage and bone in particular have rarely been definitively demonstrated[69,129]. In addition to the bone and joint manifestations of disease, in rare cases, CHIKV infection can result in more severe disease manifestations, including mortalities[41,70,77,87,137].

There are currently several existing animal models including mice and non-human primates that are considered appropriate for evaluation of CHIKV-associated disease as experimental models[42,70,167]. Two models that most closely replicate consistent joint involvement associated with CHIKV infection include the IRF 3/7 $^{-/-\ -/-}$ mice, which have a deficient type 1 interferon response, and

adult, wild-type C57BL/6 mice[55,145,150]. The IRF 3/7 $^{-/-\ -/-}$ mice develop a fatal form of disease, similar to that seen in some of the more severe manifestations of disease in people[145,150], though the C57BL/6 mice develop a more protracted form of disease, similar to that seen in the majority of human cases[55]. Both models have been shown to develop significant viremia following viral inoculation in the dorsal or ventral surface of the hind foot, exhibit evidence of some myositis, synovitis, and tendonitis associated with infection, and CHIKV has been demonstrated locally within the tissues of the foot[55,145,150]. While these two mouse models develop consistent CHIKV-associated disease, some of the manifestations of joint disease seen in humans, including damage to the articular cartilage, alterations of bone including bony lysis, have rarely, if ever been described. Additionally, none of these models have demonstrated utility for use in chronic CHIKV-associated disease studies.

By utilizing these two established animal models of disease, this study aimed to 1) demonstrate, describe and evaluate pathologic findings in both articular cartilage and bone associated with CHIKV infection, 2) examine these aspects of disease manifestations over time at various points throughout the disease course, and 3) evaluate these models for potential use in chronic studies of CHIKV-associated arthralgia/arthritis. We suspect that a thorough evaluation of bone and joint pathology associated with CHIKV infection will reveal previously unrecognized lesions in these existing mouse models. We hypothesize that CHIKV infection will result in degeneration of articular cartilage and osteoclastic bone resorption associated with synovitis.

2.2 MATERIALS AND METHODS

2.2.1 Virus

A Southeast Asian strain of CHIKV (SVO 476-96) was utilized for this project and was a generous gift from the World Reference Center for Emerging Viruses and Arboviruses at the University of Texas Medical Branch. The isolate was originally obtained from a human sample in Northeast Thailand in 1996 and was passaged twice in LLC-MK2 cells and once in Vero cells prior to being obtained by our laboratory. The virus was passaged one additional time in Vero cells prior to utilization in this project.

2.2.2 Ethics Statement

Housing of animals utilized in this study and the methods employed during animal experimental procedures were reviewed and approved by the Louisiana State University (LSU) Institutional Animal Care and Use Committee (IACUC) which complies with the guidelines stated in the National Institutes of Health's (NIH) Guide for the Care and Use of Laboratory Animals. These experiments were conducted under the approved LSU IACUC protocol #15-005 (approved in 2015).

2.2.3 Animal Models

Two established mouse models of CHIKV infection were utilized: IRF 3/7 $^{-/-\ -/-}$ mice on a C57BL/6 background (≥ 8 weeks of age; males and females) and C57BL/6J mice (≥ 8 weeks of age; females only). C57BL/6J mice were obtained from a distributor (The Jackson Laboratory, https://www.jax.org/). The IRF 3/7 $^{-/-\ -/-}$ mice were originally obtained as a generous gift from Dr. Michael Diamond (Washington University, St. Louis, MO) with permission from Dr. T. Taniguchi (University of Tokyo, Tokyo, Japan). A breeding colony was subsequently established and maintained in the BSL3 laboratory at the Louisiana State University (LSU) School of Veterinary Medicine (SVM).

Mice were housed in groups of 4 or 5 in micro-isolator cages in the BSL3 laboratory of the LSU SVM. Mice were provided water and a standard commercial mouse food (LabDiet, Land O' Lakes, Inc., St. Louis, MO) ad libitum throughout the experiments. Prior to infection, mice were initially anesthetized with isoflurane followed by intraperitoneal injection of a ketamine (40 mg/kg) and xylazine (2 mg/kg) solution. Subsequently, mice were intradermally (IRF 3/7 $^{-/-\ -/-}$ mice) or subcutaneously (C57BL/6J mice) injected in the caudoventral aspect of the hind foot near the tarsal joint with $2x10^4$ PFU of virus. As negative controls, age and sex-matched mice were injected with a similar volume (10µl) of sterile PBS. Mice were then euthanized at various timepoints throughout the disease course (1, 2, 4, 5, 6, 7 days post infection [DPI] for the IRF 3/7 $^{-/-\ -/-}$ mice and 7, 14, 21 DPI for the C57BL/6J mice). During experiments, animals were monitored a minimum of once (C57BL/6J mice) or twice (IRF-3/7$^{-/-\ -/-}$ mice) daily for clinical signs associated with illness, including lethargy, abnormal posture, joint swelling, lameness, limb gnawing, and loss of body weight. If at any point

during the experiments, mice were determined to be in significant distress or exhibited a loss of 20% or greater of initial body weight, they were immediately euthanized to reduce pain and suffering. At 5 DPI, 4 of the IRF 3/7 $^{-/-\,-/-}$ mice were moderately lethargic and were subsequently euthanized at that time. Due to the rapid progression of the fatal disease that occurs in the IRF 3/7 $^{-/-\,-/-}$ mice, 6 mice died during the experiment, though, with the exception of foot swelling, no additional clinical signs were observed in these mice prior to their death (4 mice at 5 DPI, 1 mouse at 6 DPI, and 1 mouse at 7 DPI). Mice were euthanized via CO_2 asphyxiation followed by cervical dislocation. All experiments were performed in accordance with LSU IACUC guidelines (protocol #15-005).

2.2.4 Microcomputed Tomography (μCT)

Intact hindlimbs were collected from mice and scanned using μCT. Two regions of interest (ROI) scanned for each mouse included: 1) the stifle joint extending from approximately mid-shaft of the femur to mid-shaft of the tibia and fibula, and 2) the distal hindlimb extending from the proximal aspect of the tuber calcanei to the distal phalanges. Specimens were placed in holders for scanning by μCT (Scanco model 40; Scanco Medical AG, Basserdorf, Switzerland). Samples were scanned in a transverse plane in 70% ETOH at 55kV, 0.3-second integration time, with a 16 μm voxel size in plane and a 16 μm slice thickness. To evaluate differences in bone morphology within age-matched IRF 3/7 $^{-/-\,-/-}$ mice (n=11) compared to wild-type C57BL/6J controls (n=9), the humeri were dissected free from surrounding soft tissue and scanned in 70% ETOH at 55kV, 0.3-second integration time, with a 10 μm voxel size in plane and a 10 μm slice thickness.

To evaluate trabecular bone morphology secondary to CHIKV infection within the stifle joint region, two ROIs were evaluated: 1) the proximal epiphysis of the tibia extending from the subchondral bone to the proximal physis as has been previously evaluated[35], and 2) the distal metaphysis of the femur, extending from approximately mid-shaft to the distal physis, which is considered the appropriate location to evaluate trabecular bone morphology[16]. The proximal 30% of the humerus, extending distally from the proximal physis, was the ROI used to evaluate changes in

trabecular morphology within the IRF 3/7 $^{-/-\ -/-}$ strain compared to wild-type C57BL/6J controls, and a region at midshaft was used to evaluate cortical bone.

The proper thresholds for 3D reconstructions to qualitatively evaluate overall bone morphology, in addition to appropriate thresholds to quantitatively evaluate trabecular bone, were tested and the same thresholds were used throughout the study for all ROIs. For trabecular bone, bone volume (BV), total volume (TV), BV/TV, tissue density, apparent density, trabecular number (Tb.N), trabecular thickness (Tb.Th), trabecular spacing (Tb.Sp), connectivity density (Conn.D), structural model index (SMI), bone surface (BS), and degree of anisotropy (DA) were evaluated. For cortical bone, cortical area (Ct.Ar), thickness (Ct.Th), and porosity (Ct.Po), total cross-sectional area (Tt.Ar), and Ct.Ar/Tt.Ar were evaluated. Established procedures and nomenclature were used for all variables[16].

2.2.5 Histopathology

Immediately following euthanasia, entire mice were fixed in 10% neutral buffered formalin for a minimum of 48 hours. Following fixation and after evaluation via μCT, the entire hind feet of mice (ipsilateral and contralateral) were sagittally bisected and decalcified in 10% EDTA for 21-28 days. Samples were then routinely processed for histopathologic evaluation. Briefly, samples were dehydrated in increasing concentrations of ethanol and embedded in paraffin wax. Subsequently, 4-5 μm thick sections were adhered to positively charged glass slides. Sections were routinely stained with hematoxylin and eosin (H&E) for evaluation. Standard Masson's trichrome stains were performed on select slides. All histologic evaluations were performed by a board-certified veterinary anatomic pathologist (BAG). All slides were evaluated using a Nikon Eclipse Ni-U upright microscope (Nikon Instruments Inc., Melville, New York) and digital images were obtained using an attached Olympus DP72 microscope digital camera (Olympus Corporation, Tokyo, Japan).

2.3 RESULTS

2.3.1 C57BL/6 Mice

At 7 DPI, all virally infected mice exhibited moderate to marked swelling of the inoculated feet (Figure 2.1). This swelling had resolved by 14 DPI in all mice. These findings are similar to those previously reported in this mouse model[55].

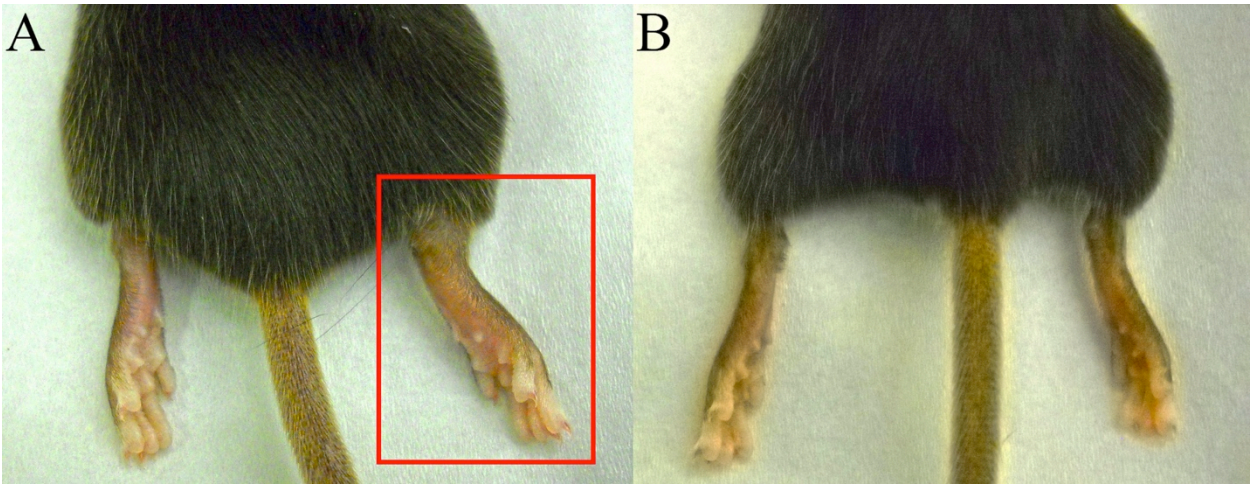

Figure 2.1. C57BL/6 mice sacrificed at 7 DPI. (A) CHIKV inoculated mouse demonstrating significant swelling of the inoculated foot (right foot; red box). (B) PBS sham inoculated mouse demonstrating no swelling associated with inoculation (right foot).

Initial histopathologic evaluation of some aspects of CHIKV infection in the feet of adult C57Bl/6 mice has been previously reported[55]. Similar findings were observed in the current experiment, including moderate mononuclear inflammation in the deep dermis and subcutis, extensive myocyte necrosis and inflammation, tendonitis, and synovitis. A more detailed histologic evaluation in the current experiment demonstrated additional novel lesions associated with CHIKV infection. An overview of the various lesions and their time courses are presented in Figure 2.2**.**

In 100% of mice, the predominant change in the skeletal muscle consisted of acute myofiber degeneration and necrosis accompanied by minimal cellular infiltrates consisting predominantly of macrophages and fewer neutrophils. Joint lesions primarily affected the tarsal joints in 100% of mice, and consisted of loss of the lining synoviocytes of the intima and infiltration of the subintima by small numbers of mononuclear cells and neutrophils. There were rare regions of equivocal cartilage necrosis in few mice, though no definitive foci were apparent. Affecting the metatarsal bones of 3 of 4

infected mice (75%), there were occasional areas of minimal to mild expansion and hypercellularity of the periosteum (periostitis). Rarely, within the tibia and metatarsal bones of 1 mouse (25%), there were small areas of bone marrow edema characterized by accumulation of variably sized pools of pale eosinophilic, homogenous material.

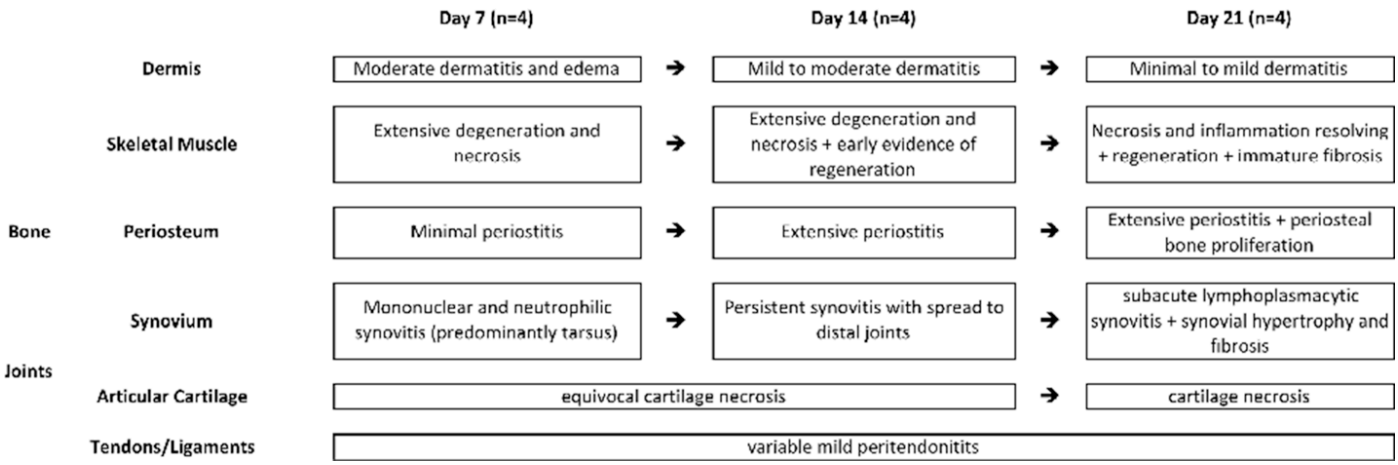

Figure 2.2. Progression of lesions in C57BL/6J mice infected with chikungunya virus.

At 14 DPI, the necrosis and inflammatory component within the skeletal muscle was similar to that observed at 7 DPI, however, there was also evidence of myofiber regeneration characterized by the presence of large myocytes containing basophilic cytoplasm and internalized nuclei exhibiting nuclear rowing. More distal joints including the tarsometatarsal, metatarsophalangeal and interphalangeal joints were also similarly affected in all mice. Similarly to 7 DPI, there were rare regions of equivocal cartilage necrosis in few mice, though no definitive foci were apparent. Four of 4 mice (100%) had consistent mild periostitis affecting the majority of the length of the metatarsal bones. Areas exhibiting more significant periostitis were often immediately adjacent to more extensive regions of necrosis and inflammation within the skeletal muscle. Bone marrow edema was not observed in any mice at this timepoint.

At 21 DPI, in the skeletal muscle, the necrosis was beginning to resolve and regeneration was more prominent and accompanied by some loose fibrous connective tissue replacing areas of myofiber dropout (Figure 2.3, A). The subintimal mononuclear infiltrates within the synovium had increased and consisted predominantly of lymphocytes and plasma cells, consistent with a subacute

lymphoplasmacytic synovitis affecting 4 of 4 mice (100%). Synoviocytes, when present, were often hypertrophic and trichrome stains demonstrated increased fibrous connective tissue within the synovium (Figure 2.3, C). Two of 4 mice (50%), had foci of necrotic articular cartilage.

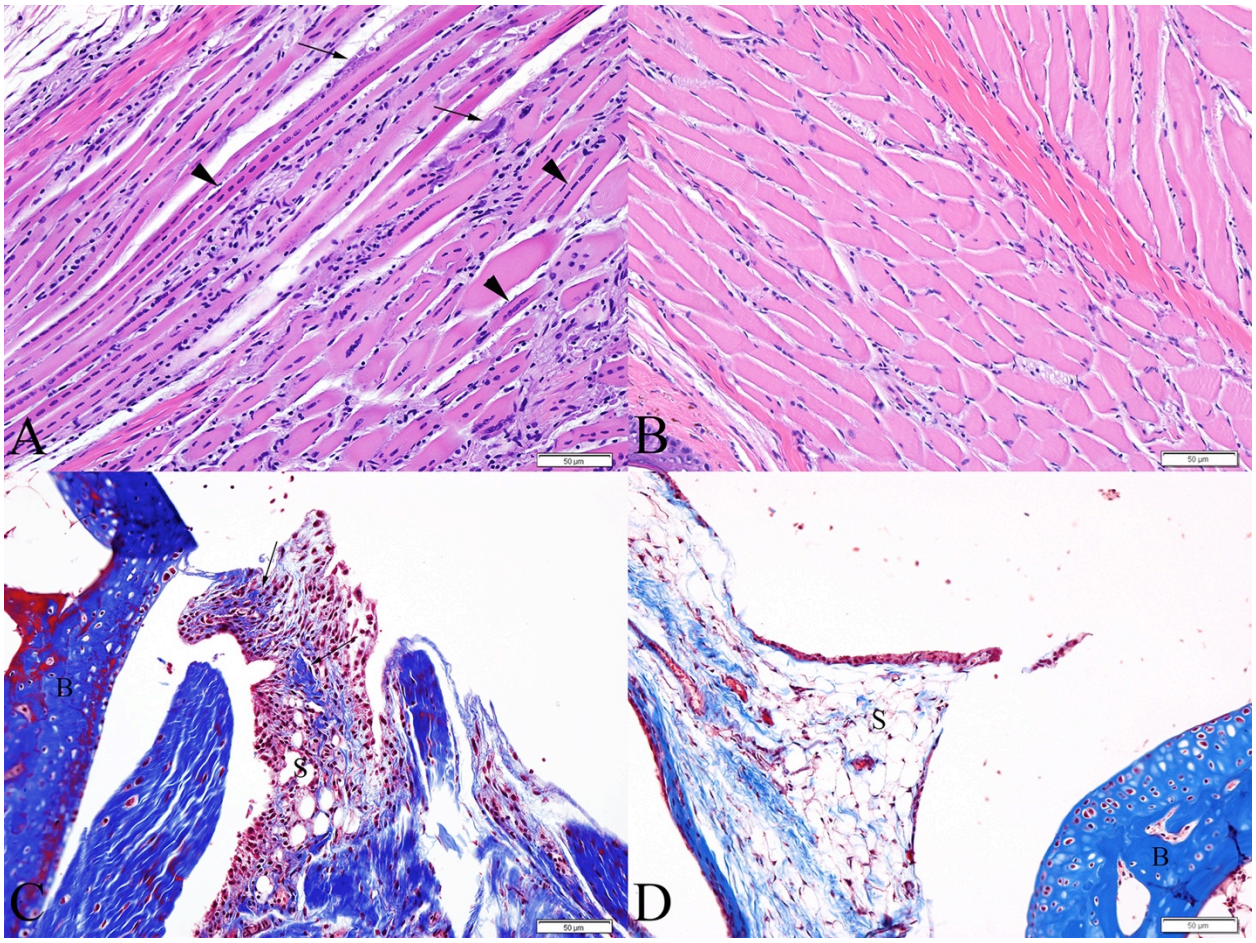

Figure 2.3. C57BL/6 mice sacrificed at 21 DPI. (A) Skeletal muscle exhibiting multifocal areas of ongoing necrosis (arrows) and extensive myofiber regeneration (arrowheads). (B) Skeletal muscle from a similar location of a normal PBS-inoculated control mouse. (C) Tibiotarsal joint demonstrating deposition of fibrous connective tissue within the synovium (arrows) (Masson's trichrome stain). (D) Tibiotarsal from a PBS-inoculated control mouse demonstrating normal synovium (Masson's trichrome stain). (S = synovium, B = bone)

Affecting 4 of 4 (100%) virally infected mice, there was extensive, moderate periostitis. In 2 of 4 (50%) of these mice, on the plantar surface of the diaphysis of the metatarsal bone, within areas of periostitis, there were focal regions of mild proliferation of immature woven bone beneath the periosteum (subperiosteal bone proliferation) (Figure 2.4, A). These foci were limited to this location and not seen in other bones of the foot. Within these areas, lining the periosteal new bone, there were numerous elliptical cells with basophilic cytoplasm, a perinuclear clear zone and

heterochromatic nuclei (consistent with activated osteoblasts). Occasionally, within the periosteum and associated with either periosteal new bone or the periosteal surface of adjacent cortical bone, there were few large, polygonal to round, multinucleated cells occasionally found within scalloped margins of bone (Howship's lacunae), consistent with osteoclasts actively resorbing bone (Figure 2.4, B). Bone marrow edema was apparent in 75% of mice.

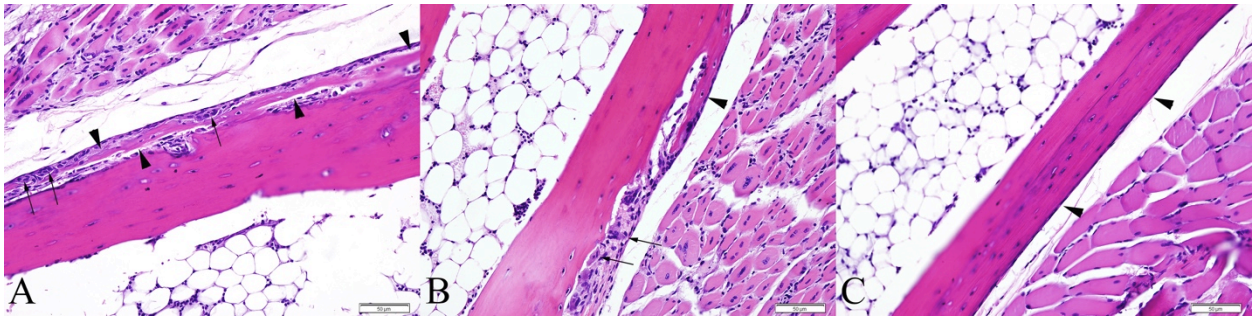

Figure 2.4. Metatarsal bones of C57BL/6J mice at 21 DPI exhibiting periosteal bone proliferation of woven bone. (A) Periosteal bone proliferation (arrowheads) and few large multinucleated cells within scalloped lacunae (osteoclasts, arrows) along the superficial margin of the periosteal new bone, just deep to the periosteal lining. (B) Periosteal bone proliferation (arrowhead) and osteoclasts (arrows) are apparent along the cortical surface of the bone. (C) Metatarsal bone from a PBS-inoculated control mouse demonstrating normal periosteum (arrowhead).

2.3.2 IRF 3/7 $^{-/-\ -/-}$ Mice

Similarly to what has been previously reported in this mouse model[145,150], grossly apparent swelling of the virus-inoculated feet was apparent by 2 DPI and reached its maximum at 4 DPI. While measureable swelling of the contralateral feet did not occur, mild hyperemia was apparent when compared to the PBS control mice (Figure 2.5). No additional significant gross findings were apparent.

Initial histopathologic evaluations of IRF 3/7 $^{-/-\ -/-}$ mice infected with CHIKV have been reported previously[145,150] and lesions similar to those described were also observed in the current experiment. These included multifocal epidermal necrosis, dermal edema, inflammation and hemorrhage, skeletal muscle necrosis, tenosynovitis, and fibrinonecrotizing vasculitis. Because these lesions have been previously described, the following results will consist of more detailed descriptions of some of these and descriptions of novel lesions. An overview of the various lesions and their time courses are presented in Figure 2.6.

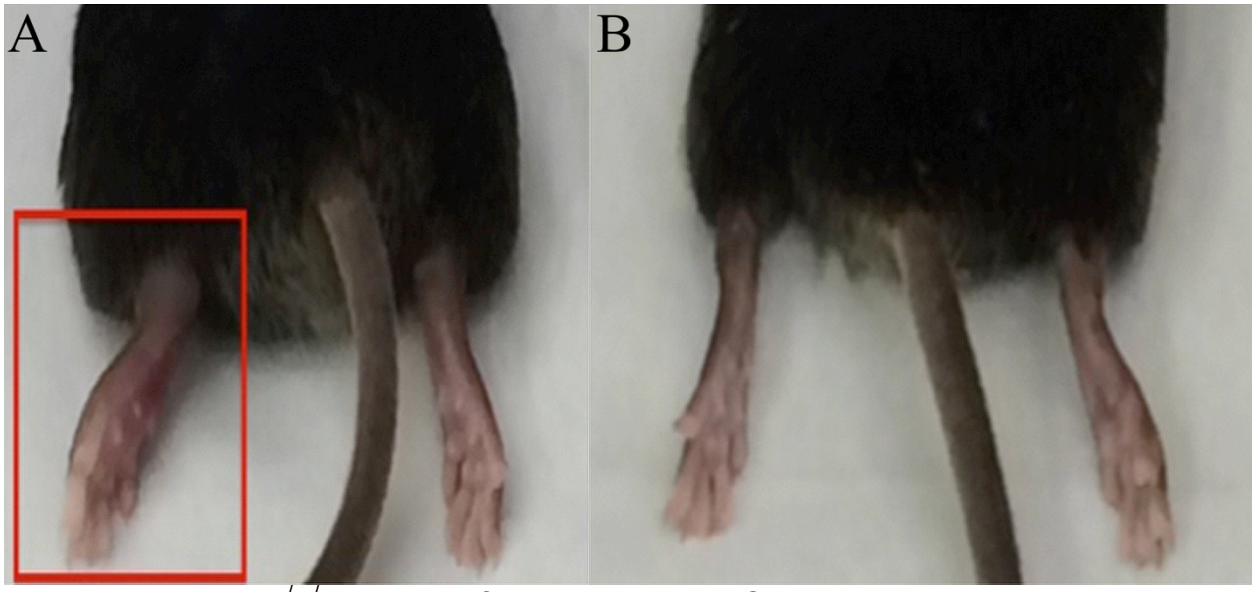

Figure 2.5. IRF 3/7 $^{-/-\ -/-}$ mice sacrificed at 5 DPI. (A) CHIKV inoculated mouse demonstrating significant swelling of the inoculated foot (left foot; red box). Mild hyperemia is apparent in the contralateral (right) foot. (B) PBS Sham inoculated mouse demonstrating no swelling associated with inoculation (left foot).

At 2 DPI, initial evidence of minimal to mild skeletal muscle degeneration was present in 6 of 6 mice (100%). While a fibrinous synovitis has been previously reported in this mouse model[145,150], the full extent and progression of the joint disease has not been described. Initial synovial degeneration and necrosis was observed at 2 DPI in the inoculated feet in 100% mice, predominantly affecting the tarsal joints. Two of 6 mice (33%) exhibited variably severe regions of bone marrow necrosis characterized by locally extensive areas of eosinophilia, loss of cellular detail, accumulation of cellular debris, and presence of cells with pyknotic, karyolytic or karyorrhectic nuclei (apoptosis and necrosis).

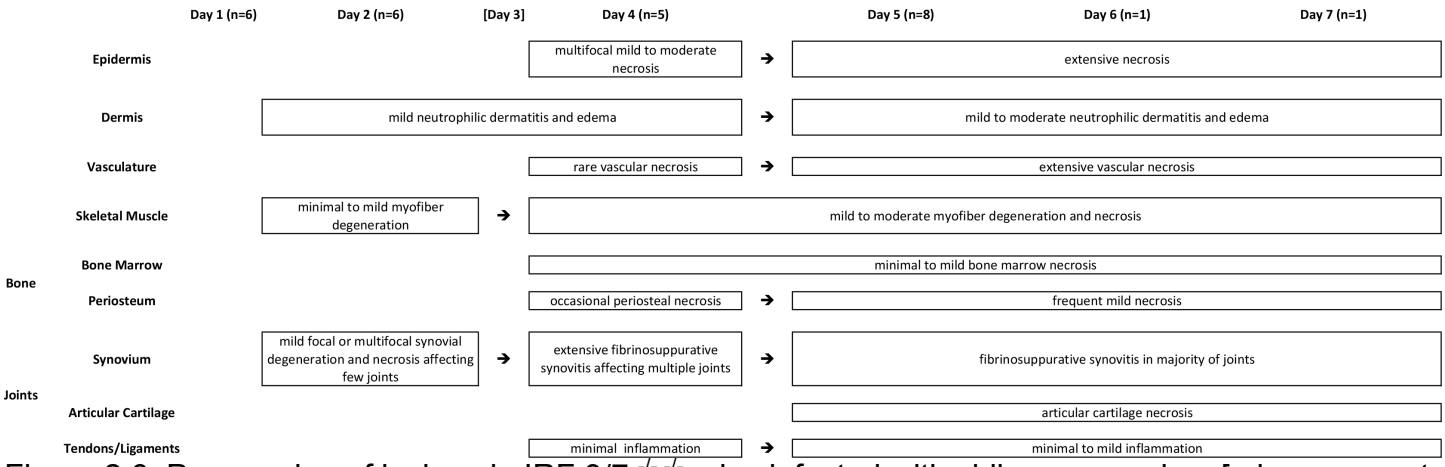

Figure 2.6. Progression of lesions in IRF 3/7 $^{-/-\ -/-}$ mice infected with chikungunya virus [mice were not evaluated on Day 3 post-infection].

By 4 DPI, lesions of skeletal muscle degeneration progressed to necrosis in 5 of 5 mice (100%). Fibrinoid vasculitis affecting small and medium caliber vessels was apparent in 5 out of 5 mice (100%), though was not widespread. There was necrosis and loss of endothelial cells, transmural fibrinoid change of the vessel walls, and occasional leukocytoclasia. Inflammatory cells within the necrotic vessel walls were rare and consisted of degenerate leukocytes. The majority of joints throughout the foot, including the intertarsal, tarsometatarsal, metatarsophalangeal, and interphalangeal joints were affected in 100% of mice. In these cases, there was partial to complete loss of the superficial synoviocytes accompanied by degeneration and necrosis of any remaining synoviocytes. The subintima was infiltrated by rare neutrophils and mononuclear cells, and variably effaced and replaced by accumulations of fibrin and necrotic debris. Three of 5 mice exhibited focally extensive regions of minimal to mild periosteal necrosis characterized by loss of cellular detail and accumulation of small amounts of fibrin and necrotic debris (Figure 2.7, A). Regions of bone marrow necrosis were present in 100% of mice (Figure 2.7, B). Occasionally, regions of necrosis also contained numerous prominent vacuolated macrophages.

By 5 DPI and later, 10 of 10 mice (100%) had extensive multifocal myocyte necrosis accompanied by minimal infiltration by rare neutrophils and macrophages. In 100% of mice, fibrinoid vasculitis was widespread and affected the majority of vessels, including occasional larger caliber vessels. Synovial lesions persisted at these timepoints in all mice (Figure 2.7, E). Additionally, 3 out of 10 mice (30%) exhibited focal areas of cartilage necrosis located immediately adjacent to regions of fibrinous synovitis. The cartilage necrosis was characterized by decreased staining intensity of the cartilage matrix and presence of pale, swollen chondrocytes often exhibiting loss of cellular detail (necrosis) (Figure 2.7, F). Eight out of 10 mice exhibited focally extensive regions of periosteal necrosis, particularly evident within the periosteum of the metatarsal bones and all mice (10/10) had multifocal and extensive regions of bone marrow necrosis. These lesions were present throughout the foot, often variably affecting numerous bones within the section extending from the tibia to the distal phalanges. In some instances, necrotic nutrient/mid-diaphyseal vessels were present near the most

severe regions of bone marrow necrosis, consistent with ischemic necrosis of bone marrow (Figure 2.8, A). Rarely, in the caudal aspect of the calcanei, regions of marrow necrosis extended into and affected the adjacent physeal cartilage.

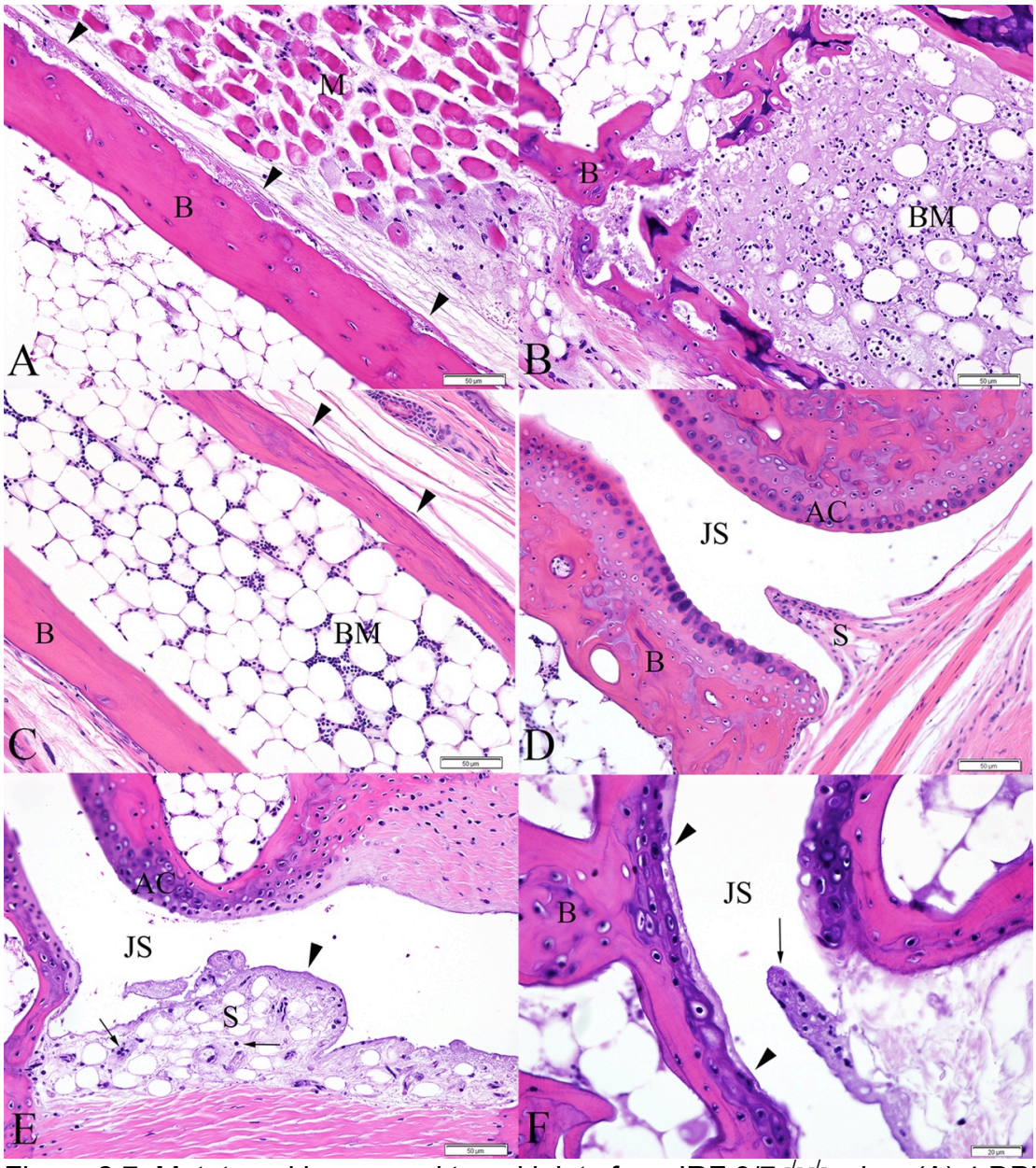

Figure 2.7. Metatarsal bones and tarsal joints from IRF 3/7 $^{-/-\ -/-}$ mice. (A) 4 DPI, periosteal necrosis of the metatarsal bone (arrowheads). The periosteum is slightly expanded by fibrin and cellular debris. (B) 4 DPI, distal aspect of metatarsal bone exhibiting extensive bone marrow necrosis. Normal bone marrow is replaced by fibrin, cellular debris, and necrotic and apoptotic cells. (C) Metatarsal bone from a PBS-inoculated control mouse demonstrating normal bone marrow and periosteum (arrowheads). (D) Synovium and articular cartilage from a normal PBS-inoculated control mouse. (E) 5 DPI, fibrinous synovitis exhibiting loss of synoviocytes, accumulation of fibrin along the intima and within the superficial subintima (arrowhead), and infiltration of the subintima by few leukocytes (arrows). (F) 6 DPI, cartilage necrosis (bounded by arrowheads) is apparent in the articular cartilage of the metatarsal bone, adjacent to a region of fibrinous synovitis (arrow). (B = bone, M = skeletal muscle, BM = bone marrow, S = synovium, JS = joint space, AC = articular cartilage)

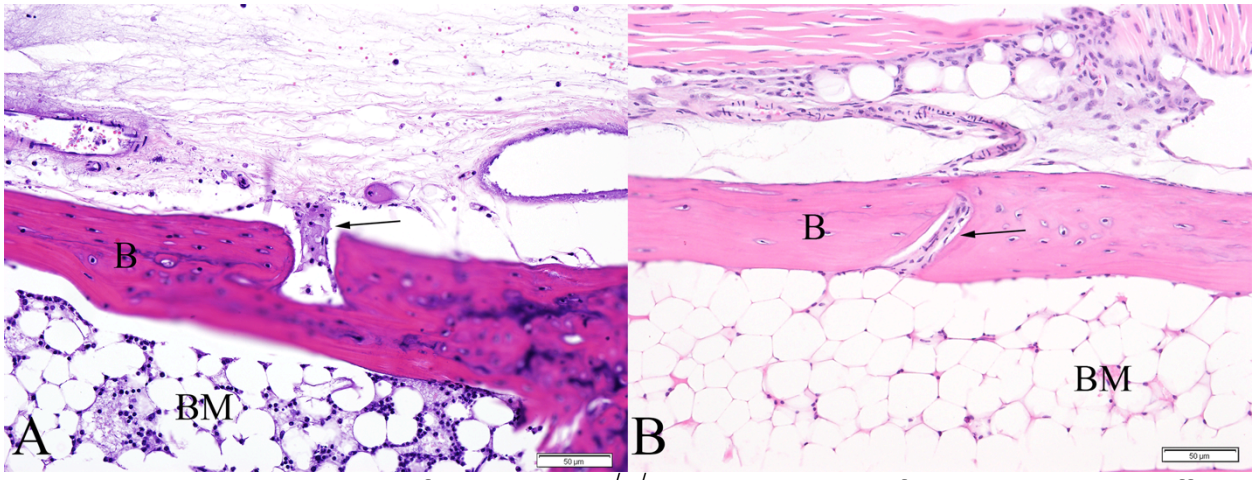

Figure 2.8. Metatarsal bones from IRF 3/7 $^{-/-\ -/-}$ mice. (A) 7 DPI, fibrinoid vasculitis affecting the mid-diaphyseal blood vessel of the metatarsal bone (arrow) associated with a region of bone marrow necrosis. (B) PBS sham inoculated mouse demonstrating normal mid-diaphyseal blood vessel of the metatarsal bone (arrow). (B = bone, M = skeletal muscle, BM = bone marrow)

In the contralateral feet of all virally inoculated mice, similar, though milder lesions of dermal edema and hemorrhage, fibrinonecrotizing vasculitis, fibrinous synovitis, and ischemic bone marrow necrosis were present at similar timepoints. None of the previously described lesions were present in either the inoculated or contralateral feet of control mice.

2.3.3 Micro-computed Tomography (µCT)

No changes in any trabecular bone parameters in wild-type C57BL/6J mice secondary to CHIKV infection were identified in either ROI evaluated (Figure 2.9). Within the wild-type C57BL/6J mice, 3 out of 4 mice (75%) at 21 DPI exhibited periosteal bone proliferation secondary to CHIKV infection, whereas this same lesion was not identified in any control mice. These lesions were readily visible on 2D µCT scans (Figure 2.10, A), and 3D reconstructions of the region identified a roughened surface of the bone (Figure 2.10, B). The first metatarsal bone of each mouse was most consistently and severely affected in all instances. The regions of periosteal bone proliferation affected between 17.48% and 46.10% of the entire bone length and the volume of the regions of periosteal bone ranged from 0.0079 mm^3 to 0.0812 mm^3. The density of these areas ranged from 458.6021 mg HA/ccm to 631.638 mg HA/ccm as compared to a density of the adjacent cortical bone between 922.7256 mg HA/ccm and 1013.2021 mg HA/ccm, consistent with the fact that immature woven bone is less dense than mature lamellar cortical bone.

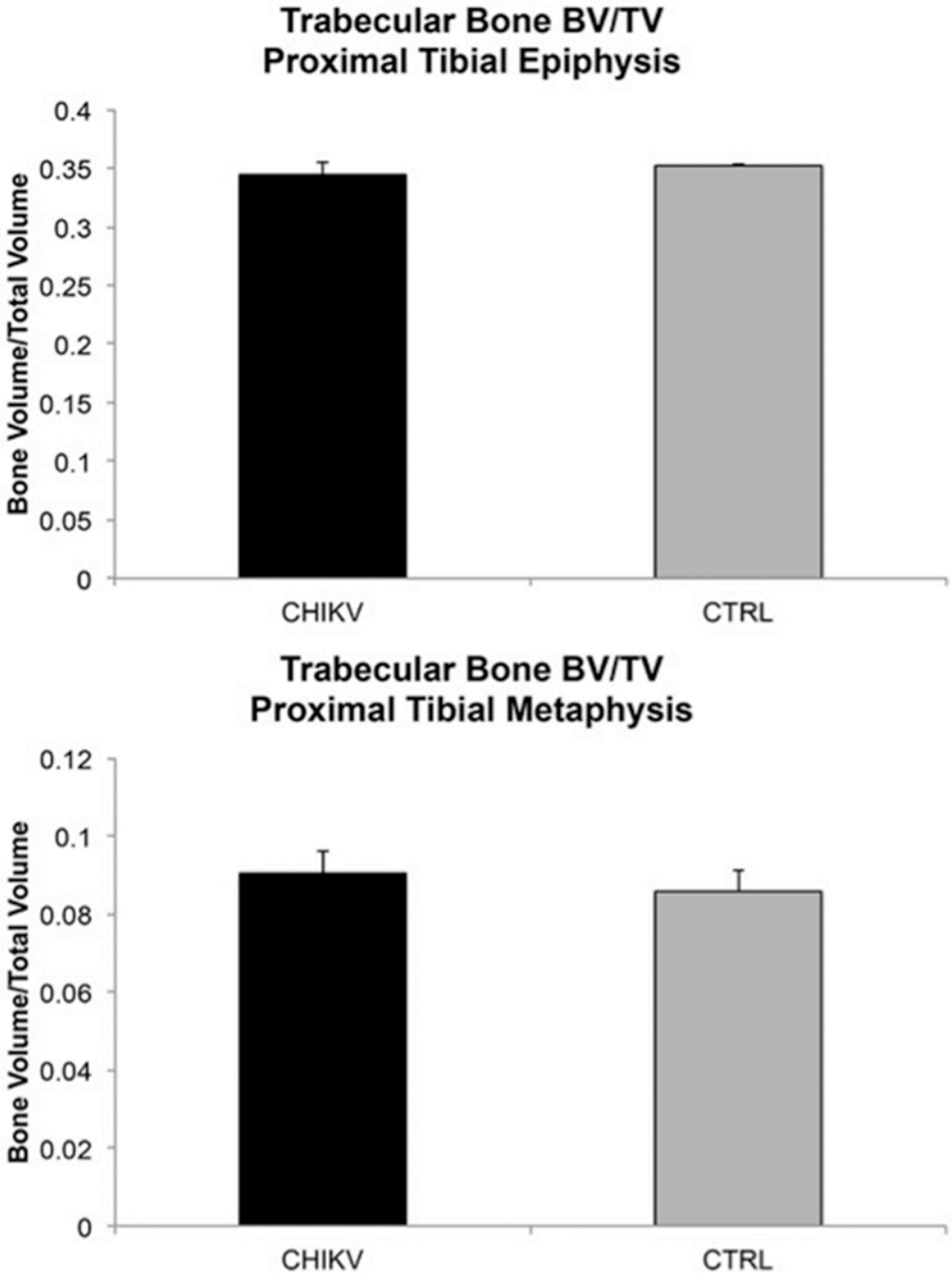

Figure 2.9. Bone volume/total volume in CHIKV and control mice. ROIs included the proximal epiphysis of the tibia and distal metaphysis of the femur. Mean ± SEM.

No changes were identified in trabecular bone between the two strains. However, several differences between the two strains were identified in cortical bone at the midshaft of the humerus (Figure 2.11). IRF 3/7 $^{-/-\,-/-}$ mice were found to have significantly higher Ct.Th ($p=0.010$). Ct.Ar/Tt.Ar also trended towards being significantly higher ($p=0.050$) in the IRF 3/7 $^{-/-\,-/-}$ mice, and Ct.Po trended towards being significantly lower ($p=0.050$).

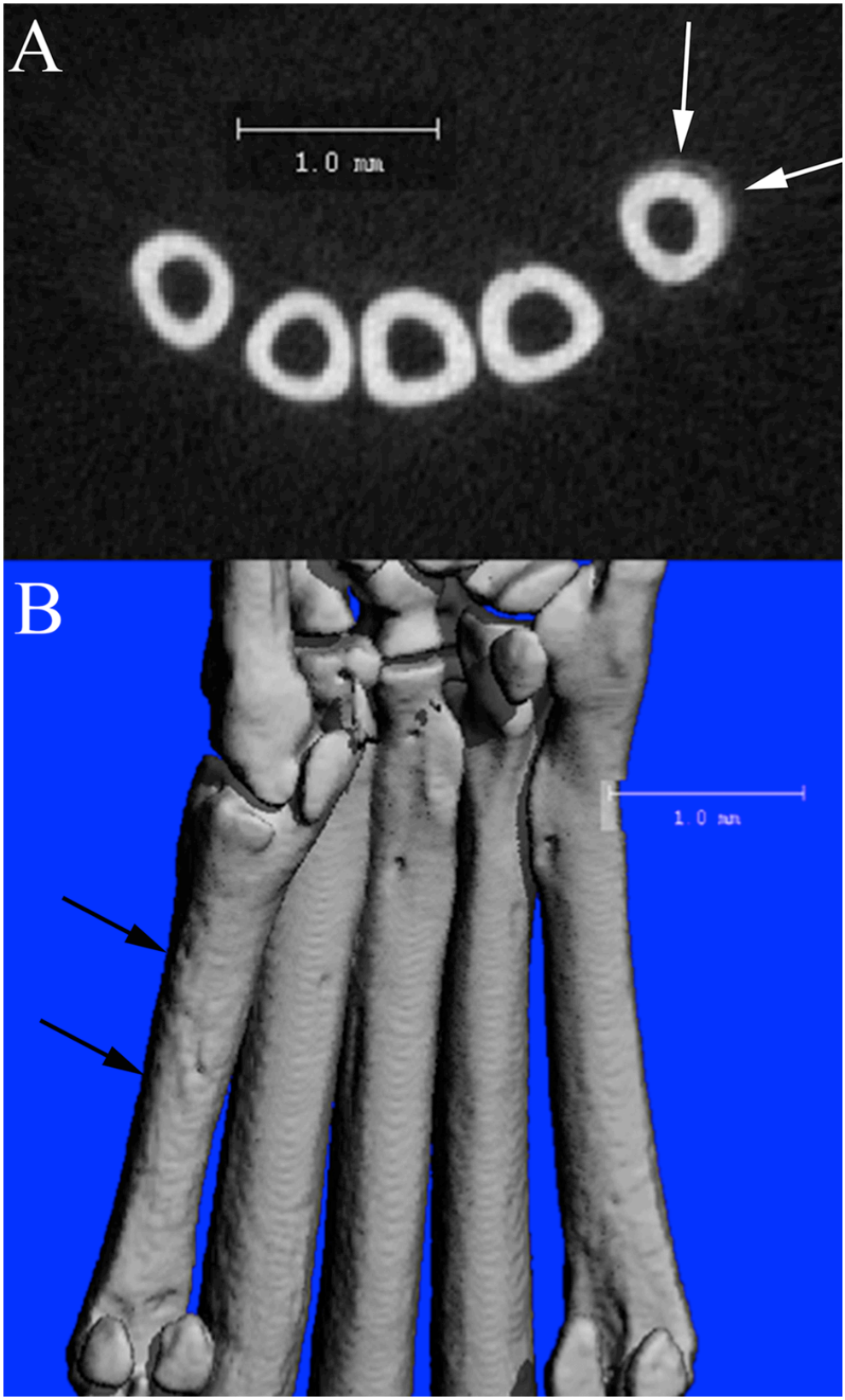

Figure 2.10. μCT scans of a CHIKV infected C57BL/6 mouse at 21 DPI. (A) 2D slice from μCT scan of the mid-metatarsal region demonstrating region of periosteal bone proliferation (arrows) on first metatarsal bone (Mt1). (B) Corresponding 3D reconstruction of the plantar metatarsal region of the same mouse, demonstrating the roughened periosteal surface on Mt1 (arrows) in the region of the proliferative lesion identified in A.

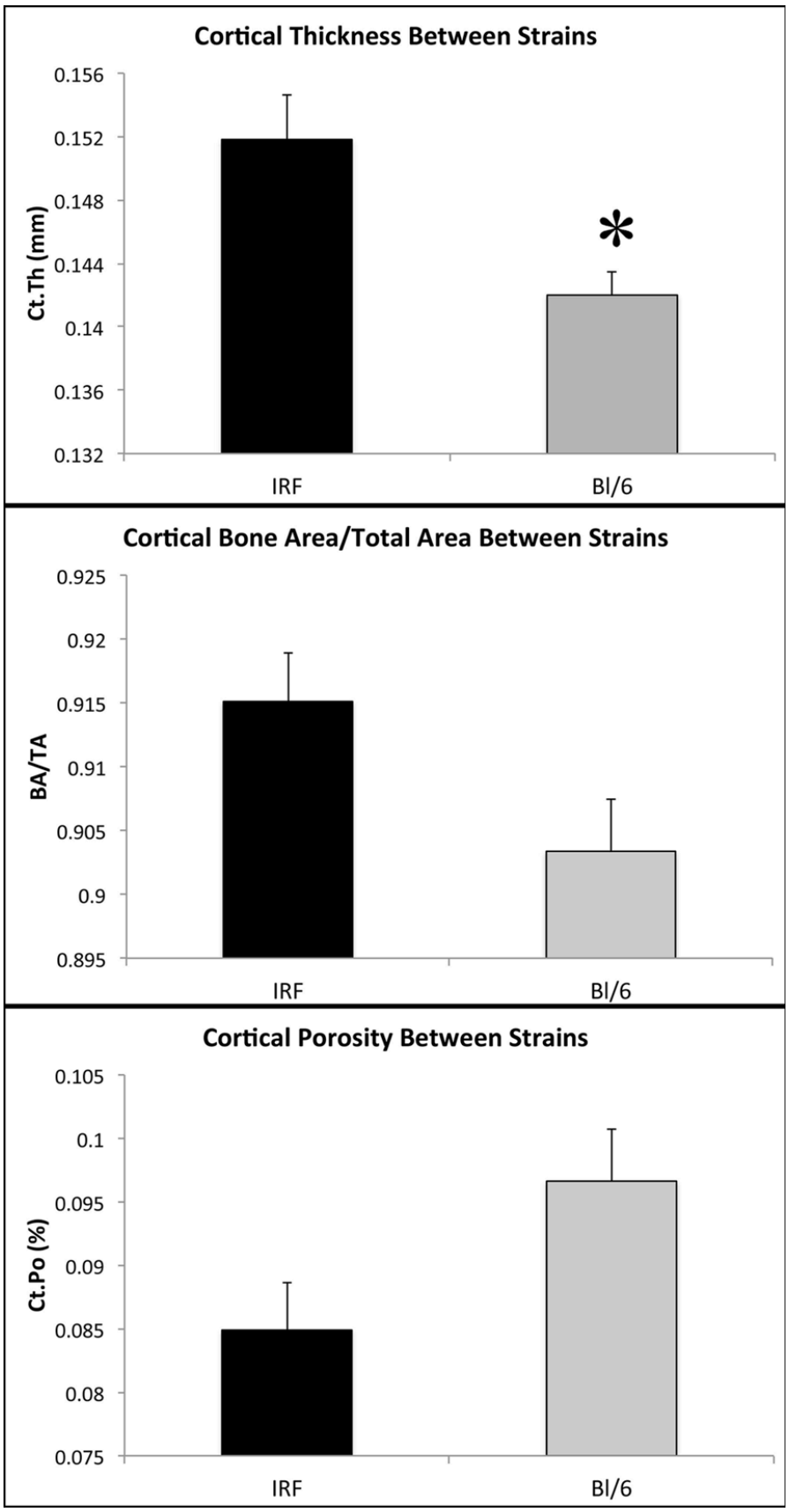

Figure 2.11. Comparison of cortical bone parameters in normal control IRF 3/7 $^{-/-\ -/-}$ and C57BL/6 mice. Specific parameters of interest include cortical bone thickness (Ct.Th), bone area/total area (BA/TA), and porosity (Ct.Po). Mean $\pm$ SEM.

2.4 DISCUSSION

These experiments demonstrated novel pathologic lesions in the bones and joints of two established mouse models of chikungunya virus (CHIKV) infection. To our knowledge, this is the first description of cartilage necrosis associated with CHIKV infection in an adult immunocompetent wild-type animal model, though chondrocyte loss has been recently described in a CCR2 $^{-/-}$ mouse model[129]. Additionally, while the presence of CHIKV RNA has been demonstrated in the periosteum[145], the results from the current experiments are the first to demonstrate consistent periostitis and the presence of periosteal bone proliferation, as well as extensive ischemic bone marrow necrosis associated with CHIKV infection. These novel lesions offer new insights into the pathogenesis of acute, chronic, and fatal CHIKV-associated diseases.

It should be noted that different routes of viral inoculation were used in the two mouse models utilized in these experiments (i.e. intradermal for IRF 3/7 $^{-/- -/-}$ mice and subcutaneous for C57BL/6 mice). Although route of inoculation can have some impact on immunological responses and disease progression, because early pathogenic mechanisms of viral infection and immune responses are not compared between the two mouse strains, this difference in technique is not considered to have significant impact on the importance of the novel lesions described herein. Experiments performed in our laboratory utilizing a subcutaneous route of infection in IRF 3/7 $^{-/- -/-}$ mice have demonstrated similar lesions at 5 DPI and later in both the ipsilateral and contralateral feet to those reported here in intradermally inoculated mice (data not shown). Therefore, the differences in disease manifestations between the two strains are considered to be predominantly a result of the specific mouse strains utilized and their different immunological responses to viral infection, rather than differences in inoculation technique[55,119,145,150]. As a result of dramatically diminished type 1 interferon response, the IRF mice develop a severe fatal form of disease and tissues demonstrate paucicellular, primarily necrotizing changes including severe, widespread fibrinoid vascular necrosis resulting in severe edema and hemorrhage[145,150]. This is in contrast to a histiocytic and lymphocytic inflammatory

response which occurs in the C57BL/6 mice, resulting in a more inflammatory condition and a milder and more protracted from of disease[55,119].

2.4.1 Cartilage – IRF 3/7 $^{-/-\ -/-}$ and C57BL/6 Mice

Early evidence of articular cartilage necrosis associated with CHIKV infection is significant because chondrocytes have limited ability to replicate and repair, therefore this damage is often considered irreversible[10,75,136]. Attempts at cartilage repair consist of proliferation of fibrocartilaginous tissue, which will gradually degenerate over time due to differences in biomechanical properties when compared to normal articular hyaline cartilage[10]. Therefore, if the initial damage to the articular cartilage is severe enough, it is often progressive[75]. Even in the absence of ongoing infection and/or inflammation, these types of lesions can progress as degenerative changes, similar to those seen in osteoarthritis[186].

2.4.2 Periostitis and Periosteal New Bone – C57BL/6 Mice

As previously mentioned, this report is the first to describe periostitis and periosteal bone proliferation associated with CHIKV infection in an animal model. Periostitis has been occasionally described in human cases of CHIKV-associated disease, often affecting the ankles and wrists, and associated with metacarpophalangeal and proximal interphalangeal stiffness[79,138]. Additionally, periostitis accompanied by periosteal bone proliferation associated with tenosynovitis was demonstrated via radiography in a patient with post-CHIKV infection disease[77].

The presence of periostitis with periosteal bone proliferation associated with CHIKV infection may shed some light on the mechanisms involved in the severe polyarthralgia that occurs with CHIKV infection both acutely and chronically. The periosteum contains numerous sympathetic nerves and thus irritation and inflammation result in significant sensation of pain[7]. Because periostitis often manifests as painful limbs, particularly as polyarthralgia/polyarthritis when affecting distal extremities, it can go unrecognized and be misdiagnosed as a myopathy or joint disease, such as rheumatoid arthritis[116]. Additionally, while periosteal bone proliferation can be a reversible process[107,116], some areas can persist. These can remain clinically inapparent, but can also interfere with adjacent tendon

or ligament function resulting in clinical manifestations such as stiffness or discomfort[107]. The current experiments suggest that pain associated with both acute and chronic cases of CHIKV-associated arthralgia may, at least in part, be a result of development of periostitis and periosteal bone proliferation.

2.4.3 Ischemic Necrosis of Bone Marrow – IRF 3/7 $^{-/-\ -/-}$ Mice

Another lesion demonstrated in these experiments that may be relevant in regard to severe and fatal manifestations of CHIKV-associated disease is widespread ischemic necrosis of bone marrow seen in the IRF 3/7 $^{-/-\ -/-}$ mice. Clinically, regardless of the inciting cause, bone marrow necrosis often presents as bone pain (75% of cases) and fever (68.5% cases) in human patients[4,78]. Ischemic bone marrow necrosis can progress to true osteonecrosis that ultimately can result in bone destruction and joint pain[54].

It is currently unknown whether ischemic bone marrow necrosis represents a significant component of severe CHIKV disease in people. This manifestation of disease has not been described in the literature in humans, possibly because bone marrow biopsies and extensive autopsies including evaluation of numerous regions of bone marrow are not commonly performed in severe and fatal cases and/or results of these autopsies may not be reported in the literature. Virus-associated vasculitis has been reported in cases of CHIKV infection in people, therefore, ischemic necrosis of tissues including bone marrow is potentially possible[50,76,139].

2.4.4 Micro-computed Tomography (µCT)

Results of these experiments that are of additional interest include the lack of significant differences in measurements of bone volumes in the virally infected C57BL/6J mice as compared to the negative control mice. It has recently been reported that infection with CHIKV resulted in significant decreases in various bone parameters, including trabecular bone mass and bone volume fraction at 3 DPI, as well as increased osteoclastic activity[35]. However, these findings were not recapitulated in the current experiments. The most likely reason for this is associated with the ages of the animals used in the respective experiments.

In the current experiment, adult, skeletally mature C57BL/6J mice were utilized, as compared to juvenile (25 day old), skeletally immature C57BL/6 mice used in the previously reported experiments[35]. Bone growth, modeling and remodeling dynamics are quite different in juveniles vs. adults and thus alterations in any of these processes can also be very different depending on the age of the individual. In experiments utilizing the juvenile model, the authors stated that there was a decreased width of the growth plates in affected mice, demonstrating potential alterations in bone growth in addition to increased osteoclastic bone resorption[35]. Therefore, the results in the immature mice, in regard to bone dynamics, may not be directly applicable to chikungunya virus disease in adult humans as active bone growth is no longer occurring. However, it is unclear if these alterations might be similar to those occurring in neonatal and juvenile cases of CHIKV infection.

The results of the previous experiments, in conjunction with those of the current experiments suggest it is possible that CHIKV affects bone growth and growth plate function in juveniles and that there is less of an effect on the mechanics of bone remodeling in an adult animal model. Therefore the current experiments may more closely replicate disease in adult patients. While decreased bone volumes were not demonstrated in the current experiments, osteoclastic bone resorption appears to still be a component of disease. Active osteoclasts were demonstrated in the areas of periosteal bone proliferation, affecting both the new woven bone as well as the adjacent existing lamellar cortical bone.

In addition to the analyses performed in regard to CHIKV infection, the normal control IRF 3/7 $^{-/- -/-}$ and wild-type C57BL/6J mice were compared for differences in normal bone structure. The results indicated that there were significant and near-significant differences in the cortical bone between these two strains. This indicates that a thorough analysis and understanding of the normal bone morphology of inbred strains of mice is essential when comparing bony changes, as this may impact results identified or the underlying mechanisms for changes. Other studies have identified significant differences in normal bone morphology and remodeling processes among popular mouse strains, including in both trabecular and cortical bone[17,18,80,118,157,172,176]. The mechanism(s) involved in the

differences in cortical bone between the two strains utilized in the current experiments is unknown, but indicate potential differences in bone growth, modeling and remodeling. Therefore appropriate choice of mouse strain utilized in studies of bone and joint pathology is essential, and a thorough evaluation and characterization of skeletal structure is necessary in all experiments.

A potential drawback of this study is that virus and/or viral antigen was not demonstrated within the tissue sections. Numerous attempts were made to develop an immunohistochemistry protocol using a commercially available anti-chikungunya virus mouse antibody (LifeSpan BioSciences, Inc., Seattle, WA) and Mouse on Mouse peroxidase and fluorescein kits (Vector Laboratories, Burlingame, CA) (data not shown). Unfortunately, background staining or fluorescence including non-specific binding of the secondary antibody was observed in these attempts and could not be diminished to a level at which the authors could be confident in the interpretation of results. However, because established mouse models were utilized in these experiments and lesions were consistent within virally inoculated animals while absent in control animals, the novel lesions described herein are still considered significant.

2.5 CONCLUSIONS

In closing, this study has demonstrated numerous novel findings in bone and joints that may aid in further determination of the pathogenesis of acute, chronic and severe forms of CHIKV-associated disease. The identification of periostitis and periosteal bone proliferation demonstrates a component of disease manifestation that may be under-recognized in human cases. Potentially progressive lesions such as cartilage necrosis and periosteal bone proliferation, and disease manifestations resulting in permanent tissue alterations, such as fibrosis within skeletal muscle and synovium, have demonstrated the utility of these mouse models in future studies focusing on chronic CHIKV-associated disease. These experiments also illustrate the importance of advanced imaging techniques in evaluation of diseases involving bones and joints, as without the use of μCT, the presence of some bony lesions may have been overlooked and certainly the extent of these lesions would not have been fully appreciated.

Currently, the mechanisms involved in the development of cartilage necrosis, periostitis and periosteal bone formation, and ischemic bone marrow necrosis are unknown. Experiments examining the local environment within the joint, including alterations in regulation of cytokine and matrix metalloproteinase production, may help elucidate the mechanisms involved in CHIKV-associated cartilage necrosis. A definitive reason for the consistently affected location of the periosteal bone proliferation is currently unknown, though possibilities could include anatomical structure of the vasculature within this region or variable severity of inflammation in surrounding tissues. Further experiments are required for clarification of the factors involved in periostitis and periosteal bone proliferation and to determine the significance of ischemic bone marrow necrosis associated with CHIKV infection. Additionally, the incorporation of evaluation via radiographs, CT and MRI into clinical studies of patients with acute and chronic CHIKV-associated arthralgia will greatly enhance the current understanding of disease pathogenesis.

CHAPTER 3: CHARACTERIZATION OF CHRONIC JOINT DISEASE ASSOCIATED WITH CHIKUNGUNYA VIRUS INFECTION

3.1 INTRODUCTION

Chikungunya virus is an alphavirus spread predominantly by *Aedes aegypti* and *Ae. albopictus* mosquitoes[184]. The distribution of the virus is subtropical and tropical and it is considered an emerging infectious disease[182]. Recently, the virus spread to the Western Hemisphere and there is an ongoing outbreak affecting 45 countries and territories throughout the Americas and the Caribbean[124]. As of June 3, 2016, there have been almost 2 million reported suspected cases and 284 deaths associated with infection[124]. Because of the presence of competent mosquito vector species in the United States, there is a concern for an outbreak occurring in the near future[99].

Infection results in disease in 95% of people, and consists predominantly of high fever, rash and debilitating polyarthralgia usually lasting for 2 weeks[6]. Additionally, it has been reported that in a certain percentage of people (14.4-87.2%), chronic or relapsing joint disease can occur, lasting months to years after resolution of the acute phase of disease[141]. Unfortunately, due to the lack of an animal model that demonstrates chronic disease, the mechanisms associated with these manifestations are currently unknown[33]. Due to some similarities with rheumatoid arthritis, it has been suggested that initial infection may result in induction of autoimmune disease[6,15]. However, the data currently are lacking to support this hypothesis. Alternatively, others have speculated that persistence of virus or viral antigen may result in ongoing immune stimulation and continued disease[109]**.** In support of this hypothesis, viral RNA has been demonstrated 16 weeks post infection in a mouse model, 90 days in a nonhuman primate model, and 18 months in a human synovial biopsy sample[65,71,93].

In regard to the joint disease that occurs following infection, it has recently been reported that cartilage necrosis, periostitis and periosteal bone proliferation can occur in a mouse model in the weeks following initial infection[60]. Unfortunately, cartilage loss cannot be diagnosed definitively via standard radiographs, and MRI has demonstrated a variable sensitivity for identification of cartilage

degeneration[132]. Therefore, substantial progression of disease may be necessary before cartilage damage is recognized. Additionally, periosteal bone proliferation may be difficult to diagnose by radiographs in early stages, therefore MRI or CT may be more useful for early detection of periostitis and periosteal bone proliferation[94,149]. However, MRI scans are rarely performed during acute stages of chikungunya virus infection, therefore alternative methods for making these diagnoses would be useful. As alterations in bone dynamics, such as increases or decreases in bone resorption can be associated with receptor activator of nuclear factor kappa-B ligand (RANKL) and osteoprotegerin (OPG), these may represent serologic parameters that can be measured and associated with disease manifestations and progressions in a clinical setting[179].

Once the onset of skeletal maturity occurs, bone is in a constant state of remodeling. This includes ongoing bone resorption and bone formation, occurring in a delicate balance to ensure that one pathway does not outweigh the other and bone homeostasis is maintained. RANKL is a ligand found on the surface of osteoblasts and when recognized by the RANK receptor on the surface of osteoclasts, differentiation, proliferation, and activation of osteoclasts is induced[164]. As osteoclasts are the cells responsible for bone resorption, increases in RANKL and subsequent RANKL-RANK interactions, can result in increased bone resorption[85]. To balance this, OPG is a soluble molecule with a similar structure to RANK, and acts as a decoy receptor, binding to RANKL, thus preventing interaction with RANK[61]. Therefore, increased levels of OPG can result in decreased activation of osteoclasts, and subsequent decreases in bone resorption[85]. Perhaps more important than the individual levels of RANKL and OPG, is their ratio to each other. Alterations in the RANKL:OPG ratio can result in an imbalance between these processes, whereby a decrease in ratio favors bone resorption and an increase favors bone protection[171].

Therefore, in disease states that result in either new bone formation or bone resorption, it is possible that significant alterations in serum levels of RANKL, OPG, or both may be detectable. It has been demonstrated that rheumatoid arthritis patients with active synovitis have increased expression of RANKL, decreased expression of OPG, and a subsequently increased RANKL:OPG ratio, and

these expression levels can be predictive of disease progression[45,66,128]. Similarly, serum levels of RANKL and RANKL:OPG ratios can be increased in patients with osteoarthritis, another disease associated with bone loss[128]. Because it has been previously demonstrated that there are alterations in bone and joints associated with CHIKV infection, it is possible that these manifestations may be associated with changes in the serum levels of RANKL and OPG.

Therefore, the goals of the current experiments were as follows: 1) demonstrate that cartilage necrosis and periosteal bone formation can be persistent and progressive lesions in chronic stages of post-CHIKV infection disease, and 2) measure RANKL and OPG levels throughout the disease process to determine their clinical utility for evaluating disease progression in people. We hypothesize that 1) cartilage necrosis and periosteal bone proliferation will progress, resulting in continued cartilage damage and ongoing periostitis in chronic stages of disease, 2) alterations in RANKL, OPG and RANKL:OPG ratio will be associated with alterations in bone, demonstrating utility for clinical diagnosis and monitoring. To evaluate these hypotheses, we utilized an established mouse model of CHIKV infection, an adult C57BL/6 mouse.

3.2 MATERIALS AND METHODS

3.2.1 Virus

A Southeast Asian strain of CHIKV (SVO 476-96) given as a generous gift from the University of Texas Medical Branch World Reference Center for Emerging Viruses and Arboviruses was used for all mouse injections. The source of the virus was a human sample in Northeast Thailand from 1996. The original isolate was passaged twice in LLC-MK2 cells followed by one passage in Vero cells prior to receipt by our laboratory. Subsequently, the virus was passaged an additional time in Vero cells prior to animal injections.

3.2.2 Ethics Statement

The Louisiana State University (LSU) Institutional Animal Care and Use Committee (IACUC) approved all methods of animal housing and experimental methods utilized in this study (LSU IACUC

protocol #15-005, approved in 2015). The LSU IACUC complies with guidelines of the National Institutes of Health's (NIH) Guide for the Care and Use of Laboratory Animals.

3.2.3 Animal Models

For all experiments, C57BL/6J mice (females; >8 weeks of age) obtained from a distributor were used (The Jackson Laboratory, https://www.jax.org/). Throughout the experiments, mice were maintained as groups of 4 to 5 individuals in micro-isolator cages in the LSU SVM BSL3 laboratory and provided with a commercial mouse diet (LabDiet, Land O' Lakes, Inc., St. Louis, MO) and water ad libitum. At the time of viral inoculation, mice were anesthetized with isoflurane and intraperitoneal injection with ketamine (40 mg/kg) and xylazine (2 mg/kg). Once anesthetized, a volume of 10µl of either $2x10^4$ PFU of virus solution or sterile PBS (negative controls) was injected subcutaneously into the caudoventral aspect of the hind foot near the tarsal joint.

During experiments, mice were monitored for clinical signs of disease including, but not limited to lethargy, loss of body weight, joint swelling, and lameness. To minimize pain and suffering throughout the experiment, if mice lost more than 20% of the initial body weight or exhibited signs of distress, they were euthanized. No mice met these criteria requiring early euthanasia during the experiments; so all mice were euthanized at the predetermined timepoints of 30 and 90 days post inoculation (DPI). Euthanasias were performed using CO_2 and subsequent cervical dislocation.

3.2.4 Serology

Prior to euthanasia, mice were anesthetized with isoflurane. Blood samples were obtained via cardiac puncture with a 23-gauge needle and syringe. Blood samples were allowed to clot at room temperature for 20 to 30 minutes. Samples were then centrifuged for 10 minutes at 10000 rpm. Serum samples were subsequently removed using a micropipette, placed in new microcentrifuge tubes, and frozen at -80C prior to performing ELISAs. Additionally, to examine earlier timepoints (14 and 21 DPI), frozen serum samples from 14 mice from previously reported experiments were included in this study. Experimental details for these have been previously reported and are similar to the current experiments[60]. These samples had been processed similarly to those described above

and frozen at -80C prior to performing ELISAs. RANKL and OPG were measured using commercially available ELISA kits following the manufacturer's instructions (Mouse TRANCE (TNFS11) ELISA Kit and Mouse OPG (TNFRSF11B) ELISA Kit, Thermo Scientific™ Pierce™, Waltham, MA, USA).

3.2.5 Microcomputed Tomography (μCT)

After euthanasia, whole mice were fixed for a minimum of 48 hours in 10% neutral buffered formalin. For μCT scanning, intact hindlimbs from all mice were collected. The region of interest for scans was the distal hindlimb from the proximal region of the tuber calcanei to the distal phalanges. Prior to evaluation, specimens were placed in proper holders in 70% ETOH and samples were then scanned by μCT (Scanco model 40; Scanco Medical AG, Basserdorf, Switzerland). Scans were performed in the transverse plane at 55kV, 0.3-second integration time, with a 16 μm resolution. For qualitative evaluation of overall bone morphology utilizing 3D reconstructions, proper thresholds were tested. The appropriate threshold was then utilized throughout the study for all specimens.

3.2.6 Histopathology

After the μCT scans were performed, fixed specimen were processed for histologic evaluation, which included transverse (30DPI) or sagittal (90 DPI) sectioning of the inoculated hind foot followed by decalcification in 10% EDTA for 3-4 weeks. Subsequently, routine processing for histologic evaluation was performed, including dehydration in increasing concentrations of ethanol and paraffin wax embedding. Sections of 4-5 μm thicknesses were adhered to glass slides and routinely stained with hematoxylin and eosin (H&E). For histologic assessment, the entire tissue sections were evaluated for pathologic changes throughout the hind foot, with particular attention paid to skeletal muscle, joints and bones. Additionally, a semi-quantitative Articular Cartilage Structure (ACS) score was determined for each section in the 90 DPI control and virus treatment groups. For consistency, evaluations were performed on the proximal intertarsal joint (articulation of the talus and central tarsal bone) of each mouse. An established ACS scoring system was utilized for these evaluations, as previously described[113]. This system assigns a score of 0 to 12 based on severity of cartilage necrosis, clefting, and area affected. A board-certified veterinary anatomic pathologist performed the

histologic evaluations (BAG). Microscopic evaluations were performed utilizing a Nikon Eclipse Ni-U upright microscope (Nikon Instruments Inc., Melville, New York) with an attached Olympus DP72 microscope digital camera (Olympus Corporation, Tokyo, Japan) for image capture.

3.2.7 Immunohistochemistry

Tissue sections were routinely deparaffinized in xylene and rehydrated in decreasing concentrations of alcohol. An antigen retrieval step was performed using a high temperature citrate-based technique (Vector® Antigen Unmasking Solution, Vector Laboratories, Inc., Burlingame, CA, USA). This was followed by an endogenous peroxidase-blocking step utilizing BLOXALL (Vector Laboratories, Inc., Burlingame, CA, USA). For identification of CHIKV antigen in tissue sections, a primary anti-chikungunya virus rabbit antibody (IBT Bioservices, Gaithersburg, MD, USA), and a commercially available reagent detection kit (ImmPRESS Reagent Anti-Rabbit Ig Peroxidase kit) and a peroxidase substrate kit (ImmPACT DAB Peroxidase Substrate kit) from Vector Laboratories, Inc. (Burlingame, CA, USA) were utilized, following the manufacturers instructions. This was followed by counterstaining with hematoxylin (Vector® Hematoxylin QS, Vector Laboratories, Inc., Burlingame, CA, USA).

3.2.8 Statistics

All statistical analyses were performed using a commercially available statistical software package (IBM SPSS Statistics version 23, IBM Corp., Armonk, New York, USA). For purposes of analyses, 14 and 21 DPI were grouped and analyzed together and 30 and 90 DPI were grouped and analyzed together because these experiments were performed at separate times and had different sample sizes and variances. Data were examined for outliers prior to analyses; any data points that were more than 2.2 interquartile ranges below the first quartile or above the third quartile were considered outliers and were removed prior to analyses. This resulted in the removal of one CHIKV-infected mouse from the 90 DPI treatment group. ANOVAs were then performed on both data groups to determine significances. For ACS scores of 90 DPI mice, a Mann Whitney U analysis was

performed to determine differences in ACS score distribution between the control and virus treatment groups.

3.3 RESULTS

3.3.1 Histology

At 30 DPI, six of six (100%) mice had evidence of ongoing myositis and skeletal muscle regeneration, similar that previously reported at 21 DPI[60]. Five of six mice (83.3%) demonstrated ongoing chronic synovitis characterized by mild synovial hyperplasia and hypertrophy accompanied by inflammatory infiltrates composed predominantly of lymphocytes and fewer macrophages. Similar inflammatory infiltrates were seen within tendon sheaths in six of six mice (100%). In three of six mice (50%) there was evidence of ongoing periosteal disease consisting of mild periosteal hypercellularity and periosteal bone proliferation, similar to that previously reported at 21 DPI (Figure 3.1, A). Rarely, there were also osteoclasts actively resorbing subperiosteal new bone and mature cortical bone. Because histologic samples were sectioned differently (in cross-section) at this timepoint to facilitate thorough evaluation of the periosteal bone, articular cartilage could not be assessed. There were no significant findings in any of the control mice at this timepoint.

At 90 DPI, five of seven mice (71.4%) displayed minimal to mild myofiber dropout with replacement fibrosis. Six of seven mice (85.7%) demonstrated a concurrent ongoing synovitis, while seven of seven mice (100%) exhibited ongoing chronic enthesitis (Figures 3.1, B and C). In all cases, inflammatory infiltrates were composed predominantly of lymphocytes with fewer macrophages and plasma cells, and mild synovial hypertrophy and hyperplasia were present. None of the mice (0%) showed any evidence of periostitis or periosteal bone proliferation. All mice (100%) in both the virus and control groups had some degree of articular cartilage abnormalities, ranging from minimal surface irregularities to full thickness fibrillation and/or clefting of the cartilage. Four of seven mice (57.1%) in the virus group exhibited cartilage clefting as compared to one (14.3%) in the control group (Figure 3.1, D). A Mann Whitney U test demonstrated that the distribution of the ACS scores were significantly higher in the virally infected group (median = 11) as compared to the PBS control group

(median = 4)(p=0.011) indicating more severe cartilage damage associated with viral infection. There were no additional significant findings in any of the control mice at this timepoint.

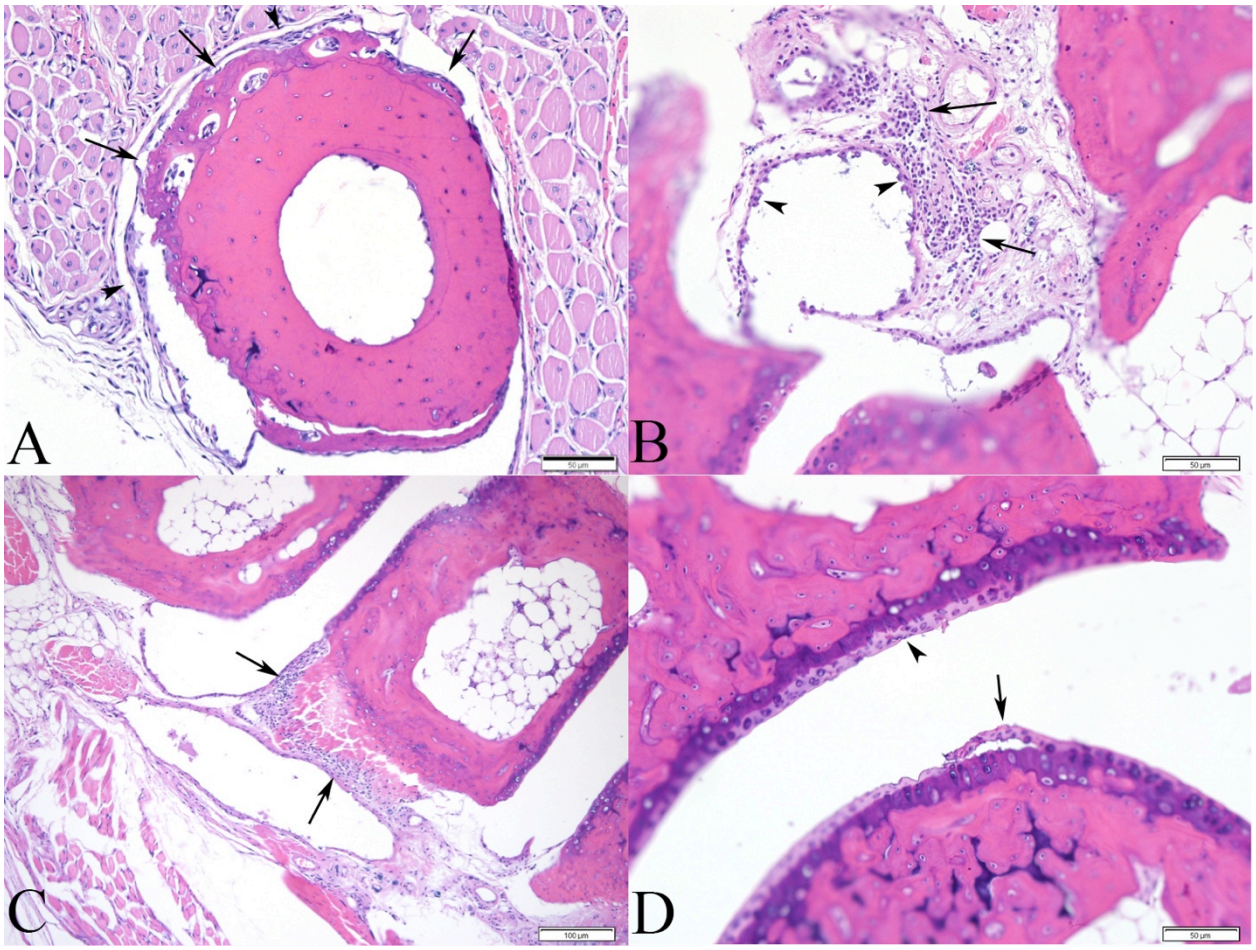

Figure 3.1. Histopathologic lesions of bones and joints in CHIKV infected mice. (A) Metatarsal bone from a 30 DPI CHIKV infected mouse demonstrating periosteal bone proliferation (arrows) and hypercellular periosteum (periostitis) (arrowheads). (B) Synovium from a 90 DPI CHIKV infected mouse demonstrating inflammatory infiltrates in the subintima composed predominantly of lymphocytes and fewer macrophages and plasma cells (synovitis) (arrows) and hypertrophic synoviocytes (arrowheads). (C) Tarsal bone and associated enthesis from a 90 DPI CHIKV infected mouse demonstrating inflammatory infiltrates composed of predominantly lymphocytes and fewer macrophages and plasma cells (enthesitis) (arrows). (D) Proximal intertarsal joint from a 90 DPI CHIKV infected mouse demonstrating ongoing damage to the articular cartilage including surface irregularities (arrowhead) and cartilage clefting with flap formation (arrow).

3.3.2 Immunohistochemistry

The immunohistochemical results were similar at 21, 30, and 90 DPI. Scattered throughout the dermis, there were numerous round to oval immunopositive cells with morphology resembling macrophages and/or dermal fibroblasts (Figure 3.2, A). There were morphologically similar immunopositive cells scattered within regions of inflammation surrounding some tendons, and

throughout the subintima of the synovium, though there was no apparent positivity within the synoviocytes themselves (Figure 3.2, B, C, and D). Rarely, there were also scattered ovoid to fusiform immunopositive cells within the perimysium surrounding skeletal muscle bundles. Due to the quality of the tissue sections, it could not be definitively determined if there was CHIKV antigen present within cartilage, bone or periosteum.

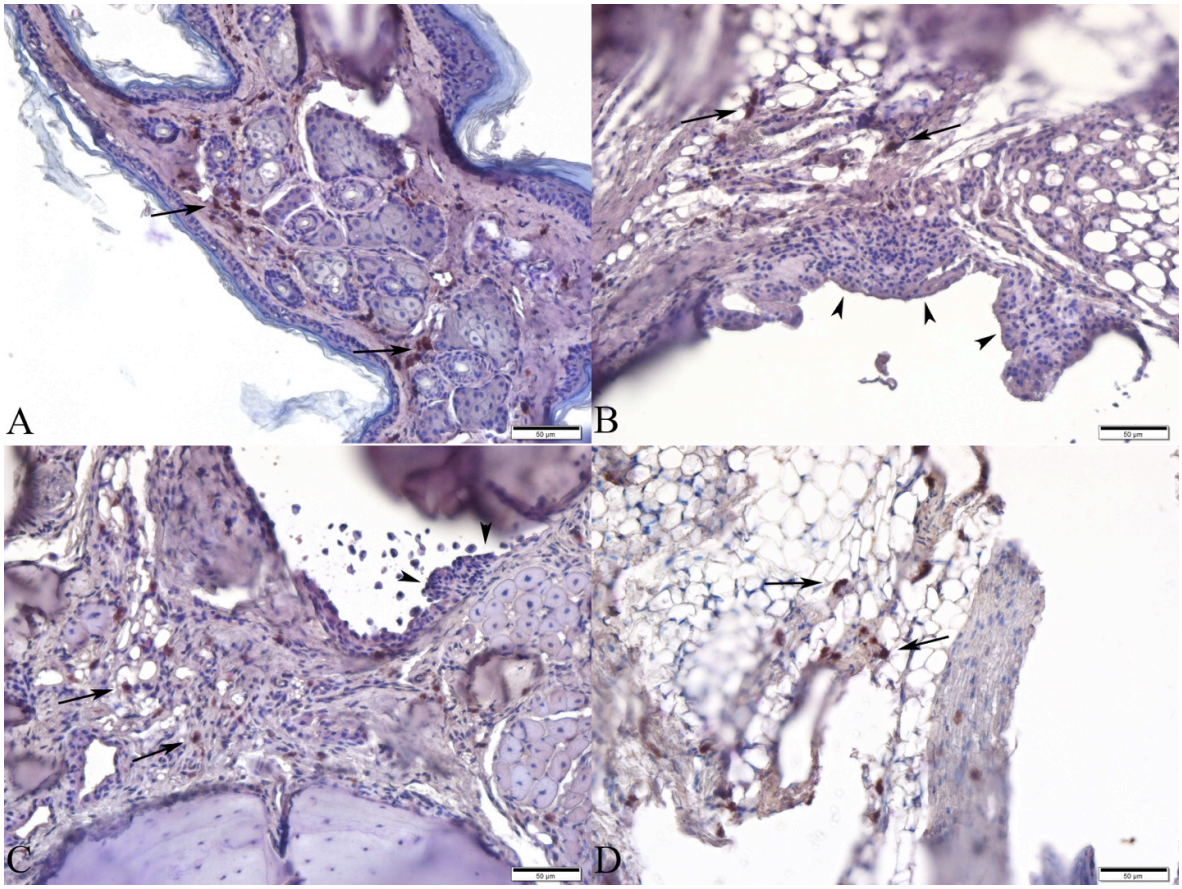

Figure 3.2. Immunohistochemistry for CHIKV antigen on tissue sections. (A) Dermis from a CHIKV infected mouse at 21 DPI. There are numerous immunopositive round to ovoid cells scattered throughout the dermis (arrows), morphology consistent with macrophages and/or dermal fibroblasts. (B and C) Synovium from a CHIKV infected mouse at 21 DPI and 30 DPI, respectively, demonstrating numerous immunopositive round to ovoid cells within the subintima of the synovium (arrows), morphology consistent with macrophages and/or fibroblasts. There is no positivity within the adjacent hyperplastic synoviocytes (arrowheads). (D) Synovium from a CHIKV infected mouse at 90 DPI demonstrating numerous immunopositive round to ovoid cells within the subintima of the synovium (arrows), morphology consistent with macrophages and/or fibroblasts.

3.3.3 Micro-computed Tomography (µCT)

At 30 DPI, there was periosteal new bone proliferation on the distal plantar aspect of the first metatarsal bone (3 out of 6 [50%] of virally infected mice) (Figure 3.3). There was no evidence periosteal bone proliferation present at 90 DPI.

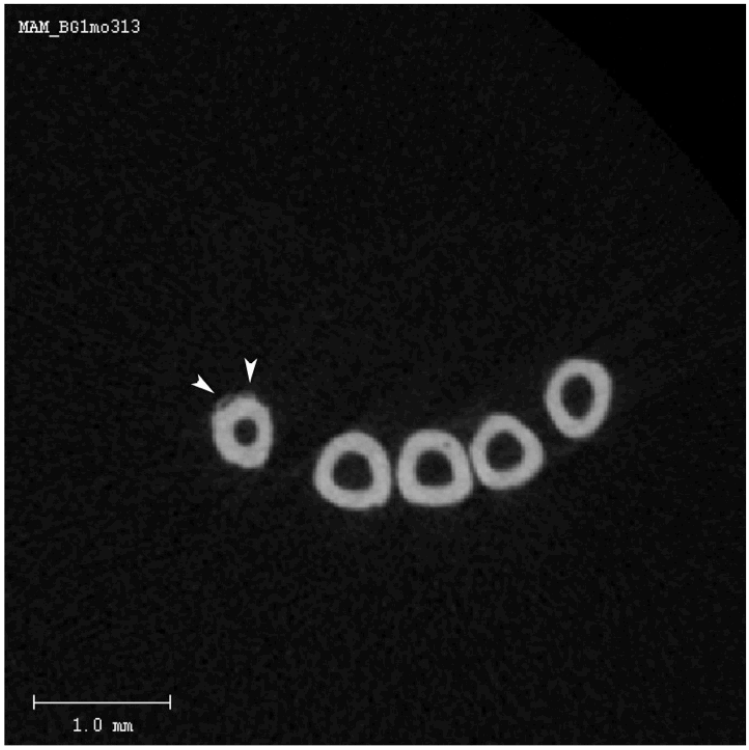

Figure 3.3. 2D slice from μCT scan of the mid-metatarsal region from a 30 DPI CHIKV infected mouse demonstrating region of periosteal bone proliferation (arrowheads) on first metatarsal bone (Mt1).

3.3.4 Serology

At 14 and 21 DPI, there were no significant differences in RANKL, OPG, or RANKL:OPG ratio at any timepoint between the control and virus groups (Figures 3.4, A, C, and E). The RANKL of the 30 DPI control group was significantly higher than the 90 DPI virus group (p=0.002)(Figure 3.4, B). The OPG in the 30 DPI virus group was significantly lower than the 90 DPI virus group (p=0.003) (Figure 3.4, D). The RANKL:OPG ratios of the 30 DPI control and 30 DPI virus groups were both significantly higher than the 90 DPI virus group (p=0.002 and 0.017, respectively)(Figure 3.4, F). Additionally, the ratio of the 90 DPI control group was higher compared to the 90 DPI virus group, and this difference approached significance (p=0.083).

3.4 DISCUSSION

These experiments demonstrated continued and permanent tissue damage at 90 DPI associated with CHIKV infection. Chronic synovitis remains at this timepoint and there is clear permanent damage to the cartilage seen in the majority of mice. However, these experiments also demonstrated that periosteal bone proliferation associated with infection, though present at 30 DPI,

has completely resolved by 90 DPI, indicating that this disease manifestation is reversible. Of additional significance, there are alterations in serum levels of RANKL, OPG, and the RANKL:OPG ratio at later timepoints, demonstrating their potential utility in a clinical setting for evaluation of chronic cases of CHIKV-induced arthralgia.

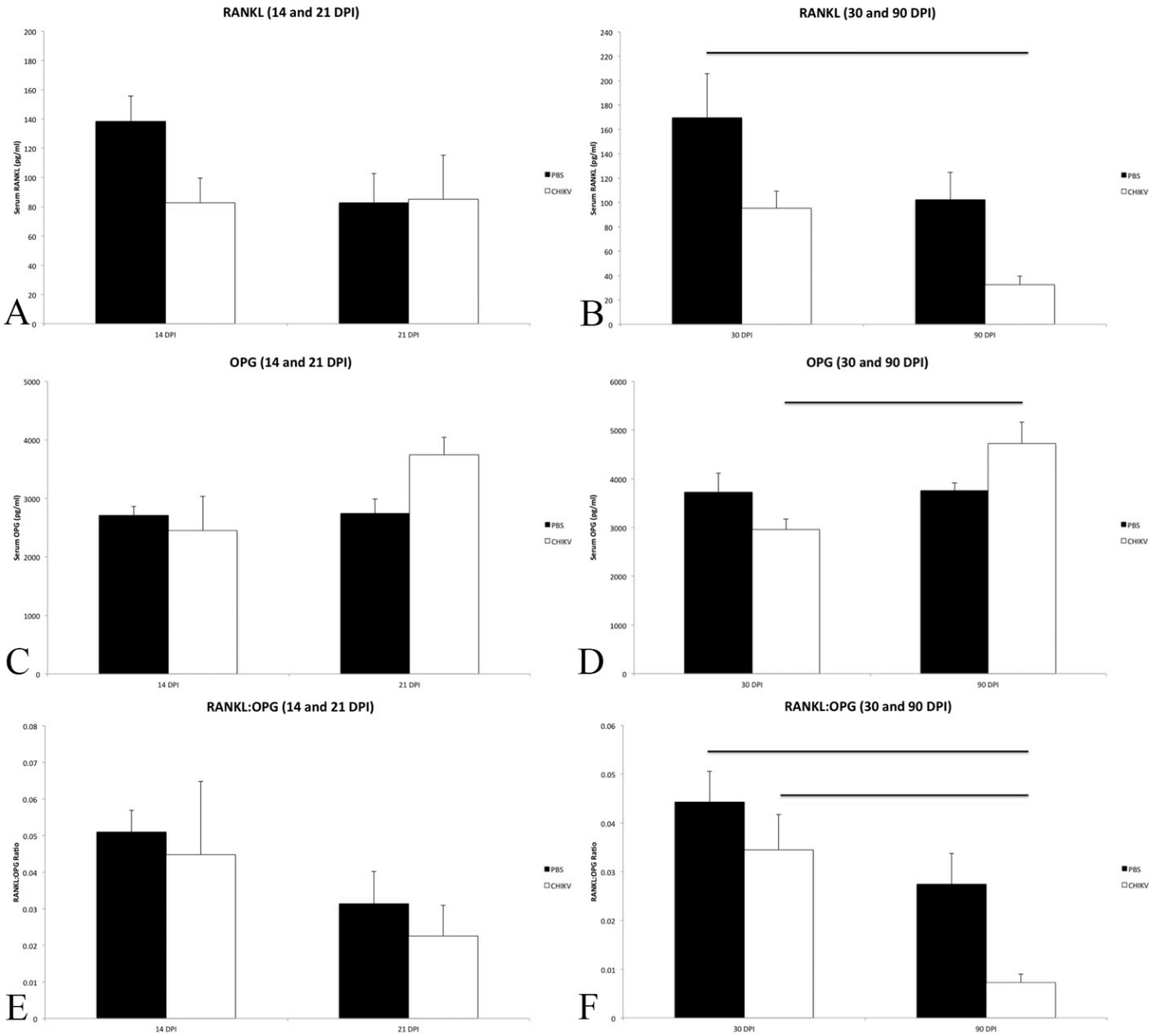

Figure 3.4. Serologic measurements of RANKL, OPG and RANKL:OPG ratio for mice at various timepoints. DPI = days post inoculation, PBS = PBS control mice, CHIKV = chikungunya virus infected mice. Mean ± SEM. Horizontal bars denote significant differences.

Presence of synovitis in chronic stages of post-CHIKV infection-associated disease has been previously reported in a juvenile C57BL/6 mouse model[119]. Caution should be taken when utilizing juvenile animal models for specific purposes of studying diseases associated with bones and joints as

these animals have immature skeletons and thus, alterations may not necessarily reflect disease manifestations in a skeletally mature patient[19]. Therefore, the current studies have confirmed that chronic synovitis also occurs in an adult animal model and are thus relevant for studying bone and joint manifestations associated with chronic CHIKV disease. Additionally, these experiments have demonstrated that there is persistence of viral antigen associated with the ongoing synovitis, demonstrating a potential mechanism for continued joint disease. Although viral persistence has been previously demonstrated in a mouse model[65], the location of virus or viral antigen has not been determined. In the current experiments, viral antigen has been demonstrated in macrophages and/or fibroblasts within the dermis, peritendinous tissues, and the synovial subintima. This corroborates previous evidence that has demonstrated persistence of CHIKV antigen in the synovium of a patient[24] and virus in synovial macrophages in NHPs[93]. The presence of persistent viral antigen and synovitis can be associated with ongoing joint pain and thus demonstrates a potential mechanism for chronic arthralgia seen in some patients[100].

Interestingly, while true synovitis was seen in 85.7% of virus-infected mice, 100% of mice demonstrated chronic enthesitis at 90 DPI. Although chronic CHIKV-associated arthritis has been compared to rheumatoid arthritis due to a number of clinical similarities, enthesitis is not considered a common finding in RA, but rather is more common in some of the spondyloarthropathies which are most often associated with axial skeletal disease such as sacroiliac pain[16,79,146]. Though chronic CHIKV-associated joint disease is most commonly described as affecting joints of the appendicular skeleton, axial pain has been described in 28-32% of cases as well[181]. Therefore, chronic CHIKV-associated arthritis may have a more broad spectrum of clinical presentations than is commonly recognized for cases of autoimmune arthritis such as RA. In fact, in some reports regarding chronic CHIKV-associated arthralgia, patients met the criteria to be diagnosed with various chronic inflammatory rheumatisms, such as rheumatoid arthritis, spondyloarthropathy, and undifferentiated polyarthritis, indicating that this may represent a heterogeneous group of disorders and/or disease manifestations[79]. It should also be noted that the pain associated with enthesitis is considered to be

severe and debilitating, sometimes lasting for years[47], similar to what is described in cases of CHIKV-associated arthralgia. As enthesitis requires advanced imaging such as MRI or ultrasound[112], this may be an underappreciated component of sources of pain and disease in CHIKV patients, particularly in the chronic stages.

Additionally, the finding of continued and progressive cartilage damage at 90 DPI indicates another potential mechanism that may occur in some chronic cases of CHIKV-induced joint disease. While there were cartilage lesions seen in both the control and virally infected groups, the severity of lesions was significantly higher in the virally infected mice. The presence of the cartilage lesions seen in both treatment groups is likely a result of degenerative changes associated with naturally occurring osteoarthritis. At the 90 DPI timepoint, these mice were 24.6 weeks old and C57BL/6 mice are reported to have relatively high incidences of spontaneous development of osteoarthritis, visible by 16 weeks of age[14,110]. Although these degenerative changes were seen in both treatment groups, they were significantly more severe in the virally infected group, suggesting that viral infection may exacerbate these lesions in the articular cartilage. The cartilage degeneration and necrosis that has been previously reported in this mouse model[60] has progressed to more severe disease at 90 DPI including cartilage thinning, fibrillation and necrosis.

Chondrocytes have only minimal abilities to replicate and repair, therefore the lesions described in the current experiments represent irreversible and progressive damage to the articular cartilage[10,75,136]. Additionally, it should be noted that presence of cartilage flaps resulting in full thickness loss of cartilage indicates that alterations in subchondral bone (i.e. sclerosis) will follow[186]. Because there are currently no effective treatments for reversing damage to articular cartilage, this indicates that prevention of this disease manifestation is essential, as the initial cartilage damage occurs during the acute to subacute stages of infection[60].

Conversely, though periosteal bone proliferation can in some instances be a progressive condition[108], the current experiments demonstrated that the bone proliferation seen in this mouse model has completely resolved by 90 DPI. Therefore, while this manifestation may have clinical

significance during the acute phase of disease, continued pain associated with periostitis and periosteal bone proliferation likely does not occur in this model. However, it should be recognized that standard treatment options for pain associated with acute and subacute stages of CHIKV-infection generally rely on the use of NSAIDs, which can often be ineffective for treating pain associated with periostitis and periosteal bone proliferation[161]. Therefore, alternative treatment options may be worth investigating, including bisphosphonates such as pamidronate and zoledronic acid which are often used in cases of severe pain associated with periosteal disease[11,121].

Of additional interest are the RANKL, OPG, and RANKL:OPG ratio results. It has been reported in a juvenile mouse model of CHIKV infection that significant decreases in bone density by 3 DPI and an associated increase in the RANKL:OPG ratio favoring bone resorption occur[35]. However, we have previously reported that significant decreases in bone density do not occur in this adult mouse model of disease[60]. As previously mentioned, care must be taken when using a skeletally immature animal model to study bone and joint disease, as bone dynamics can be quite different in skeletally mature animals. Because significant alterations in bone density do not occur at 14 and 21 DPI, it is not surprising that there was also no alteration in RANKL or OPG at these timepoints.

However, there was a significantly decreased RANKL:OPG ratio at 90 DPI associated with viral infection, as compared to the negative control and the virally infected group at 30 DPI, and a trend towards significance when compared to the negative control group at 90 DPI (Figure 3.3, F). These alterations in serological parameters would result in an overall favoring of bone protection rather than bone resorption. In other words, there would likely be less bone resorption occurring in the virally infected mice at 90 DPI when compared to those at 30 DPI, and to the 30 DPI and 90 DPI control mice.

There are several possible reasons for these alterations at this timepoint in the disease. This could correspond to repairs from the damage done at earlier timepoints. At 21 DPI, we have previously reported osteoclastic bone resorption of both the periosteal new bone and the normal cortical bone[60], which was also observed at 30 DPI. Though bone resorption would be necessary to

resolve the periosteal new bone proliferation, bone formation would also need to occur in order to repair the resorption that occurred in the cortical bone. It would be very interesting to look at additional timepoints between 30 and 90 DPI, because there may be a stage during which bone resorption is favored to resolve the bone proliferation, followed by a shift towards bone protection at a later timepoint, to stop the resorption and favor formation to resolve any damage to the cortical bone.

Additionally, it has been reported that increased levels of OPG and subsequent reduction in the RANKL:OPG ratio have been associated with decreased activation of endosteal osteoclasts, but not periosteal osteoclasts, suggesting that alterations in the RANKL:OPG pathways may not have as strong an impact on periosteal bone resorption[82]. Therefore, it is possible a decreased RANKL:OPG ratio may allow resorption of the periosteal new bone, while protecting against osteoclastic bone resorption within the endocortical space. Further investigations may determine if there is a clinical utility to these alterations in RANKL:OPG ratio. The current experiments indicate that there is a decrease in RANKL:OPG ratio throughout the course of disease, the timing of which coincides with complete resolution of the periosteal bone proliferation. Therefore, it is possible that serum levels of RANKL and OPG could be tracked during acute to subacute stages of disease to determine when these aspects of disease are resolving, thus aiding in treatment decisions.

In addition to examining timepoints between 30 and 90 DPI, future studies should focus on later timepoints to continue tracking and evaluating the ongoing synovitis and cartilage damage. Currently, there are no established animal models of chronic CHIKV-associated joint disease that demonstrate cartilage loss and bony lysis believed to occur in human cases[69,167]. However, the presence of synovitis at 90 DPI, in conjunction with significant cartilage damage and loss, suggests that disease could continue to progress in this mouse model. It would be interesting to examine later timepoints to determine if the synovitis ultimately resolves and evaluate progression of cartilage lesions and potential changes in underlying subchondral bone. If these lesions in fact progress, it is possible that alterations in the subchondral bone such as sclerosis and/or bony lysis could also

occur[95,156]. Therefore, the animal model utilized in the current experiments has potential utility for studying more chronic CHIKV-associated bone and joint disease.

Furthermore, because we have demonstrated persistence of CHIKV antigen associated with synovitis and ongoing cartilage damage, experiments examining mechanisms of the cartilage changes can be performed. Loss of proteoglycans and subsequent cartilage degeneration and necrosis can be a result of ongoing synovitis and production of matrix metalloproteinases (MMP) by synoviocytes[84,154] and some pro-inflammatory cytokines (such as IL-1β and TNF-α)[59,131]. Additionally, chondrocyte apoptosis can be considered a mechanism of cartilage damage[187], and CHIKV has been shown to induce apoptosis in various cell types[46,83,92,180,183]. Therefore, evaluation of local expression of these cytokines and the potential for chondrocyte apoptosis could help elucidate specific mechanisms of cartilage damage associated with CHIKV infection.

In addition, examining serological markers of bone formation such as bone alkaline phosphatase and osteocalcin, or examining alterations in bone morphogenic protein expression would be helpful, particularly at the earlier timepoints when active bone formation is occurring. Serological parameters associated with bone formation could correlate with the periosteal bone proliferation seen at the 3 to 4 week timepoint and thus, could be useful in a clinical setting for early identification of these manifestations of disease.

CHAPTER 4: CHIKUNGUNYA VIRUS INFECTION ALTERS NEW BONE FORMATION ASSOCIATED WITH PROGRESSION OF PRE-EXISTING OSTEOARTHRITIS

4.1 INTRODUCTION

Chikungunya virus (CHIKV) is an RNA virus in the alphavirus group, which includes both the New (encephalitic) and Old (arthritogenic) alphaviruses[126]. It is spread by mosquitoes, predominantly *Aedes aegypti* and *Ae. albopictus*, and can be found throughout tropical and subtropical regions, resulting in potential risk to over 1 billion people[182]. Recently, in October of 2013, an outbreak began in the Caribbean and has subsequently spread throughout Central and South America, resulting in almost 2 million reported suspected cases[124]. This represents the first major outbreak in the western hemisphere and currently affects 45 countries and territories[124]. There have been 3490 reported cases in the United States since the outbreak began, including 12 locally acquired cases in Florida in 2014[29,30]. There were an additional 4912 cases in US territories (Puerto Rico, the US Virgin Islands, and America Samoa), the majorities of which were locally acquired cases[29,30].

The vast majority of people that become infected after a mosquito bite will develop disease, consisting predominantly of high fever, extensive rash and debilitating polyarthralgia, for which the virus was named[6]. Chikungunya is a Tanzanian Makonde word roughly translated as “that which bends upward”, and refers to the extensive joint distortion as a result of severe pain associated with infection[116]. This debilitating polyarthralgia can last for weeks in many people, who are often bedridden as a result. Additionally, in 12-82% of cases, it has been reported that an ongoing or chronic arthralgia and/or arthritis can occur following resolution of the initial acute phase of disease[25,52,151,160,181]. The mechanisms associated with development of these chronic forms of disease are currently unknown. However, it has been recently reported that infection with CHIKV in mouse models of disease can result in cartilage necrosis, periostitis, and periosteal bone proliferation, indicating potential avenues for ongoing joint disease[60]. Additionally, more severe acute arthralgia

and ongoing chronic arthritis associated with CHIKV infection have been correlated with pre-existing joint disease, such as osteoarthritis (OA)[151,160].

It is estimated that 22.7% (52.5 million) of adults in the United states have been diagnosed with OA and nearly half of these have subsequent reduction in mobility or activity[28]. Furthermore, by the year 2030, estimates indicate that 67 million adults (25% of the US population) will have clinically diagnosed arthritis[28]. Thus, OA is a widespread problem in the United States, indicating a very real risk that people infected with CHIKV may have an underlying pre-existing joint disease at the time of infection.

Joint damage, particularly that which involves the articular cartilage, is considered to be irreversible[75]. Therefore, current treatment regimens are centered on alleviating symptoms, rather than repairing current damage or preventing future damage[97,148,189]. As cartilage loss has been demonstrated in both OA and more recently in CHIKV-induced disease[60], a more thorough understanding of the interactions of these diseases is required to prevent severe irreversible damage within the joint. In addition to cartilage necrosis, alterations in bone occur as OA progresses. Changes vary depending on the stage of disease, but can include increases in subchondral bone and formation of periarticular osteophytes[49,74,89]. Some of these changes in bone have been linked to alterations in receptor activator of NF-κB ligand (RANKL) and osteoprotegerin (OPG)[166].

RANKL and OPG are intimately involved in bone homeostasis, specifically in regard to regulating bone resorption. RANKL is expressed on the surface of osteoblasts and when it interacts with RANK on the surfaces of osteoclast precursors, it induces their differentiation, proliferation and activation[164]. In order to regulate this pro-bone resorption pathway, a soluble decoy receptor (OPG) binds to RANKL, blocking its ability to interact with RANK[61]. In some instances of OA, it has been demonstrated that alterations in RANKL and OPG expression within the subchondral bone could result in a shift towards bone formation, rather than bone resorption, and in fact, these alterations in the RANKL:OPG ratio corresponded to increased subchondral bone thickness[166]. Conversely, it has been demonstrated that CHIKV infection can result in increases in the RANKL:OPG ratio which may

favor bone resorption[35]. As a result, there may be conflicting changes in RANKL and OPG associated with CHIKV infection as compared to OA, and the potential interactions between these alterations are unknown.

Therefore, the goals of these experiments were to 1) determine if infection with CHIKV would result in more rapid progression of pre-existing OA, and 2) identify any alterations in RANKL and OPG that may be related to alterations in bone remodeling dynamics and disease manifestations in CHIKV associated disease, OA, and concurrent CHIKV arthritis and OA. We hypothesize that 1) concurrent CHIKV infection will result in more severe cartilage necrosis and synovitis, and alterations in bone formation associated with pre-existing OA, and 2) differences in disease manifestations and severity will be associated with alterations in RANKL and OPG. To address this hypothesis, we utilized an established mouse model of surgically induced OA (destabilization of the medial meniscus surgical technique [DMM]) in a mouse strain also established as a model of CHIKV infection, the C57BL/6 strain[55,57,60,113].

4.2 MATERIALS AND METHODS

4.2.1 Virus

A Southeast Asian strain of CHIKV (SVO 476-96) initially isolated from a human sample in Northeast Thailand in 1996 was utilized for all mouse inoculations. This isolate was given as a generous gift from the University of Texas Medical Branch World Reference Center for Emerging Viruses and Arboviruses. After initial collection, the virus was passaged twice in LLC-MK2 cells and once in Vero cells. After our laboratory received the isolate, the virus was passaged again in Vero cells before utilization in experiments.

4.2.2 Ethics Statement

All animal housing and experimental methods in this study were approved by the Louisiana State University (LSU) Institutional Animal Care and Use Committee (IACUC) (LSU IACUC protocol #15-005 approval in 2015) in compliance with the guidelines of the National Institutes of Health's (NIH) Guide for the Care and Use of Laboratory Animals.

4.2.3 Animal Models

Adult (12 weeks of age), female C57BL/6J mice were obtained from a distributor (The Jackson Laboratory, https://www.jax.org/). Mice were housed in the LSU SVM BSL3 laboratory in micro-isolator cages in groups of 4 to 5 individuals. All mice had ad libitum access to water and a commercial mouse diet (LabDiet, Land O' Lakes, Inc., St. Louis, MO, USA) throughout the experiments.

4.2.3.a Destabilization of the Medial Meniscus (DMM) Surgeries

Immediately prior to surgeries, mice were given subcutaneous injections of gentamicin (5mg/kg, diluted in 0.1ml sterile saline) and carprofen (5mg/kg, diluted in 0.1ml of sterile saline). Mice were subsequently maintained under anesthesia using isoflurane. DMM surgeries were performed on the stifle of the right hindlimb of all DMM mice (virus and controls) as previously described[57]. Briefly, parasagittal skin incisions were made on the craniomedial aspect of the stifle joint, just medial to midline. The patellar ligament was visualized, retracted laterally and the medial meniscal ligament was transected. The joint capsule and skin incision were closed using 5-0 coated VICRYL® (polyglactin 910) suture (Ethicon USA, LLC, Somerville, NJ, USA), followed by closure with a wound clip (BD BBL™ AUTOCLIP wound clips, Becton, Dickinson and Company, Franklin Lakes, NJ, USA). Mice were monitored daily following surgeries; additional gentamicin and carprofen injections were given post-op at 24 and 48 hours, and 12 and 24 hours, respectively. Wound clips were removed 7 days after surgery, though some mice had removed their wound clips prior to this. Previous experiments performed by one of the authors (MAM) have demonstrated that Sham surgeries consisting of surgical incision and routine closures resulted in no significant alterations in the joints; therefore Sham groups in the current experiments only received intra-articular injections (see below).

4.2.3.b Viral Inoculations

Following the DMM surgeries, mice were allowed to recover for a period of 1 week before receiving intra-articular injections. During experiments and prior to viral inoculation, mice were initially anesthetized with isoflurane followed by intraperitoneal injection with ketamine (40 mg/kg) and

xylazine (2 mg/kg). Subsequently, mice were intra-articularly injected in the medial aspect of the right stifle joint with 10µl of either $2x10^4$ PFU of virus solution, sterile PBS (8 week post-DMM negative controls) or Vero cell culture media (4 week post-DMM negative controls). The experiments included the following treatment groups: at the 4 week post-surgery/3 week post-inoculation timepoint, there were 4 treatment groups consisting of virally inoculated and control inoculated mice that had received the DMM surgery (DMM+CHIKV and DMM+Media, respectively), and virally inoculated and control inoculated mice that received no surgery (Sham+CHIKV and Sham+Media, respectively); at the 8 week post-surgery/7 week post-inoculation timepoint, there were 3 treatment groups consisting of virally inoculated and control inoculated mice that had received the DMM surgery (DMM+CHIKV and DMM+PBS, respectively), and virally inoculated mice that received no surgery (Sham+CHIKV).

Throughout the entire experimental timeframes, mice were monitored for clinical signs of disease such as lethargy, lameness, joint swelling, or loss of body weight. If more than 20% of the initial body weight was lost or signs of pain or distress were observed during experiments, mice would be immediately euthanized to minimize pain and suffering. However, none of the mice in these experiments met any of these criteria, therefore all mice were euthanized at the predetermined experimental timepoints (4 weeks and 8 weeks post-surgery/3 and 7 weeks post-inoculation). All mice were euthanized via asphyxiation in a CO_2 chamber, followed by cervical dislocation.

4.2.4 Serology

For blood sample collections, mice were initially anesthetized with isoflurane. Samples were collected via cardiac puncture with a 23-gauge needle and syringe. Mice were then euthanized as described above. Blood samples were transferred to microcentrifuge tubes and allowed to clot at room temperature for 20 to 30 minutes. Subsequently, clotted blood samples were centrifuged for 10 minutes at 10000 rpm, after which serum was removed using a micropipettor and placed in new microcentrifuge tubes. Prior to performing ELISAs, serum samples were frozen and stored at -80C. For analyses, samples were allowed to thaw at room temperature and commercially available ELISA kits for RANKL and OPG were performed, following the manufacturer's instructions (Mouse TRANCE

(TNFS11) ELISA Kit and Mouse OPG (TNFRSF11B) ELISA Kit, Thermo Scientific™ Pierce™, Waltham, MA, USA).

4.2.5 Microcomputed tomography (μCT)

Immediately following euthanasia, mice were fixed in 10% neutral buffered formalin for a minimum of 48 hours. All μCT scans were performed on intact hindlimbs and the region of interest consisted of the stifle joint extending from approximately mid-shaft of the femur to mid-shaft of the tibia and fibula. Hindlimbs were placed in holders in 70% ETOH and scanned using a bench top μCT scanner (Scanco model 40; Scanco Medical AG, Basserdorf, Switzerland). Samples were oriented for scanning in a transverse plane and the following scanning parameters were used: 55kV, 0.3-second integration time, and a resolution of 8 μm.

Prior to analyses, all scans were examined to determine proper thresholds for evaluation of osteophyte and subchondral bone volume (BV) and total volume (TV), and for 3D reconstructions to evaluate overall bone morphology. These thresholds were tested for each specimen and the same thresholds were used throughout the study. Established procedures and nomenclature were used for all variables[16].

4.2.6 Histopathology

After μCT evaluations were performed, the right stifle joints including distal femur and proximal tibia and fibula were decalcified in 10% EDTA. Routine processing for histologic evaluation was performed on all samples. This included dehydration in increasing concentrations of ethanol and embedding in paraffin wax. This was followed by adherence of 4-5 μm thick sections to glass slides and routine staining with hematoxylin and eosin (H&E) for evaluation. Serial sections were also obtained and stained with Safranin O to evaluate articular cartilage. Histologic evaluations were performed by a board-certified veterinary anatomic pathologist (BAG) and an orthopedic researcher experienced in evaluation of osteoarthritic joints (MAM), who were blinded to treatment groups. A Nikon Eclipse Ni-U upright microscope (Nikon Instruments Inc., Melville, New York) was utilized for

microscopic evaluations. An attached Olympus DP72 microscope digital camera (Olympus Corporation, Tokyo, Japan) was utilized for digital image capture.

Presence or absence and severity of synovitis in samples was assessed using a modified version of the grading system described by Krenn *et al*.[90]. Total synovitis scores (TSS) were determined separately for the synovial cells, inflammation and synovial stromal activation. Eight regions of the synovium here evaluated to determine hyperplasia scores (0-3) after which these results were averaged to determine the mean score; the maximum hyperplasia score was also determined (0-3). For inflammation, a score of 0-3 was determined for inflammatory cell infiltrates and a separate score of 0-3 for presence of fibrin and/or fibrinoid necrosis. An additional 0-3 score was determined for synovial stromal activation. All scores were then combined to determine a total synovitis score (0-15). Additionally, histologic assessment included determination of a Safranin-O staining score, as previously described[113]. Histomorphologic assessments were performed on the 8 week post-surgery groups only, using an OsteoMeasure bone histomorphometry system (OsteoMetrics, Atlanta, GA) as previously described[113]. Evaluated parameters included articular cartilage area (AC.Ar) and thickness (AC.Th), subchondral bone area (SCB.Ar) and thickness (SCB.Th), chondrocyte cell death area (CCD.Ar), proportion of dead chondrocytes (CCD/AC), chondrocyte number (Chond#) and area of abaxial osteophytes (Ab.OP).

4.2.7 Statistics

SPSS statistics version 23 was used for all analyses (IBM SPSS Statistics, IBM Corp., Armonk, New York, USA). Data from 4 week and 8 week post-surgery mice were analyzed separately as the experiments were performed at different times and there were slight differences in treatments (i.e. sham inoculations utilized cell culture media for the 4 week groups and sterile PBS for the 8 week groups). ANOVAs were performed for RANKL, OPG, RANKL:OPG ratio, histomorphometry, and μCT data. Kruskal Wallis tests were performed for the Total Synovitis Scores (TSS).

4.3 RESULTS

4.3.1 Serology

4.3.1.a RANKL

At 4 weeks, in the groups that did not undergo the DMM surgery, RANKL was significantly increased in the virally infected mice (Sham+CHIKV) compared to the control group (Sham+Media) (p=0.006), indicating an increase in RANKL associated with viral infection (Figure 4.1, A). However, in the groups that received DMM surgery, there was no significant difference between the virally infected mice and the control group. There was a significant difference between the Sham+CHIKV group and the DMM+Media group (p=0.001). At 8 weeks, there were no significant differences between any of the groups (Figure 4.1, B).

4.3.1.b OPG

At 4 weeks, the only significant result was a lower OPG level in the Sham+CHIKV group as compared to the DMM+Media group (p=0.007) (Figure 4.1, C). Similarly, within the 8-week groups, the Sham+CHIKV group had a significantly lower OPG than the DMM+PBS group (p=0.004) (Figure 4.1, D).

4.3.1.c RANKL:OPG Ratio

At 4 weeks, the RANKL:OPG ratio was significantly higher in the Sham+CHIKV group than in all other groups (vs. Sham+Media, p=0.000; vs. DMM+Media, p=0.000; vs. DMM+CHIKV, p=0.001) (Figure 4.1, E). At 8 weeks, there were no significant differences between any of the groups (Figure 4.1, F).

4.3.2 Histology/Histomorphometry

4.3.2.a Synovium

At 4 weeks, a Kruskal Wallis test indicated that there was a significant difference in distribution of the Total Synovitis scores (TSS) between the three treatment groups (p=0.006). Further pairwise comparisons using the Dunn-Bonferroni approach indicated that the only significant difference in TSS was between the DMM+Media (median = 4.25) and the Sham+Media groups (median = 0)(p=0.013).

At 8 weeks, a Kruskal Wallis test indicated that there was a significant difference in distribution of the TSS between the three treatment groups (p=0.033). Further pairwise comparisons using the Dunn-Bonferroni approach indicated that the difference between Sham+CHIKV (median = 1.06) and DMM+PBS (median = 3.75) groups approached significance (p=0.051).

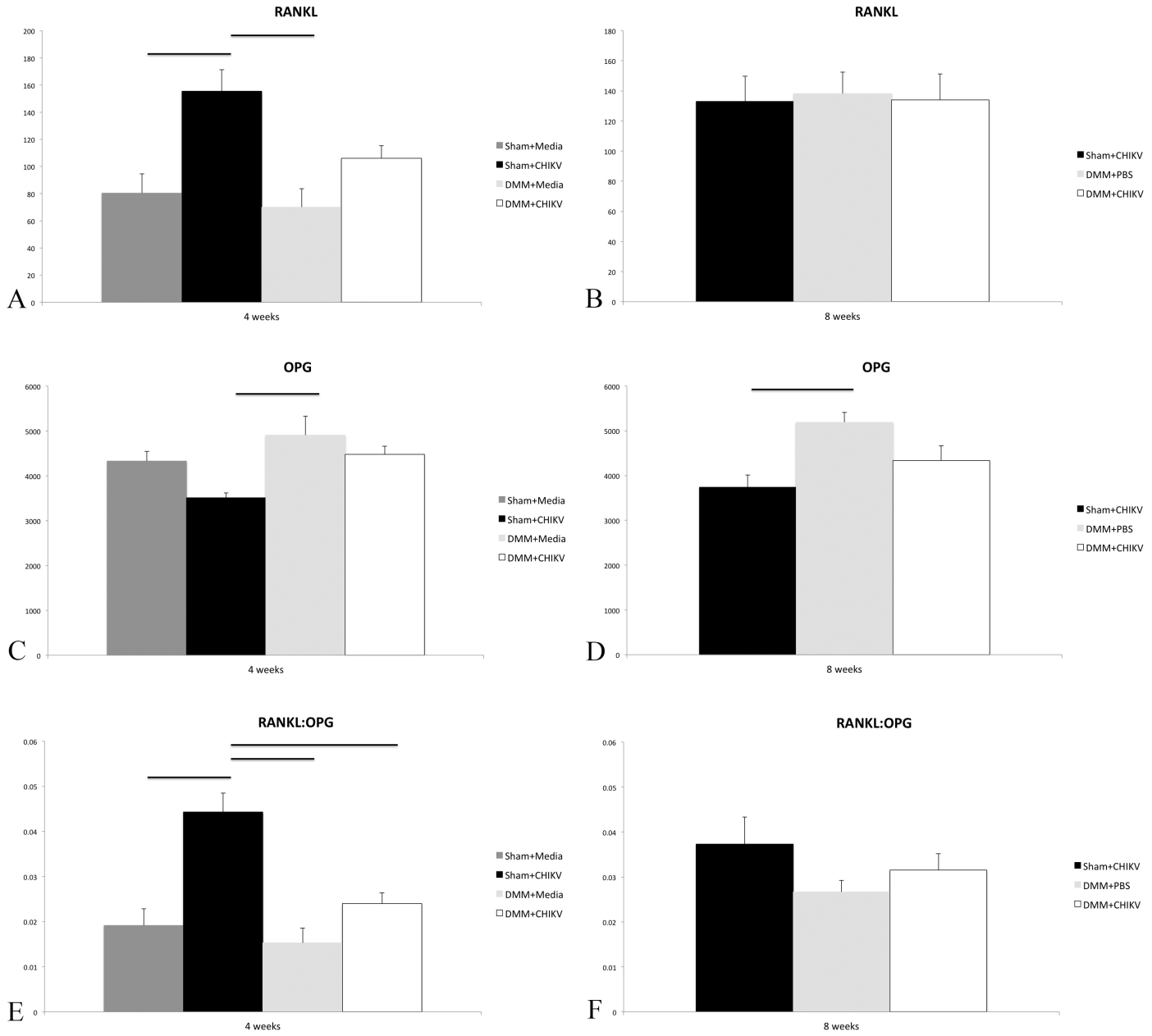

Figure 4.1. Serologic measurements of RANKL, OPG and RANKL:OPG ratio for mice at 4 and 8 weeks post-surgery/3 and 7 weeks post-inoculation. Mean ± SEM. Horizontal bars denote significant differences.

4.3.2.b Articular Cartilage

At 8 weeks post-surgery, both the DMM+CHIKV and the Sham+CHIKV groups had significantly lower AC.Ar than the DMM+PBS group (p=0.027 and p=0.001, respectively) (Figure 4.2, A). Similarly, both the DMM+CHIKV and the Sham+CHIKV groups had significantly lower AC.Th than the DMM+PBS group (p=0.033 and p=0.002, respectively) (Figure 4.2, B).

4.3.2.c Chondrocyte Cell Death

Some degree of cartilage necrosis was histologically apparent in all treatment groups (Figure 4.3, A, C, and E). Both the DMM+PBS and DMM+CHIKV groups had significantly higher CCD.Ar than the Sham+CHIKV group (p=0.000 and p=0.001, respectively) (Figure 4.2, C). Similarly, both the DMM+PBS and DMM+CHIKV groups had significantly higher CCD/AC than the Sham+CHIKV group (p=0.000 and p=0.001, respectively) (Figure 4.2, D).

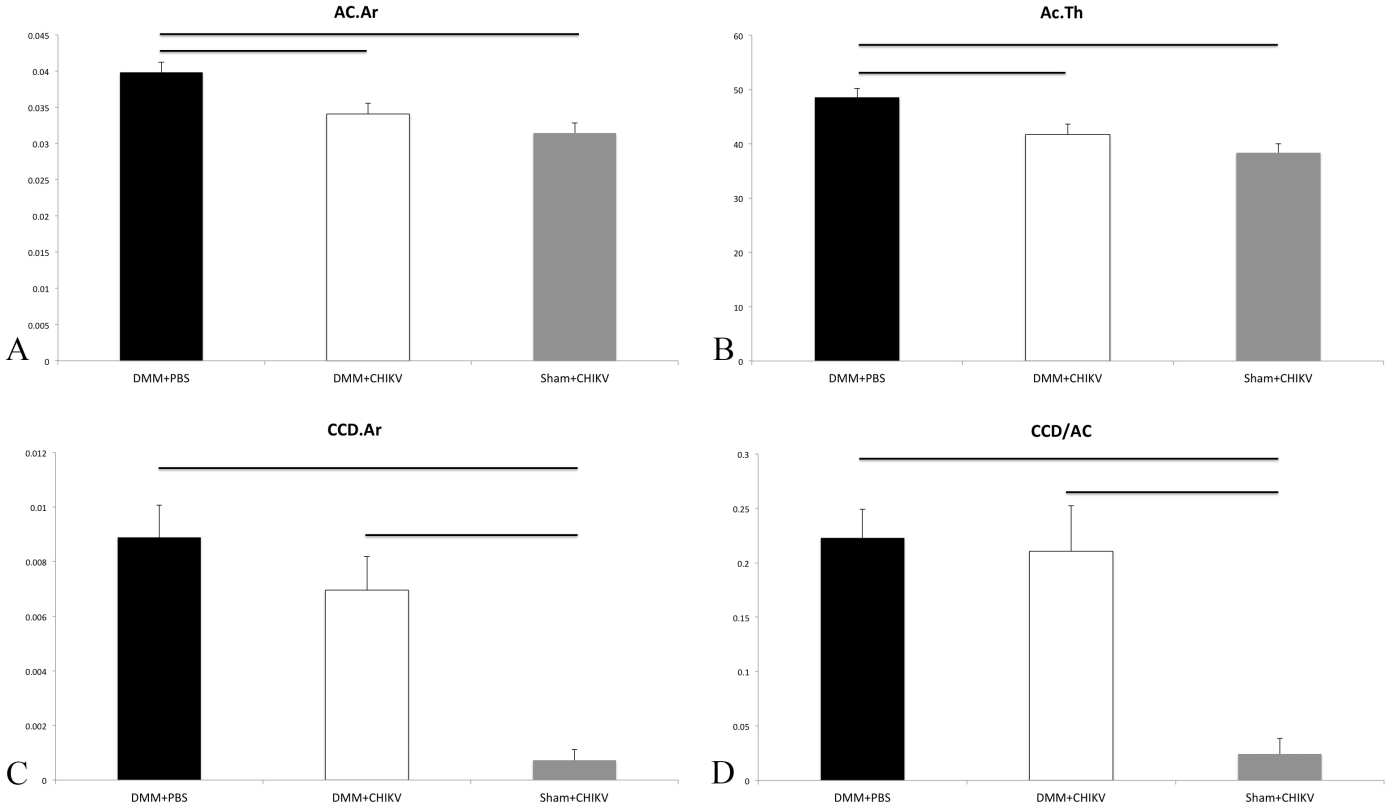

Figure 4.2. Histomorphometry results for articular cartilage measurements at 8 weeks post-surgery/7 weeks post-inoculation, including articular cartilage area (AC.Ar) and thickness (AC.Th), chondrocyte cell death area (CCD.Ar), and proportion of dead chondrocytes (CCD/AC). Mean ± SEM. Horizontal bars denote significant differences.

4.3.2.d ACS and Safranin O Stains

There were no significant differences in the ACS scores between any of the treatment groups. There was a significant difference in the distribution of the Safranin O scores in the medial stifle joint compartment, as indicated by a Kruskal Wallis test (p=0.002). Further pairwise comparisons using the Dunn-Bonferroni approach indicated that the Safranin O scores for the Sham+CHIKV group (median = 0) were significantly lower than those for both the DMM+PBS (median = 10) and DMM+CHIKV (median = 7) groups (p=0.003 and p=0.013, respectively)(Figure 4.3, B, D, and F). There were no significant differences in the distribution of the Safranin O scores in the lateral stifle joint compartment.

4.3.2.e Subchondral Bone

The DMM+CHIKV group had a significantly higher SCB.Ar than the Sham+CHIKV group (p=0.004) (Figure 4.4, A). Similarly, the DMM+CHIKV group had a significantly higher SCB.Th than the Sham+CHIKV group (p=0.001) (Figure 4.4, B).

4.3.2.f Abaxial Osteophytes

Both the DMM+CHIKV and Sham+CHIKV groups had significantly lower Ab.OP than the DMM+PBS group (p=0.043 and p=0.000, respectively) (Figure 4.4, C). Also, the Sham+CHIKV group had a significantly lower Ab.OP than the DMM+CHIKV group (p=0.000).

4.3.3 Microcomputed Tomography (μCT)

4.3.3.a Subchondral Bone

BV was significantly greater in the DMM+PBS group as compared to both the DMM+CHIKV and the Sham+CHIKV groups at 8 weeks post-surgery (p=0.011 and p=0.000, respectively) (Figure 4.5, A). Additionally, tissue density in the DMM+CHIKV group was significantly greater than the Sham+CHIKV group (p = 0.001) (Figure 4.5, B).

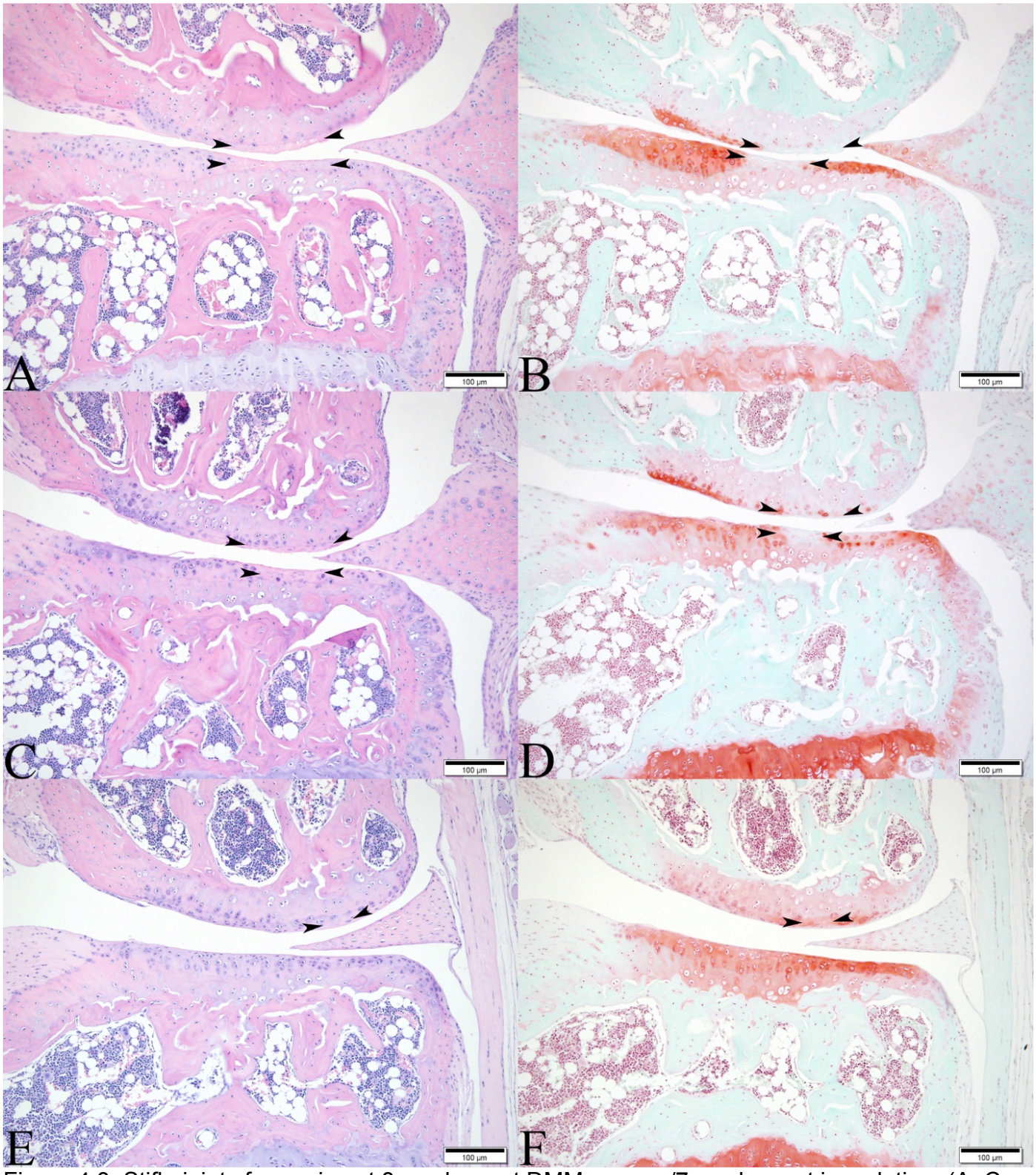

Figure 4.3. Stifle joints from mice at 8 weeks post DMM surgery/7 weeks post inoculation. (A, C, and E) Images demonstrating regions of articular cartilage necrosis bounded by arrowheads (A – DMM+PBS, C – DMM+CHIKV, E – Sham+CHIKV) (H&E). (B, D, and F) Corresponding Safranin O stains from the same mice in A, C, and E, exhibiting decreased uptake of stain indicating loss of proteoglycans (bounded by arrowheads), which correspond with the regions of cartilage necrosis (B – DMM+PBS, D – DMM+CHIKV, F – Sham+CHIKV) (Safranin O).

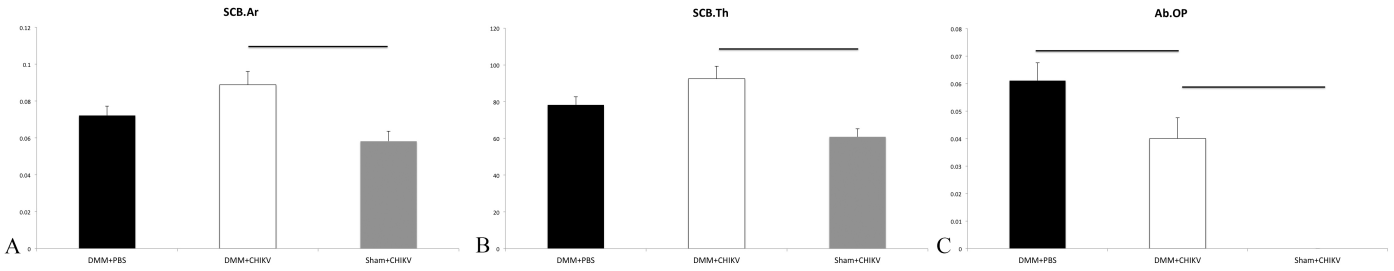

Figure 4.4. Histomorphometry results for subchondral bone and osteophyte measurements at 8 weeks post-surgery/7 weeks post-inoculation, including subchondral bone area (SCB.Ar) and thickness (SCB.Th), and area of abaxial osteophytes (Ab.OP). Mean ± SEM. Horizontal bars denote significant differences.

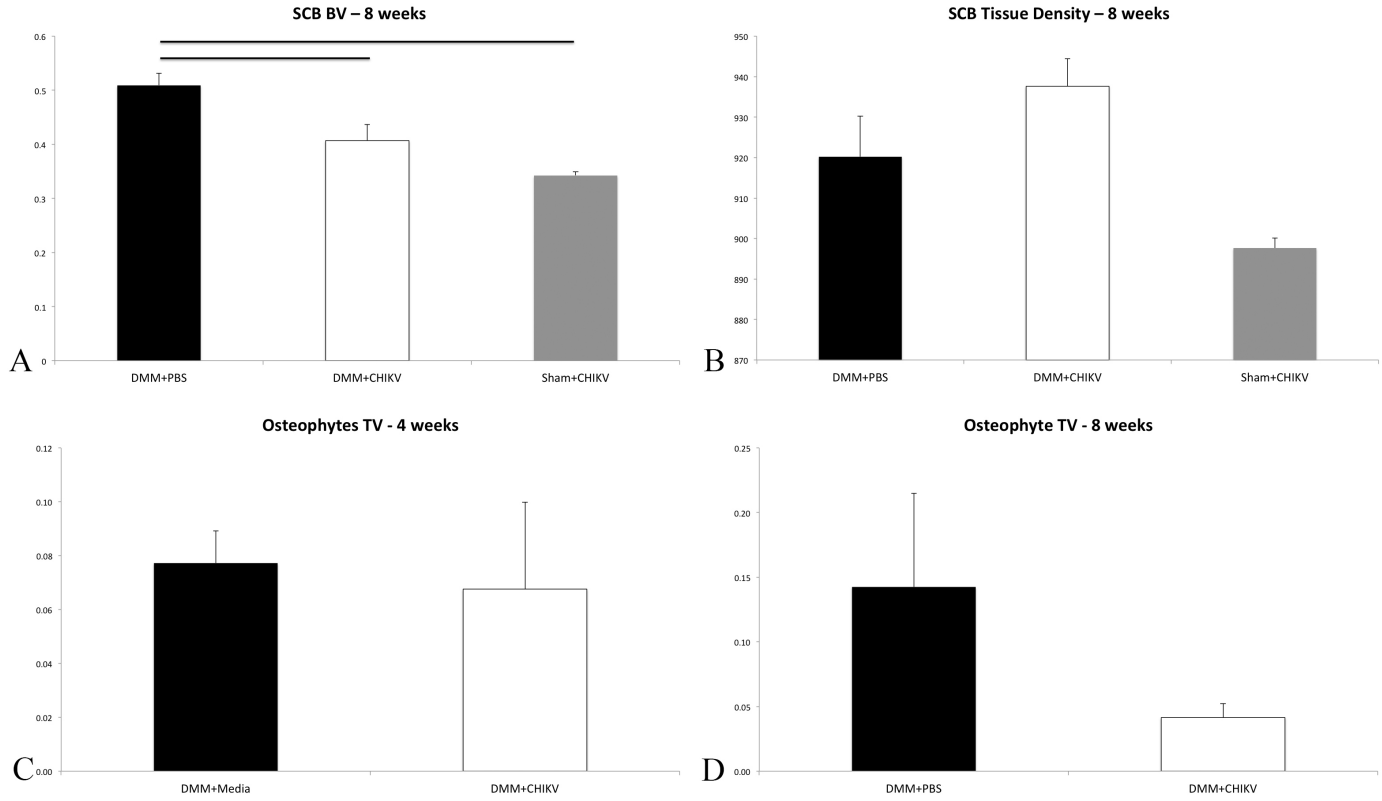

Figure 4.5. µCT results for subchondral bone and osteophyte measurements at 4 weeks post surgery/3 weeks post inoculation and 8 weeks post surgery/7 weeks post inoculation, including total medial + cranial osteophyte volume (Osteophyte TV), total subchondral bone volume (SCB BV), and subchondral bone tissue density (SCB Tissue Density). Mean ± SEM. Horizontal bars denote significant differences.

4.3.3.b Medial + Cranial Osteophytes

There were no significant differences in the combined medial and cranial osteophyte TV between any of the groups at either 4 or 8 weeks (Figure 4.5, C and D). However, subjective evaluation of the 3D reconstructions of stifle joints at 8 weeks post DMM surgery demonstrated more extensive proliferation of new bone in the DMM+PBS as compared to the DMM+CHIKV groups

(Figure 4.6). There was no observable proliferation of osteophytes in the Sham+CHIKV group. There was also clear medial displacement of the medial meniscus in both the DMM+PBS and DMM+CHIKV groups demonstrating successful DMM surgeries, while there was no displacement of the medial meniscus in the Sham+CHIKV group.

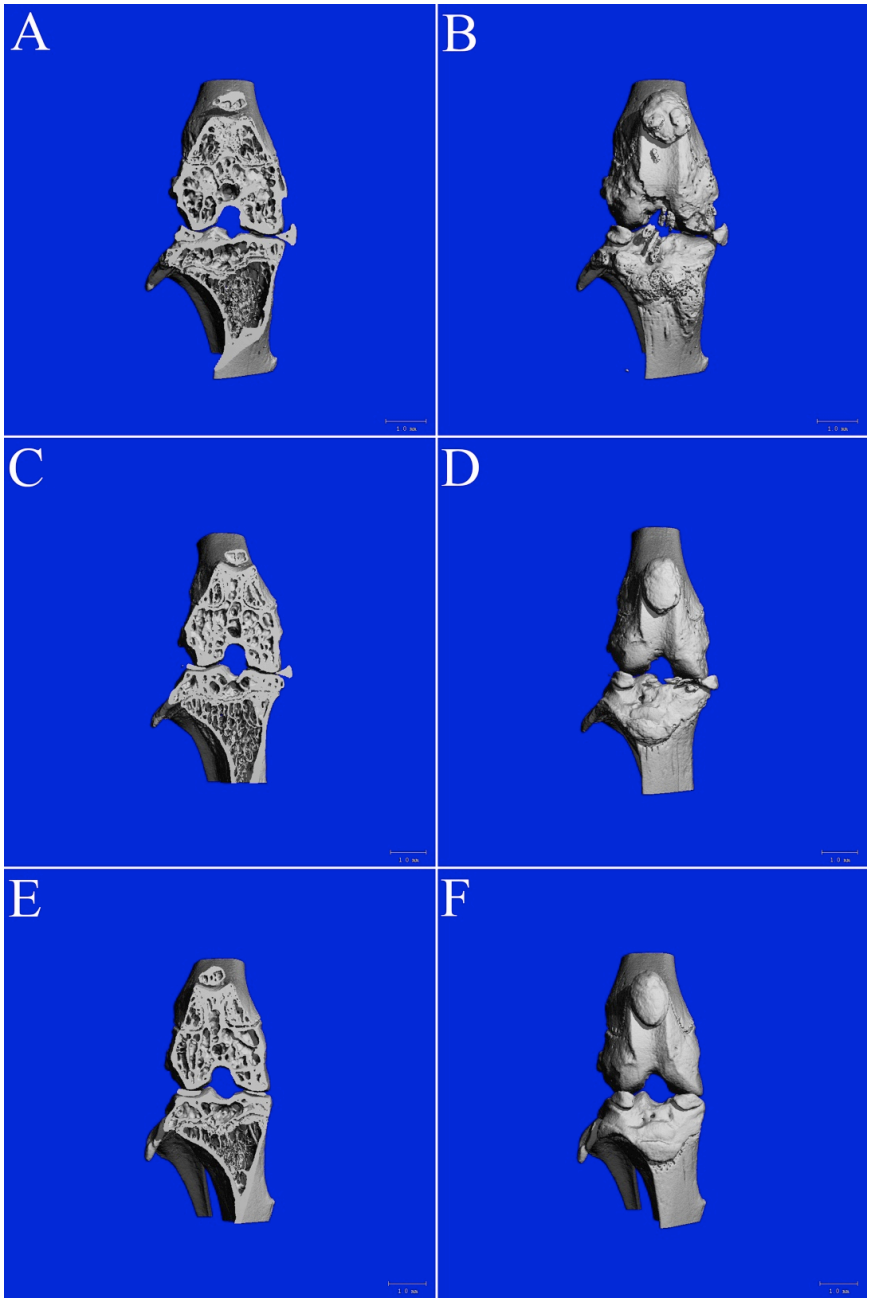

Figure 4.6. µCT 3D reconstructions of stifle joints from mice at 8 weeks post-surgery/7 weeks post-inoculations. (A and B) DMM+PBS group – demonstrating medial displacement of the medial meniscus and proliferative osteophytes, most severe on medial and cranial aspects of the femur and tibia, as well as on the distal aspect of the patella. (C and D) DMM+CHIKV group – demonstrating medial displacement of the medial meniscus and less prominent proliferative osteophytes on medial and cranial aspects of the femur and tibia. (E and F) Sham+CHIKV group – demonstrating no medial displacement of the medial meniscus and no obvious osteophyte proliferation.

4.4 DISCUSSION

4.4.1 Serology

These experiments demonstrated that at 3 weeks post-inoculation, CHIKV infection alone resulted in a significant increase in the RANKL:OPG ratio, as a result of an increase in RANKL and concurrent decrease in OPG. It has been previously reported that CHIKV infection can result in transient increases in RANKL:OPG ratios of protein levels and mRNA expression within infected joints in a mouse model of CHIKV infection; however, serological measurements were not evaluated[35]. Additionally in that study, Chen *et al*. demonstrated a return to normal in mRNA expression by 3 DPI, and it should be noted, that juvenile mice were utilized. As bone modeling dynamics in immature skeletons are much different than bone remodeling in mature skeletons, caution should be taken when interpreting those results[40,169]. However, the current experiments demonstrated that similar alterations in RANKL and OPG can occur at later timepoints post infection in an adult animal model, providing additional supporting evidence that CHIKV infection alters RANKL and OPG and thus, bone remodeling dynamics.

Chen *et al*. also demonstrated significant increases in serum RANKL and RANKL:OPG ratios in human serum samples from people infected with CHIKV; results which were mirrored in the mouse model in the current experiments[35]. It has also been demonstrated *in vitro* that CHIKV can infect human osteoblasts and result in increases in RANKL and decreases in OPG, demonstrating that alterations in bone dynamics may, at least in part, be a direct result of viral infection of osteoblasts[122]. Increases in RANKL:OPG ratio would favor bone resorption over bone protection, consistent with reports that CHIKV infection may result in erosive lesions of bone[103,104].

Interestingly, though results indicated that viral infection alone was associated with an increase in the RANKL:OPG ratio, there was no significant difference between the DMM+Control groups and the DMM+CHIKV groups at either 4 or 8 weeks post-surgery. This suggests that pre-existing OA may suppress or prevent the effects that CHIKV infection has on systemic levels of RANKL and OPG. The mechanism of this is unclear, however, as the pathophysiology of OA includes significant new bone

formation in the form of development of osteophytes and subchondral bone sclerosis[130], a RANKL:OPG ratio that favors bone protection or formation may be a component of disease. Thus, in regard to RANKL:OPG ratios, it seems that the necessity of new bone formation associated with progression of OA outweighs the potential bone resorptive trend associated with CHIKV infection. Unfortunately, the published data regarding OA, RANKL and OPG in humans is limited and sometimes conflicting, in regard to the direction of alteration in the RANKL:OPG ratio[166]. These differences are potentially due to variations in bone dynamics throughout the disease course and the heterogeneity of pathogenesis of OA. Within the DMM surgery groups, though not statistically significant, the mice concurrently infected with CHIKV did have increased RANKL:OPG ratios as compared to their control counterparts. It is possible that larger group sizes for future experiments may help determine if these differences could be significant. Regardless, it seems clear that CHIKV infection can impact RANKL and OPG levels, demonstrating a potential impact on bone dynamics.

It should be noted that it has been previously suggested that serologic RANKL and OPG protein measurements may sometimes be unreliable and not reflect local expression[88]. Therefore future studies examining mRNA and protein expression within the affected tissues could further elucidate the impact of CHIKV on alteration of bone dynamics and clarify some of the discrepancies seen in the current experiments. However, because relatively rapid and inexpensive measurements of serum RANKL and OPG can be performed in a clinical setting, these may be more practical during widespread disease outbreaks. As such, since there is a clear difference in the RANKL:OPG ratios between Sham+CHIKV and DMM+CHIKV animals at the 3-week post infection timepoint, these measurements could be useful in differentiating between CHIKV infection and CHIKV infection with concurrent underlying OA during the acute stages of infection. Advanced imaging techniques are the mainstay for diagnosing OA[132], though these may not be available for patient assessment in some regions affected by CHIKV. The ability to differentiate these disease processes serologically could be useful in a clinical setting as it may guide treatment decisions.

4.4.2 Synovitis

There were no significant differences in Total synovitis scores (TSS) between the DMM+Control groups and the DMM+CHIKV groups at either 4 or 8 weeks post-surgery. However, at 4 weeks there was a significantly higher TSS for the DMM+Media group as compared to the Sham+Media group; at 8 weeks the difference between the DMM+PBS groups and the Sham+Media group approached significance. This may suggest that at these stages of disease, OA results in more significant synovial alterations than CHIKV infection. This is an unexpected finding, because CHIKV is considered to be an inflammatory arthritis, while OA is degenerative and inflammation is generally considered to be secondary[104,166]. Therefore, one might expect that synovitis associated with CHIKV infection be more severe than that associated with OA. However, it is possible that inflammation is more severe in earlier stages of OA, as seen in these experiments, whereas the inflammation associated with CHIKV infection may be subsiding at these same timepoints. Therefore additional timepoints (both earlier and later) should be examined to determine the relationship between inflammation and disease progression for both OA and CHIKV.

4.4.3 Articular Cartilage

CHIKV infection alone resulted in chondrocyte cell death in some mice, consistent with our previously reported results utilizing the footpad injection mouse model, and further demonstrating that CHIKV infection can cause articular cartilage damage during subacute stages of disease[60]. However, OA resulted in more severe chondrocyte necrosis than CHIKV alone, and concurrent CHIKV infection did not cause any increase in chondrocyte death in animals with pre-existing OA, demonstrating that infection does not exacerbate this particular disease manifestation.

The results indicating that both the Sham+CHIKV and DMM+CHIKV groups have smaller articular cartilage area and thickness than those in the DMM+PBS group were the opposite of what was expected. It has been previously demonstrated that OA results in decreased articular cartilage thickness and area as it progresses and generally, these decreases are associated with increased cartilage necrosis[114]. While the differences in area and thickness were statistically significant, the data

only represent differences of approximately 0.007 mm^2 and 7-10 microns, respectively, and therefore may be biologically insignificant and simply represent slight differences in plane of section that happened to coincide with treatment groups.

4.4.4 Osteophytes

Although the μCT analyses did not demonstrate a significant difference in osteophyte volume, the data showed a higher osteophyte volume in the DMM+PBS group as compared to the DMM+CHIKV group. Furthermore, histomorphometry data confirmed that CHIKV infection had a significant impact on osteophyte formation. While CHIKV infection alone does not result in any osteophyte formation at these timepoints, CHIKV infection in an animal with pre-existing OA resulted in significantly smaller osteophytes as compared to mice with OA alone. This suggests that CHIKV infection may have an inhibitory effect on osteophyte bone formation.

When considering these findings in conjunction with the aforementioned alterations in the RANKL:OPG ratio, these results indicate that CHIKV alters RANKL and OPG levels to create an environment which favors bone resorption over bone protection or formation, which ultimately may impact and subsequently decrease the formation of osteophytes at later timepoints. Though this alteration in the RANKL:OPG ratio does not completely prevent the new bone osteophyte formation, it may result in a slight alteration in the balance in the formation-resorption axis, thus slowing the progression of osteophyte formation. Though the serological levels of RANKL and OPG were not significantly different between the DMM+Control and the DMM+CHIKV groups, the RANKL:OPG ratio in the latter was higher than that in the former. Additionally, it is possible that local expression is affected, though not systemically observable. As previously discussed, future studies comparing local mRNA and protein expression may resolve this discrepancy.

4.4.5 Subchondral Bone

The significantly increased subchondral bone area and thickness in the DMM+CHIKV mice compared to the Sham+CHIKV mice indicates that the OA surgery results in an increase in subchondral bone associated with progression of OA. These results are consistent with the current

literature regarding OA pathogenesis, which states that OA results in subchondral bone sclerosis[49,89]. Interestingly, the results from the μCT analyses were slightly different in that the DMM+PBS group had a significantly higher subchondral bone BV than both the DMM+CHIKV and Sham+CHIKV groups. Though the BV of the DMM+CHIKV and Sham+CHIKV did not differ significantly, the DMM+CHIKV group was higher than the Sham+CHIKV group. These data may suggest that while OA results in expected increases in subchondral bone, concurrent infection with CHIKV diminishes the amount of new subchondral bone formed. This suppressive effect on new bone formation is similar to that described above concerning osteophyte bone formation. In regard to measurements of subchondral bone, the μCT results may be considered more accurate than the histomorphometry, as μCT measures 3D total subchondral bone volume, whereas the histomorphometry evaluation measures thickness and area from a single 2D image[16] and only evaluated the medial compartment of the joint.

4.4.6 Clinical Significance

Interestingly, when considering the results of decreased osteophyte formation and subchondral bone sclerosis associated with CHIKV infection in a mouse with pre-existing OA, one might be tempted to conclude that CHIKV infection actually slows the progression of OA rather than exacerbating disease as hypothesized. However, care should be taken when drawing this conclusion. While increases in osteophyte volumes and subchondral bone volume are standard parameters for measuring OA severity, they are not the only factors to consider[74]. In regard to OA pathophysiology, though there is still much controversy regarding underlying mechanisms of disease, cartilage damage and loss is often considered a primary lesion, and subchondral bone sclerosis and osteophyte formation secondary developments which represent the adaptive response of bone to combat the pathologic changes in cartilage loss and joint instability resulting from alterations in load within the joint[49,58]. The articular cartilage and subchondral bone are intimately interconnected from a functional and physiological perspective, and alterations in either can impact the structure and function of the other[95]. In fact, it has been demonstrated that histomorphometric alterations in subchondral bone

directly correlate with cartilage lesion severity[12]. Some studies have also suggested that osteophytes are important in maintaining joint stability in cases of osteoarthritis[58]. Therefore, CHIKV infection may be suppressing the adaptive response of bone to cartilage loss and joint instability by diminishing new bone formation.

Of additional consideration, alterations in subchondral bone and osteophytes do not necessarily correlate with clinically appreciable pain associated with OA. In fact, many studies have found that MRI results such as synovitis, effusion, and cartilage volume/thickness often better correlate with clinical pain[74,96,101]. Studies have also shown that radiological severity of OA, which includes evaluation of subchondral bone changes and osteophytes, often poorly correlate with clinically appreciable pain, particularly in OA involving the knee joint[101]. Some reports have also stated that there is inadequate long-term pain outcomes in patients that underwent knee replacement surgeries, though this procedure should ensure that the structural changes such as osteophyte formation and subchondral bone sclerosis are “cured”[74].

Furthermore, in the current experiments, CHIKV infection had no impact on the progression or severity of cartilage necrosis in cases of pre-existing OA. Additionally, the synovitis scores for OA and OA+CHIKV were similar, indicating that CHIKV infection does not alter this aspect of OA disease at the timepoints examined. As previously stated, presence and severity of synovitis correlates well with clinical assessments of pain[74]. Therefore, at the stage of disease examined in this project, the presence of OA may be more painful than CHIKV alone and higher levels of pain felt by some patients in acute stages of infection may warrant more thorough clinical evaluation including advanced imaging, so that other concurrent arthritic diseases can be ruled out.

When considering all of these findings together, one could conclude that while CHIKV infection does not exacerbate cartilage necrosis and synovitis associated with OA at these timepoints, it does suppress the natural responses of bone aimed at counteracting the effects of these primary lesions. Therefore, one could view the impacts of CHIKV on OA progression as detrimental, because they prevent these responses, and uncouple the cartilage/subchondral bone/osteophyte relationship that

occurs with OA progression. It is unclear at this point what long-term impact these alterations may or may not have on OA progression or clinical presentation. It has been determined that cartilage and subchondral bone changes can have feedback effects on each other, such that as cartilage degenerates, subchondral bone sclerosis occurs, altering the redistribution and absorption of forces, resulting in additional cartilage degeneration[186]. It is currently unclear if the diminished subchondral bone formation associated with concurrent CHIKV infection may impact the progression of cartilage necrosis.

Additionally, in a clinical setting, care should be taken when evaluating patients with concurrent OA and CHIKV-associated joint disease, because the current data demonstrate that CHIKV has a suppressive effect on the secondary changes associated with OA, which are often used to radiologically determine disease severity[20]. In other words, when evaluating patients with both diseases concurrently, standard methods of determining OA disease severity, such as evaluation of osteophytes and subchondral bone, may underestimate the severity of underlying cartilage damage and synovial changes. Of additional importance from a clinical perspective, because CHIKV and OA have opposite effects on bone dynamics (i.e. resorption vs. formation, respectively), care should be taken when utilizing any treatment options that may impact bone dynamics (such as bisphosphonates or RANKL antagonists) in cases of concurrent disease.

In conclusion, CHIKV infection has a significant impact on the progression of pre-existing OA, though not in the way that was hypothesized. CHIKV infection does not result in exacerbation of cartilage necrosis or synovitis associated with the pre-existing disease at the timepoints examined in these experiments. However, in regard to disease manifestations of OA associated with new bone formation, CHIKV has a suppressive effect, which may be associated with alterations in the systemic levels of RANKL and OPG. The long-term implications for these alterations in regard to the continued progression of OA are unclear. Further experiments focusing on later timepoints would help elucidate the effects of these concurrent disease processes. Additionally, examination of local protein and

mRNA expression of RANKL and OPG within affected joints could help further elucidate the impacts of CHIKV infection on bone remodeling dynamics.

CHAPTER 5: SUMMARY AND DISCUSSION

Chikungunya virus (CHIKV) is widespread throughout the tropics and subtropics and subsequently has the potential to affect more than 1 billion people, representing a significant threat to human health and well-being[182]. Infection results in disease in 95% of people, and manifestations consist of high fever, rash and a severe, debilitating polyarthralgia[6,181]. Because current therapies are only supportive, infected people often suffer throughout the acute stage of disease, and as a result, many remain bedridden for 1-3 weeks during the acute stages, resulting in absence from work and lost wages[162]. This results in a significant reduction in quality of life and, in conjunction with the medical expenses associated with diagnostics, therapeutics, and hospitalization, represents a substantial economic impact, on top of the direct health effects[134,162,174]. It has also been reported that in a variable proportion of patients, chronic arthralgia/arthritis may develop in the months to years following resolution of acute symptoms[141]. The mechanisms of this aspect of disease are currently unknown. The research presented in this dissertation focused on elucidating the pathogenesis of bone and joint disease associated with CHIKV infection. The results of this work have advanced the understanding of disease processes and have demonstrated previously un- or under-recognized manifestations.

By using three different mouse models, we have demonstrated in chapters 2, 3, and 4 that CHIKV infection can cause irreversible and progressive cartilage damage. While cartilage necrosis is assumed to occur in human cases of CHIKV-induced arthritis and has recently been demonstrated in an immunodeficient mouse model[129], the extent of these manifestations and their progression had not been previously confirmed or reported. These findings are significant because cartilage necrosis is often considered irreversible[75], demonstrating that early intervention during acute CHIKV disease when these lesions occur is crucial. Also, the progression of these cartilage lesions in subacute or chronic stages of disease, in conjunction with persistent CHIKV antigen within the synovium and other tissues, suggests a mechanism by which at least some of the reported chronic cases of CHIKV-induced joint disease may occur.

In addition, the presence of significant periostitis and periosteal bone proliferation during the 21-30 DPI time periods of disease identifies a novel mechanism for the severe pain manifestations experienced in humans. The periosteum is a highly innervated structure and thus any pathologic disturbances have the potential to result in severe pain[7]. In fact, periostitis and periosteal bone proliferation, which can occur in other diseases such as hypertrophic pulmonary osteoarthropathy, are considered extremely painful and traditional anti-inflammatory and pain management medications, such as NSAIDs, have variable success rates[121]. This may, in part, explain why there is also a variable success rate of NSAID use for pain relief in acute stages of CHIKV disease. Therefore, this finding may suggest that alternative strategies for pain management that focus on alleviation of this manifestation, such as bisphosphonates, may be of benefit[121].

Furthermore, while correlations have been made between pre-existing joint diseases such as osteoarthritis (OA) and more severe CHIKV joint disease, no studies have attempted to examine the interactions between these two diseases. Our research has demonstrated that CHIKV infection and subsequent disease can have a significant impact on manifestations associated with pre-existing OA (Chapter 4). As OA affects 22.7% (52.5 million) of adults in the United States alone, the likelihood that any infected individuals may have subclinical or clinical OA prior to infection is high[28]. Therefore, an understanding of the impact that CHIKV-induced disease may have on pre-existing OA is essential.

The results reported here demonstrate that CHIKV infection results in significant reductions in new bone formation (subchondral bone and osteophytes) that is usually associated with progression of OA. As this new bone formation is often considered a compensatory response to primary cartilage damage and joint instability[49,58], this impact can be considered a detrimental effect on pre-existing disease. Of additional note, cartilage damage cannot be easily assessed in patients with joint disease, therefore progression of these secondary bony changes are often used as indicators of overall disease progression and severity[20]. Because CHIKV has a suppressive effect on these aspects of disease, the ability to monitor disease progression using these manifestations may be impaired. In other words, progression of alterations in subchondral bone and osteophyte proliferation

may underestimate cartilage damage and changes in joint stability in patients that have concurrent OA and CHIKV-associated joint disease.

Of additional importance, we have demonstrated in Chapters 2 and 3 that CHIKV infection results in alterations in the serological parameters RANKL and OPG in two of our mouse models. Furthermore, these alterations are associated with some of the aforementioned changes in bone, such as resolution/reversal of the periosteal bone proliferation seen in the C57BL/6 footpad model, and potentially also with changes in subchondral bone and osteophytes in the OA/CHIKV model. With additional research, the significance of these alterations and their exact correlations with disease manifestations can be elucidated and their potential utility in a clinical setting as disease-monitoring tools can be determined. It is possible that these measurements could be used as surrogates for disease manifestations in bone to assess and track these alterations, so that continued evaluation via advanced imaging might not be necessary.

It should be noted that the use of multiple mouse models in these studies has both positive and negative connotations. Demonstration of some of the similar manifestations in multiple models adds credence to the conclusions that these are important manifestations of CHIKV induced disease, particularly with respect to cartilage damage. However, there are some challenges and drawbacks to each of the models utilized. With respect to the IRF 3/7 $^{-/-\,-/-}$ mice, because CHIKV results in severe, fatal disease within 7 days of infection, this model cannot be used for subacute or chronic studies. Additionally, because this type of severe disease is rare in humans[73], the significance and relevance of some of the manifestations demonstrated, such as widespread vasculitis and ischemic bone marrow necrosis, are unknown. Because full autopsies on fatal cases of CHIKV are rarely performed and/or reported, it is unclear if similar manifestations occur in people in those cases[73].

When considering the C57BL/6 footpad injection mouse model, there are many positives and negatives. Because this model develops more protracted disease similar to that seen in people, and no alterations to the innate or adaptive immune responses have been made in these mice, manifestations in these mice may be more closely mirror those in humans. This model also allows

introduction of the virus via a more natural route, as compared to the intra-articular model (to be discussed below). Furthermore, this model could be easily altered to deliver virus via mosquito, resulting in a completely natural route of infection. Additionally, because adult mice were utilized, as compared to juveniles utilized in other CHIKV studies, the alterations on bone dynamics and joint manifestations as they relate to adult patients with CHIKV disease are likely more accurate. We have also demonstrated progressive cartilage damage, ongoing synovitis, and persistence of viral antigen associated with CHIKV infection in this model, thus demonstrating its potential use in more detailed studies of chronic CHIKV disease.

The biggest drawback to this model lies in the anatomical location of the virus inoculation and the subsequent joints that are examined. Because joint manifestations at sites distant to the injection are inconsistent, only joints of the inoculated foot can be evaluated in detail. These joints are quite challenging to evaluate via histology and obtaining adequate and comparable tissue samples between individuals is extremely challenging. This makes assessment of local changes in the joints, in addition to potential alterations of cytokine expression in the synovium (when assessed by *in situ hybridization*) difficult, if not impossible. Additionally, these small joints have very thin layers of articular cartilage, and are not as similar to human joints as some of the larger mouse joints, such as the stifle. One must also consider that some degree of joint disease was demonstrated in chronic stages, even in the control mice within this cohort, likely as a result of naturally occurring OA. Because these are difficult joints to evaluate and progression of OA has not been extensively studied in this location, interpretation of these findings as they relate to CHIKV infection can be challenging.

The C57BL/6 intra-articular injection model solves some of these problems. The stifle joint is considered much more similar to human joints, and extensive evaluation of these joints has been performed in numerous studies[110,114,169]. Additionally, it is easier to process these tissues for histologic evaluation and ensure that consistent samples are obtained for comparisons. The biggest downside to this model is the somewhat “unnatural” route of inoculation. In order to ensure that viral arthritis occurs in the stifle, the virus has to be directly injected into the joint space, which would not

occur in natural infections. However, intra-articular injection of infectious agents for evaluation of joint manifestations has been utilized for other diseases, particularly in regard to septic arthritis[5,21,81,106,165], and thus should be considered a viable model. Unfortunately, because virus is not injected into the surrounding tissues, some of the manifestations, such as periostitis and periosteal bone proliferation may not occur, as these may require virus outside of the joint space and/or inflammation in the adjacent tissues. As long as these potential drawbacks are recognized prior to experimentation, all of the mouse models utilized in these studies can contribute to the current knowledge regarding CHIKV-induced disease.

To build upon the results presented here and continue to add to the body of CHIKV pathogenesis research, additional experiments can be performed to further elucidate specific mechanisms of disease and their manifestations. Because we have determined that the adult C57BL/6 mouse model demonstrates chronic cartilage damage and synovitis associated with persistence of viral antigen, this model can be utilized for further experiments examining chronic CHIKV-induced disease. While in previous experiments, RT-PCR has demonstrated virus in joint associated tissues of mice and primates 16 weeks and 90 days post-infection, respectively, localization of antigen within the joints themselves was not demonstrated[65,93]. The results presented herein clearly indicate that viral antigen remains within the subintima of the synovium demonstrating a mechanism for ongoing synovitis and joint pain.

In future experiments, the footpad and intra-articular models can be used to further evaluate local expression of cytokines, including RANKL, OPG, and others that are associated with acute inflammation and ongoing joint damage (e.g. IL-1β, IL-6, TNF-alpha, MMPs). This will help determine exact mechanisms of ongoing joint damage and potential avenues for therapeutic intervention. *In vitro* experiments have shown that CHIKV can infect osteoblasts and result in alterations in RANKL and OPG production[122]. Therefore, these mouse models could be used to determine if similar mechanisms occur *in vivo*. Alternatively, or perhaps concurrently, CHIKV could alter RANKL production and osteoclastogenesis via infection of synoviocytes, as has also been demonstrated *in*

vitro[127]. Because of the quality of the tissue sections utilized for IHC in the current experiments, it could not be definitively determined if viral antigen is present within bone, cartilage or periosteum, specifically. By utilizing the intra-articular injection model, with which more consistent and higher quality samples can be procured, these specific tissues can be evaluated for persistence of viral antigen.

While we have shown that CHIKV infection can have a negative impact on pre-existing joint disease such as OA, the long-term effects on disease progression are still unknown. Examination of later timepoints, such as 16 weeks post-surgery, will help further establish the impacts of initial CHIKV infection on OA progression. It is currently unclear how alteration of the compensatory changes in subchondral bone and osteophyte proliferation may affect the overall progression of OA, including ongoing cartilage damage and synovitis.

The current research has demonstrated novel mechanisms of bone and joint disease including potential new sources of pain, which may have consequences for intervention and treatment strategies in cases of CHIKV infection. It has also demonstrated potential mechanisms of continued joint damage, including lending additional support to the hypothesis that persistence of viral antigen plays a role in chronic disease. These are also the first experiments to demonstrate a negative impact of CHIKV infection and subsequent joint disease on pre-existing OA, which could have tremendous importance in disease management regarding the current ongoing and potentially expanding outbreak in the western hemisphere.

While the results presented in this dissertation add to our understanding of CHIKV-associated joint disease, as discussed in Chapter 1, challenges still exist in determining all of the pathogenic mechanisms involved in CHIIKV-associated arthritis, particularly in regard to the use of animal models and chronic disease. To date, no animal models have demonstrated the lesions and progression of chronic disease that has been reported in people[167]. However, it is still unclear whether this is due to inadequacy of the animal models or to the ambiguities surrounding chronic CHIKV-associated arthritis. Although there have been numerous cases of chronic CHIKV-associated

joint disease reported in the literature, none have actually determined a causal relationship with viral infection[79,163]. Rather, these diagnoses were made based on a presence of chronic joint disease and CHIKV infection at some point in the past. None of these reports adequately eliminated pre-existing joint disease at the time of initial infection, and in many cases, did not rule out other causes of chronic joint disease[13,15,160]. In fact, some reports have determined that people diagnosed with chronic CHIKV-associated joint disease meet the requirements to be diagnosed with rheumatoid arthritis, spondyloarthropathy, or other immune-mediated joint disease[79].

While some researchers have stated that this suggests CHIKV infection may result in development of these immune-mediated disease, or that viral persistence is to blame[23,24,65,105], it is highly possible that many of these people could have developed these conditions in the absence of CHIKV infection, or had unrecognized subclinical disease at the time of infection. Thus, what are currently defined as cases of chronic CHIKV-associated arthritis likely represent a heterogeneous group of disorders with varying pathogeneses. When one considers that even a fairly well studied condition such as rheumatoid arthritis is still poorly understood, it becomes clear how difficult determining the potential pathogenesis of chronic CHIKV arthritis is.

Therefore, as we move forward, it is necessary to perform prospective studies in human cases, in which pre-exiting joint disease is ruled out at the initial time of infection via advanced imaging techniques such as MRI, followed by monitoring for development of chronic disease. Additionally, more thorough clinical evaluations during both acute and chronic stages of disease, including synovial fluid analyses and evaluation of synovial biopsies, would help establish any potential relationships between viral infection and development of chronic joint disease. This, coupled with continued use of the animal models described herein will ultimately be necessary to determine the pathogenesis of both acute and chronic disease associated with CHIKV infection.

REFERENCES

1 Ahola, T. *et al.* Therapeutics and vaccines against chikungunya virus. *Vector borne and zoonotic diseases (Larchmont, N.Y.)* **15**, 250-257, doi:10.1089/vbz.2014.1681 (2015).

2 Ajene, A. N., Fischer Walker, C. L. & Black, R. E. Enteric pathogens and reactive arthritis: a systematic review of Campylobacter, salmonella and Shigella-associated reactive arthritis. *Journal of health, population, and nutrition* **31**, 299-307 (2013).

3 Akahata, W. *et al.* A virus-like particle vaccine for epidemic Chikungunya virus protects nonhuman primates against infection. *Nature medicine* **16**, 334-338, doi:10.1038/nm.2105 (2010).

4 Al-Gwaiz, L. A. Bone marrow necrosis. *Annals of Saudi medicine* **17**, 374-376 (1997).

5 Ali, A. *et al.* Antibiotic-killed Staphylococcus aureus induces destructive arthritis in mice. *Arthritis & rheumatology (Hoboken, N.J.)* **67**, 107-116, doi:10.1002/art.38902 (2015).

6 Ali Ou Alla, S. & Combe, B. Arthritis after infection with Chikungunya virus. *Best practice & research. Clinical rheumatology* **25**, 337-346, doi:10.1016/j.berh.2011.03.005 (2011).

7 Allen, M. R., Hock, J. M. & Burr, D. B. Periosteum: biology, regulation, and response to osteoporosis therapies. *Bone* **35**, 1003-1012, doi:10.1016/j.bone.2004.07.014 (2004).

8 Assuncao-Miranda, I., Cruz-Oliveira, C. & Da Poian, A. T. Molecular mechanisms involved in the pathogenesis of alphavirus-induced arthritis. *BioMed research international* **2013**, 973516, doi:10.1155/2013/973516 (2013).

9 Benedict, M. Q., Levine, R. S., Hawley, W. A. & Lounibos, L. P. Spread of the tiger: global risk of invasion by the mosquito Aedes albopictus. *Vector borne and zoonotic diseases (Larchmont, N.Y.)* **7**, 76-85, doi:10.1089/vbz.2006.0562 (2007).

10 Beris, A. E., Lykissas, M. G., Papageorgiou, C. D. & Georgoulis, A. D. Advances in articular cartilage repair. *Injury* **36 Suppl 4**, S14-23, doi:10.1016/j.injury.2005.10.007 (2005).

11 Bernardo, S. G., Emer, J. J., Burnett, M. E. & Gordon, M. Hypertrophic osteoarthropathy presenting as unilateral cellulitis with successful treatment using pamidronate disodium. *The Journal of clinical and aesthetic dermatology* **5**, 37-46 (2012).

12 Bobinac, D., Spanjol, J., Zoricic, S. & Maric, I. Changes in articular cartilage and subchondral bone histomorphometry in osteoarthritic knee joints in humans. *Bone* **32**, 284-290 (2003).

13 Borgherini, G. *et al.* Persistent arthralgia associated with chikungunya virus: a study of 88 adult patients on reunion island. *Clin Infect Dis* **47**, 469-475, doi:10.1086/590003 (2008).

14 Botter, S. M. *et al.* Cartilage damage pattern in relation to subchondral plate thickness in a collagenase-induced model of osteoarthritis. *Osteoarthritis and cartilage / OARS, Osteoarthritis Research Society* **16**, 506-514, doi:10.1016/j.joca.2007.08.005 (2008).

15 Bouquillard, E. & Combe, B. A report of 21 cases of rheumatoid arthritis following Chikungunya fever. A mean follow-up of two years. *Joint Bone Spine* **76**, 654-657, doi:10.1016/j.jbspin.2009.08.005 (2009).

16 Bouxsein, M. L. *et al.* Guidelines for assessment of bone microstructure in rodents using micro-computed tomography. *J Bone Miner Res* **25**, 1468-1486, doi:10.1002/jbmr.141 (2010).

17 Bouxsein, M. L. *et al.* Ovariectomy-induced bone loss varies among inbred strains of mice. *J Bone Miner Res* **20**, 1085-1092, doi:10.1359/jbmr.050307 (2005).

18 Bouxsein, M. L. *et al.* Mapping quantitative trait loci for vertebral trabecular bone volume fraction and microarchitecture in mice. *J Bone Miner Res* **19**, 587-599, doi:10.1359/jbmr.0301255 (2004).

19 Boyce, B. F. & Xing, L. Functions of RANKL/RANK/OPG in bone modeling and remodeling. *Archives of biochemistry and biophysics* **473**, 139-146, doi:10.1016/j.abb.2008.03.018 (2008).

20 Braun, H. J. & Gold, G. E. Diagnosis of osteoarthritis: imaging. *Bone* **51**, 278-288, doi:10.1016/j.bone.2011.11.019 (2012).

21 Bremell, T., Lange, S., Yacoub, A., Ryden, C. & Tarkowski, A. Experimental Staphylococcus aureus arthritis in mice. *Infection and immunity* **59**, 2615-2623 (1991).

22 Brighton, S. W., Prozesky, O. W. & de la Harpe, A. L. Chikungunya virus infection. A retrospective study of 107 cases. *South African medical journal = Suid-Afrikaanse tydskrif vir geneeskunde* **63**, 313-315 (1983).

23 Burt, F., Chen, W. & Mahalingam, S. Chikungunya virus and arthritic disease. *The Lancet. Infectious diseases* **14**, 789-790, doi:10.1016/s1473-3099(14)70869-2 (2014).

24 Burt, F. J., Rolph, M. S., Rulli, N. E., Mahalingam, S. & Heise, M. T. Chikungunya: a re-emerging virus. *Lancet* **379**, 662-671, doi:10.1016/s0140-6736(11)60281-x (2012).

25 Calabrese, L. H. Emerging viral infections and arthritis: the role of the rheumatologist. *Nature clinical practice. Rheumatology* **4**, 2-3, doi:10.1038/ncprheum0679 (2008).

26 Carmona, R. J., Shaikh, S. & Khalidi, N. A. Chikungunya viral polyarthritis. *J Rheumatol* **35**, 935-936 (2008).

27 Cavrini, F. *et al.* Chikungunya: an emerging and spreading arthropod-borne viral disease. *Journal of infection in developing countries* **3**, 744-752 (2009).

28 CDC. Prevalence of doctor-diagnosed arthritis and arthritis-attributable activity limitation--United States, 2010-2012. *MMWR. Morbidity and mortality weekly report* **62**, 869-873 (2013).

29 CDC. *CDC: Chikungunya Virus, 2014 final data for the United States*, <http://www.cdc.gov/chikungunya/geo/united-states-2014.html> (2014).

30 CDC. *CDC: Chikungunya Virus, 2015 final data for the United States*, <https://www.cdc.gov/chikungunya/geo/united-states-2015.html> (2015).

31 CDC. *CDC: National Notifiable Diseases Surveillance System (NNDSS)*, <https://wwwn.cdc.gov/nndss/> (2015).

32 Chaaitanya, I. K. *et al.* Role of proinflammatory cytokines and chemokines in chronic arthropathy in CHIKV infection. *Viral immunology* **24**, 265-271, doi:10.1089/vim.2010.0123 (2011).

33 Chan, Y.-H., Lum, F.-M. & Ng, L. Limitations of Current in Vivo Mouse Models for the Study of Chikungunya Virus Pathogenesis. *Medical Sciences* **3**, 64 (2015).

34 Chen, W. *et al.* Arthritogenic alphaviruses: new insights into arthritis and bone pathology. *Trends Microbiol* **23**, 35-43, doi:10.1016/j.tim.2014.09.005 (2015).

35 Chen, W. *et al.* Bindarit, an inhibitor of monocyte chemotactic protein synthesis, protects against bone loss induced by chikungunya virus infection. *Journal of virology* **89**, 581-593, doi:10.1128/jvi.02034-14 (2015).

36 Chopra, A., Anuradha, V., Ghorpade, R. & Saluja, M. Acute Chikungunya and persistent musculoskeletal pain following the 2006 Indian epidemic: a 2-year prospective rural community study. *Epidemiology and infection* **140**, 842-850, doi:10.1017/s0950268811001300 (2012).

37 Chopra, A. *et al.* Chikungunya virus aches and pains: an emerging challenge. *Arthritis and rheumatism* **58**, 2921-2922, doi:10.1002/art.23753 (2008).

38 Chopra, A., Saluja, M. & Venugopalan, A. Effectiveness of chloroquine and inflammatory cytokine response in patients with early persistent musculoskeletal pain and arthritis following chikungunya virus infection. *Arthritis Rheumatol* **66**, 319-326, doi:10.1002/art.38221 (2014).

39 Chow, A. *et al.* Persistent arthralgia induced by Chikungunya virus infection is associated with interleukin-6 and granulocyte macrophage colony-stimulating factor. *The Journal of infectious diseases* **203**, 149-157, doi:10.1093/infdis/jiq042 (2011).

40 Clarke, B. Normal bone anatomy and physiology. *Clinical journal of the American Society of Nephrology : CJASN* **3 Suppl 3**, S131-139, doi:10.2215/cjn.04151206 (2008).

41 Couderc, T. *et al.* A mouse model for Chikungunya: young age and inefficient type-I interferon signaling are risk factors for severe disease. *PLoS pathogens* **4**, e29, doi:10.1371/journal.ppat.0040029 (2008).

42 Couderc, T. & Lecuit, M. Focus on Chikungunya pathophysiology in human and animal models. *Microbes and infection / Institut Pasteur* **11**, 1197-1205, doi:10.1016/j.micinf.2009.09.002 (2009).

43 Couderc, T. & Lecuit, M. Chikungunya virus pathogenesis: From bedside to bench. *Antiviral research* **121**, 120-131, doi:10.1016/j.antiviral.2015.07.002 (2015).

44 Couturier, E. *et al.* Impaired quality of life after chikungunya virus infection: a 2-year follow-up study. *Rheumatology (Oxford)* **51**, 1315-1322, doi:10.1093/rheumatology/kes015 (2012).

45 Crotti, T. N. *et al.* Receptor activator NF-kappaB ligand (RANKL) expression in synovial tissue from patients with rheumatoid arthritis, spondyloarthropathy, osteoarthritis, and from normal patients: semiquantitative and quantitative analysis. *Annals of the rheumatic diseases* **61**, 1047-1054 (2002).

46 Cruz, D. J. *et al.* Identification of novel compounds inhibiting chikungunya virus-induced cell death by high throughput screening of a kinase inhibitor library. *PLoS neglected tropical diseases* **7**, e2471, doi:10.1371/journal.pntd.0002471 (2013).

47 D'Agostino, M. A. & Olivieri, I. Enthesitis. *Best practice & research. Clinical rheumatology* **20**, 473-486, doi:10.1016/j.berh.2006.03.007 (2006).

48 Dagley, A. *et al.* Protection against Chikungunya virus induced arthralgia following prophylactic treatment with adenovirus vectored interferon (mDEF201). *Antiviral research* **108c**, 1-9, doi:10.1016/j.antiviral.2014.05.004 (2014).

49 Das, S. K. & Farooqi, A. Osteoarthritis. *Best practice & research. Clinical rheumatology* **22**, 657-675, doi:10.1016/j.berh.2008.07.002 (2008).

50 Das, T. *et al.* Chikungunya fever: CNS infection and pathologies of a re-emerging arbovirus. *Progress in neurobiology* **91**, 121-129, doi:10.1016/j.pneurobio.2009.12.006 (2010).

51 Delogu, L. G., Deidda, S., Delitala, G. & Manetti, R. Infectious diseases and autoimmunity. *Journal of infection in developing countries* **5**, 679-687 (2011).

52 Dupuis-Maguiraga, L. *et al.* Chikungunya disease: infection-associated markers from the acute to the chronic phase of arbovirus-induced arthralgia. *PLoS neglected tropical diseases* **6**, e1446, doi:10.1371/journal.pntd.0001446 (2012).

53 Foissac, M., Javelle, E., Ray, S., Guerin, B. & Simon, F. Post-Chikungunya rheumatoid arthritis, Saint Martin. *Emerg Infect Dis* **21**, 530-532, doi:10.3201/eid2103.141397 (2015).

54 Fondi, C. & Franchi, A. Definition of bone necrosis by the pathologist. *Clinical cases in mineral and bone metabolism : the official journal of the Italian Society of Osteoporosis, Mineral Metabolism, and Skeletal Diseases* **4**, 21-26 (2007).

55 Gardner, J. *et al.* Chikungunya virus arthritis in adult wild-type mice. *Journal of virology* **84**, 8021-8032, doi:10.1128/jvi.02603-09 (2010).

56 Gerardin, P. *et al.* Predictors of Chikungunya rheumatism: a prognostic survey ancillary to the TELECHIK cohort study. *Arthritis research & therapy* **15**, R9, doi:10.1186/ar4137 (2013).

57 Glasson, S. S., Blanchet, T. J. & Morris, E. A. The surgical destabilization of the medial meniscus (DMM) model of osteoarthritis in the 129/SvEv mouse. *Osteoarthritis and cartilage / OARS, Osteoarthritis Research Society* **15**, 1061-1069, doi:10.1016/j.joca.2007.03.006 (2007).

58 Goldring, M. B. & Goldring, S. R. Articular cartilage and subchondral bone in the pathogenesis of osteoarthritis. *Annals of the New York Academy of Sciences* **1192**, 230-237, doi:10.1111/j.1749-6632.2009.05240.x (2010).

59 Goldring, S. R. Pathogenesis of bone and cartilage destruction in rheumatoid arthritis. *Rheumatology (Oxford)* **42 Suppl 2**, ii11-16, doi:10.1093/rheumatology/keg327 (2003).

60 Goupil, B. A. *et al.* Novel Lesions of Bones and Joints Associated with Chikungunya Virus Infection in Two Mouse Models of Disease: New Insights into Disease Pathogenesis. *PloS one* **11**, e0155243, doi:10.1371/journal.pone.0155243 (2016).

61 Grimaud, E. *et al.* Receptor activator of nuclear factor kappaB ligand (RANKL)/osteoprotegerin (OPG) ratio is increased in severe osteolysis. *The American journal of pathology* **163**, 2021-2031 (2003).

62 Hallengard, D. *et al.* Novel attenuated Chikungunya vaccine candidates elicit protective immunity in C57BL/6 mice. *Journal of virology* **88**, 2858-2866, doi:10.1128/jvi.03453-13 (2014).

63 Harrus, S. & Baneth, G. Drivers for the emergence and re-emergence of vector-borne protozoal and bacterial diseases. *Int J Parasitol* **35**, 1309-1318, doi:10.1016/j.ijpara.2005.06.005 (2005).

64 Hassan, R. *et al.* Chikungunya - an emerging infection in Bangladesh: a case series. *J Med Case Rep* **8**, 67, doi:10.1186/1752-1947-8-67 (2014).

65 Hawman, D. W. *et al.* Chronic joint disease caused by persistent Chikungunya virus infection is controlled by the adaptive immune response. *Journal of virology* **87**, 13878-13888, doi:10.1128/jvi.02666-13 (2013).

66 Haynes, D. R. *et al.* Osteoprotegerin expression in synovial tissue from patients with rheumatoid arthritis, spondyloarthropathies and osteoarthritis and normal controls. *Rheumatology (Oxford, England)* **42**, 123-134 (2003).

67 Heise, M. T., Simpson, D. A. & Johnston, R. E. Sindbis-group alphavirus replication in periosteum and endosteum of long bones in adult mice. *Journal of virology* **74**, 9294-9299 (2000).

68 Her, Z. *et al.* Active infection of human blood monocytes by Chikungunya virus triggers an innate immune response. *Journal of immunology (Baltimore, Md. : 1950)* **184**, 5903-5913, doi:10.4049/jimmunol.0904181 (2010).

69 Herrero, L. J. *et al.* Pentosan Polysulfate: a Novel Glycosaminoglycan-Like Molecule for Effective Treatment of Alphavirus-Induced Cartilage Destruction and Inflammatory Disease. *Journal of virology* **89**, 8063-8076, doi:10.1128/jvi.00224-15 (2015).

70 Higgs, S. & Ziegler, S. A. A nonhuman primate model of chikungunya disease. *The Journal of clinical investigation* **120**, 657-660, doi:10.1172/jci42392 (2010).

71 Hoarau, J. J. *et al.* Persistent chronic inflammation and infection by Chikungunya arthritogenic alphavirus in spite of a robust host immune response. *Journal of immunology (Baltimore, Md. : 1950)* **184**, 5914-5927, doi:10.4049/jimmunol.0900255 (2010).

72 Hodgson, R. J., O'Connor, P. J. & Grainger, A. J. Tendon and ligament imaging. *Br J Radiol* **85**, 1157-1172, doi:10.1259/bjr/34786470 (2012).

73 Hoz, J. M. *et al.* Fatal cases of Chikungunya virus infection in Colombia: Diagnostic and treatment challenges. *Journal of clinical virology : the official publication of the Pan American Society for Clinical Virology* **69**, 27-29, doi:10.1016/j.jcv.2015.05.021 (2015).

74 Hunter, D. J., Guermazi, A., Roemer, F., Zhang, Y. & Neogi, T. Structural correlates of pain in joints with osteoarthritis. *Osteoarthritis and cartilage / OARS, Osteoarthritis Research Society* **21**, 1170-1178, doi:10.1016/j.joca.2013.05.017 (2013).

75 Hunziker, E. B., Lippuner, K., Keel, M. J. & Shintani, N. An educational review of cartilage repair: precepts & practice--myths & misconceptions--progress & prospects. *Osteoarthritis Cartilage* **23**, 334-350, doi:10.1016/j.joca.2014.12.011 (2015).

76 Inamadar, A. C., Palit, A., Sampagavi, V. V., Raghunath, S. & Deshmukh, N. S. Cutaneous manifestations of chikungunya fever: observations made during a recent outbreak in south India. *International journal of dermatology* **47**, 154-159, doi:10.1111/j.1365-4632.2008.03478.x (2008).

77 Jaffar-Bandjee, M. C. *et al.* Chikungunya virus takes centre stage in virally induced arthritis: possible cellular and molecular mechanisms to pathogenesis. *Microbes and infection / Institut Pasteur* **11**, 1206-1218, doi:10.1016/j.micinf.2009.10.001 (2009).

78 Janssens, A. M., Offner, F. C. & Van Hove, W. Z. Bone marrow necrosis. *Cancer* **88**, 1769-1780 (2000).

79 Javelle, E. *et al.* Specific management of post-chikungunya rheumatic disorders: a retrospective study of 159 cases in Reunion Island from 2006-2012. *PLoS neglected tropical diseases* **9**, e0003603, doi:10.1371/journal.pntd.0003603 (2015).

80 Jepsen, K. J., Akkus, O. J., Majeska, R. J. & Nadeau, J. H. Hierarchical relationship between bone traits and mechanical properties in inbred mice. *Mammalian genome : official journal of the International Mammalian Genome Society* **14**, 97-104, doi:10.1007/s00335-002-3045-y (2003).

81 Johnson, A. H., Campbell, W. G., Jr. & Callahan, B. C. Infection of rabbit knee joints after intra-articular injection of Staphylococcus aureus. Comparison with joints injected with Staphylococcus albus. *The American journal of pathology* **60**, 165-202 (1970).

82 Jones, D. H., Kong, Y. Y. & Penninger, J. M. Role of RANKL and RANK in bone loss and arthritis. *Annals of the rheumatic diseases* **61 Suppl 2**, ii32-39 (2002).

83 Joubert, P. E. *et al.* Chikungunya-induced cell death is limited by ER and oxidative stress-induced autophagy. *Autophagy* **8**, 1261-1263, doi:10.4161/auto.20751 (2012).

84 Karouzakis, E., Neidhart, M., Gay, R. E. & Gay, S. Molecular and cellular basis of rheumatoid joint destruction. *Immunology letters* **106**, 8-13, doi:10.1016/j.imlet.2006.04.011 (2006).

85 Kearns, A. E., Khosla, S. & Kostenuik, P. J. Receptor activator of nuclear factor kappaB ligand and osteoprotegerin regulation of bone remodeling in health and disease. *Endocrine reviews* **29**, 155-192, doi:10.1210/er.2007-0014 (2008).

86 Kelvin, A. A. *et al.* Inflammatory cytokine expression is associated with chikungunya virus resolution and symptom severity. *PLoS neglected tropical diseases* **5**, e1279, doi:10.1371/journal.pntd.0001279 (2011).

87 Khasnis, A. A., Schoen, R. T. & Calabrese, L. H. Emerging viral infections in rheumatic diseases. *Seminars in arthritis and rheumatism* **41**, 236-246, doi:10.1016/j.semarthrit.2011.01.008 (2011).

88 Kostenuik, P. J. Osteoprotegerin and RANKL regulate bone resorption, density, geometry and strength. *Current opinion in pharmacology* **5**, 618-625, doi:10.1016/j.coph.2005.06.005 (2005).

89 Krasnokutsky, S., Attur, M., Palmer, G., Samuels, J. & Abramson, S. B. Current concepts in the pathogenesis of osteoarthritis. *Osteoarthritis and cartilage / OARS, Osteoarthritis Research Society* **16 Suppl 3**, S1-3, doi:10.1016/j.joca.2008.06.025 (2008).

90 Krenn, V. *et al.* Grading of chronic synovitis--a histopathological grading system for molecular and diagnostic pathology. *Pathology, research and practice* **198**, 317-325, doi:10.1078/0344-0338-5710261 (2002).

91 Kularatne, S. A. *et al.* Epidemiology, clinical manifestations, and long-term outcomes of a major outbreak of chikungunya in a hamlet in sri lanka, in 2007: a longitudinal cohort study. *J Trop Med* **2012**, 639178, doi:10.1155/2012/639178 (2012).

92 Kumar, S. *et al.* Mouse macrophage innate immune response to Chikungunya virus infection. *Virology journal* **9**, 313, doi:10.1186/1743-422x-9-313 (2012).

93 Labadie, K. *et al.* Chikungunya disease in nonhuman primates involves long-term viral persistence in macrophages. *The Journal of clinical investigation* **120**, 894-906, doi:10.1172/jci40104 (2010).

94 Lang, P., Genant, H. K., Jergesen, H. E. & Murray, W. R. Imaging of the hip joint. Computed tomography versus magnetic resonance imaging. *Clinical orthopaedics and related research*, 135-153 (1992).

95 Li, G. *et al.* Subchondral bone in osteoarthritis: insight into risk factors and microstructural changes. *Arthritis research & therapy* **15**, 223, doi:10.1186/ar4405 (2013).

96 Liu, L. *et al.* Correlation between synovitis detected on enhanced-magnetic resonance imaging and a histological analysis with a patient-oriented outcome measure for Japanese patients with

end-stage knee osteoarthritis receiving joint replacement surgery. *Clinical rheumatology* **29**, 1185-1190, doi:10.1007/s10067-010-1522-3 (2010).

97 Lubowitz, J. H., Provencher, M. T., Brand, J. C. & Rossi, M. J. Arthroscopic arthritis options are on the horizon. *Arthroscopy : the journal of arthroscopic & related surgery : official publication of the Arthroscopy Association of North America and the International Arthroscopy Association* **31**, 389-392, doi:10.1016/j.arthro.2015.01.003 (2015).

98 Lui, N. L., Leong, H. N. & Thumboo, J. Polyarthritis in four patients with chikungunya arthritis. *Singapore medical journal* **53**, 241-243 (2012).

99 Madariaga, M., Ticona, E. & Resurrecion, C. Chikungunya: bending over the Americas and the rest of the world. *The Brazilian journal of infectious diseases : an official publication of the Brazilian Society of Infectious Diseases* **20**, 91-98, doi:10.1016/j.bjid.2015.10.004 (2016).

100 Malfait, A. M. Osteoarthritis year in review 2015: biology. *Osteoarthritis and cartilage / OARS, Osteoarthritis Research Society* **24**, 21-26, doi:10.1016/j.joca.2015.09.010 (2016).

101 Malfait, A. M., Little, C. B. & McDougall, J. J. A commentary on modelling osteoarthritis pain in small animals. *Osteoarthritis and cartilage / OARS, Osteoarthritis Research Society* **21**, 1316-1326, doi:10.1016/j.joca.2013.06.003 (2013).

102 Mallilankaraman, K. *et al.* A DNA vaccine against chikungunya virus is protective in mice and induces neutralizing antibodies in mice and nonhuman primates. *PLoS neglected tropical diseases* **5**, e928, doi:10.1371/journal.pntd.0000928 (2011).

103 Malvy, D. *et al.* Destructive arthritis in a patient with chikungunya virus infection with persistent specific IgM antibodies. *BMC infectious diseases* **9**, 200, doi:10.1186/1471-2334-9-200 (2009).

104 Manimunda, S. P. *et al.* Clinical progression of chikungunya fever during acute and chronic arthritic stages and the changes in joint morphology as revealed by imaging. *Transactions of the Royal Society of Tropical Medicine and Hygiene* **104**, 392-399, doi:10.1016/j.trstmh.2010.01.011 (2010).

105 Mathew, A. J. *et al.* Rheumatic-musculoskeletal pain and disorders in a naive group of individuals 15 months following a Chikungunya viral epidemic in south India: a population based observational study. *Int J Clin Pract* **65**, 1306-1312, doi:10.1111/j.1742-1241.2011.02792.x (2011).

106 Mathews, C. J., Weston, V. C., Jones, A., Field, M. & Coakley, G. Bacterial septic arthritis in adults. *Lancet (London, England)* **375**, 846-855, doi:10.1016/s0140-6736(09)61595-6 (2010).

107 Maxie, M. G. *Jubb, Kennedy, Palmer's Pathology of Domestic Animals*. Sixth edn, Vol. 1 (Elsevier Limited, 2015).

108 Maxie, M. G. *Jubb, Kennedy, Palmer's Pathology of Domestic Animals*. Sixth edn, Vol. 2 (Elsevier Limited, 2015).

109 McCarthy, M. K. & Morrison, T. E. Chronic chikungunya virus musculoskeletal disease: what are the underlying mechanisms? *Future microbiology* **11**, 331-334, doi:10.2217/fmb.15.147 (2016).

110 McCoy, A. M. Animal Models of Osteoarthritis: Comparisons and Key Considerations. *Veterinary pathology* **52**, 803-818, doi:10.1177/0300985815588611 (2015).

111 McGill, P. E. Viral infections: alpha-viral arthropathy. *Baillieres Clin Rheumatol* **9**, 145-150 (1995).

112 McGonagle, D. Diagnosis and treatment of enthesitis. *Rheumatic diseases clinics of North America* **29**, 549-560 (2003).

113 McNulty, M. A. *et al.* A Comprehensive Histological Assessment of Osteoarthritis Lesions in Mice. *Cartilage* **2**, 354-363, doi:10.1177/1947603511402665 (2011).

114 McNulty, M. A. *et al.* Histopathology of naturally occurring and surgically induced osteoarthritis in mice. *Osteoarthritis and cartilage / OARS, Osteoarthritis Research Society* **20**, 949-956, doi:10.1016/j.joca.2012.05.001 (2012).

115 McQueen, F. M. Magnetic resonance imaging in early inflammatory arthritis: what is its role? *Rheumatology (Oxford)* **39**, 700-706 (2000).

116 Mizuno, Y. *et al.* Clinical and radiological features of imported chikungunya fever in Japan: a study of six cases at the National Center for Global Health and Medicine. *J Infect Chemother* **17**, 419-423, doi:10.1007/s10156-010-0124-y (2011).

117 Mokhtarian, F., Zhang, Z., Shi, Y., Gonzales, E. & Sobel, R. A. Molecular mimicry between a viral peptide and a myelin oligodendrocyte glycoprotein peptide induces autoimmune demyelinating disease in mice. *Journal of neuroimmunology* **95**, 43-54 (1999).

118 Moran, M. M. *et al.* Intramembranous bone regeneration differs among common inbred mouse strains following marrow ablation. *J Orthop Res* **33**, 1374-1381, doi:10.1002/jor.22901 (2015).

119 Morrison, T. E. *et al.* A mouse model of chikungunya virus-induced musculoskeletal inflammatory disease: evidence of arthritis, tenosynovitis, myositis, and persistence. *The American journal of pathology* **178**, 32-40, doi:10.1016/j.ajpath.2010.11.018 (2011).

120 Nakaya, H. I. *et al.* Gene profiling of Chikungunya virus arthritis in a mouse model reveals significant overlap with rheumatoid arthritis. *Arthritis and rheumatism* **64**, 3553-3563, doi:10.1002/art.34631 (2012).

121 Nguyen, S. & Hojjati, M. Review of current therapies for secondary hypertrophic pulmonary osteoarthropathy. *Clinical rheumatology* **30**, 7-13, doi:10.1007/s10067-010-1563-7 (2011).

122 Noret, M. *et al.* Interleukin 6, RANKL, and osteoprotegerin expression by chikungunya virus-infected human osteoblasts. *The Journal of infectious diseases* **206**, 455-457: 457-459, doi:10.1093/infdis/jis368 (2012).

123 PAHO. *Pan American Health Organization*, <http://www.paho.org/hq/> (2015).

124 PAHO. *Chikungunya: Statistic Data*, <http://www.paho.org/hq/index.php?option=com_topics&view=readall&cid=5927&Itemid=40931&lang=en> (2016).

125 Pardigon, N. The biology of chikungunya: a brief review of what we still do not know. *Pathologie-biologie* **57**, 127-132, doi:10.1016/j.patbio.2008.02.016 (2009).

126 Paredes, A., Weaver, S., Watowich, S. & Chiu, W. Structural biology of old world and new world alphaviruses. *Arch Virol Suppl*, 179-185 (2005).

127 Phuklia, W. *et al.* Osteoclastogenesis induced by CHIKV-infected fibroblast-like synoviocytes: a possible interplay between synoviocytes and monocytes/macrophages in CHIKV-induced arthralgia/arthritis. *Virus Res* **177**, 179-188, doi:10.1016/j.virusres.2013.08.011 (2013).

128 Pilichou, A. *et al.* High levels of synovial fluid osteoprotegerin (OPG) and increased serum ratio of receptor activator of nuclear factor-kappa B ligand (RANKL) to OPG correlate with disease severity in patients with primary knee osteoarthritis. *Clinical biochemistry* **41**, 746-749, doi:10.1016/j.clinbiochem.2008.02.011 (2008).

129 Poo, Y. S. *et al.* CCR2 Deficiency Promotes Exacerbated Chronic Erosive Neutrophil-Dominated Chikungunya Virus Arthritis. *Journal of virology* **88**, 6862-6872, doi:10.1128/jvi.03364-13 (2014).

130 Poulet, B. & Staines, K. A. New developments in osteoarthritis and cartilage biology. *Current opinion in pharmacology* **28**, 8-13, doi:10.1016/j.coph.2016.02.009 (2016).

131 Punzi, L., Frigato, M., Frallonardo, P. & Ramonda, R. Inflammatory osteoarthritis of the hand. *Best practice & research. Clinical rheumatology* **24**, 301-312, doi:10.1016/j.berh.2009.12.007 (2010).

132 Quatman, C. E., Hettrich, C. M., Schmitt, L. C. & Spindler, K. P. The Clinical Utility and Diagnostic Performance of MRI for Identification of Early and Advanced Knee Osteoarthritis: A Systematic Review. *The American journal of sports medicine* **39**, 1557-1568, doi:10.1177/0363546511407612 (2011).

133 Rahim, A. A., Thekkekara, R. J., Bina, T. & Paul, B. J. Disability with Persistent Pain Following an Epidemic of Chikungunya in Rural South India. *J Rheumatol* **43**, 440-444, doi:10.3899/jrheum.141609 (2016).

134 Ramachandran, V. *et al.* Impact of Chikungunya on health related quality of life Chennai, South India. *PloS one* **7**, e51519, doi:10.1371/journal.pone.0051519 (2012).

135 Ravichandran, R. & Manian, M. Ribavirin therapy for Chikungunya arthritis. *Journal of infection in developing countries* **2**, 140-142 (2008).

136 Redman, S. N., Oldfield, S. F. & Archer, C. W. Current strategies for articular cartilage repair. *European cells & materials* **9**, 23-32; discussion 23-32 (2005).

137 Renault, P. *et al.* A major epidemic of chikungunya virus infection on Reunion Island, France, 2005-2006. *The American journal of tropical medicine and hygiene* **77**, 727-731 (2007).

138 Ribera, A. *et al.* Emerging chronic rheumatologic demonstrations post-chikungunya in la reunion. *Annals of the rheumatic diseases* **67** (2008).

139 Robin, S. *et al.* Severe bullous skin lesions associated with Chikungunya virus infection in small infants. *European journal of pediatrics* **169**, 67-72, doi:10.1007/s00431-009-0986-0 (2010).

140 Rodriguez-Morales, A. J. *et al.* Post-chikungunya chronic arthralgia: Results from a retrospective follow-up study of 131 cases in Tolima, Colombia. *Travel medicine and infectious disease* **14**, 58-59, doi:10.1016/j.tmaid.2015.09.001 (2016).

141 Rodriguez-Morales, A. J., Cardona-Ospina, J. A., Villamil-Gomez, W. & Paniz-Mondolfi, A. E. How many patients with post-chikungunya chronic inflammatory rheumatism can we expect in the new endemic areas of Latin America? *Rheumatology international*, doi:10.1007/s00296-015-3302-5 (2015).

142 Roques, P. & Gras, G. Chikungunya fever: focus on peripheral markers of pathogenesis. *The Journal of infectious diseases* **203**, 141-143, doi:10.1093/infdis/jiq026 (2011).

143 Rosario, V. *et al.* Chikungunya infection in the general population and in patients with rheumatoid arthritis on biological therapy. *Clin Rheumatol*, doi:10.1007/s10067-015-2979-x (2015).

144 Roth, A. *et al.* Concurrent outbreaks of dengue, chikungunya and Zika virus infections - an unprecedented epidemic wave of mosquito-borne viruses in the Pacific 2012-2014. *Euro surveillance : bulletin Europeen sur les maladies transmissibles = European communicable disease bulletin* **19** (2014).

145 Rudd, P. A. *et al.* Interferon response factors 3 and 7 protect against Chikungunya virus hemorrhagic fever and shock. *Journal of virology* **86**, 9888-9898, doi:10.1128/jvi.00956-12 (2012).

146 Ruddy, S., Harris, E. D., Sledge, C. B. & Kelley, W. N. *Kelley's textbook of rheumatology*. 6th edn, (W.B. Saunders Co., 2001).

147 Rulli, N. E. *et al.* Protection from arthritis and myositis in a mouse model of acute chikungunya virus disease by bindarit, an inhibitor of monocyte chemotactic protein-1 synthesis. *The Journal of infectious diseases* **204**, 1026-1030, doi:10.1093/infdis/jir470 (2011).

148 Runhaar, J., Luijsterburg, P., Dekker, J. & Bierma-Zeinstra, S. M. Identifying potential working mechanisms behind the positive effects of exercise therapy on pain and function in osteoarthritis; a systematic review. *Osteoarthritis and cartilage / OARS, Osteoarthritis Research Society* **23**, 1071-1082, doi:10.1016/j.joca.2014.12.027 (2015).

149 Sainani, N. I. *et al.* MRI diagnosis of hypertrophic osteoarthropathy from a remote childhood malignancy. *Skeletal radiology* **36 Suppl 1**, S63-66, doi:10.1007/s00256-006-0186-1 (2007).

150 Schilte, C. *et al.* Cutting edge: independent roles for IRF-3 and IRF-7 in hematopoietic and nonhematopoietic cells during host response to Chikungunya infection. *Journal of immunology (Baltimore, Md. : 1950)* **188**, 2967-2971, doi:10.4049/jimmunol.1103185 (2012).

151 Schilte, C. *et al.* Chikungunya virus-associated long-term arthralgia: a 36-month prospective longitudinal study. *PLoS neglected tropical diseases* **7**, e2137, doi:10.1371/journal.pntd.0002137 (2013).

152 Schwartz, K. L., Giga, A. & Boggild, A. K. Chikungunya fever in Canada: fever and polyarthritis in a returned traveller. *CMAJ : Canadian Medical Association journal = journal de l'Association medicale canadienne* **186**, 772-774, doi:10.1503/cmaj.130680 (2014).

153 Sebastian, M. R., Lodha, R. & Kabra, S. K. Chikungunya infection in children. *Indian J Pediatr* **76**, 185-189, doi:10.1007/s12098-009-0049-6 (2009).

154 Seemayer, C. A., Neidhart, M., Jungel, A., Gay, R. E. & Gay, S. Synovial fibroblasts in joint destruction of rheumatoid arthritis. *Drug Discovery: Disease Mechanisms* **2**, 359-365 (2005).

155 Selmi, C. & Gershwin, M. E. Diagnosis and classification of reactive arthritis. *Autoimmun Rev* **13**, 546-549, doi:10.1016/j.autrev.2014.01.005 (2014).

156 Sharma, A. R., Jagga, S., Lee, S. S. & Nam, J. S. Interplay between cartilage and subchondral bone contributing to pathogenesis of osteoarthritis. *International journal of molecular sciences* **14**, 19805-19830, doi:10.3390/ijms141019805 (2013).

157 Sheng, M. H. *et al.* Histomorphometric studies show that bone formation and bone mineral apposition rates are greater in C3H/HeJ (high-density) than C57BL/6J (low-density) mice during growth. *Bone* **25**, 421-429 (1999).

158 Simon, F. *et al.* French guidelines for the management of chikungunya (acute and persistent presentations). November 2014. *Medecine et maladies infectieuses* **45**, 243-263, doi:10.1016/j.medmal.2015.05.007 (2015).

159 Simon, F. *et al.* Chikungunya infection: an emerging rheumatism among travelers returned from Indian Ocean islands. Report of 47 cases. *Medicine* **86**, 123-137, doi:10.1097/MD/0b013e31806010a5 (2007).

160 Sissoko, D. *et al.* Post-epidemic Chikungunya disease on Reunion Island: course of rheumatic manifestations and associated factors over a 15-month period. *PLoS neglected tropical diseases* **3**, e389, doi:10.1371/journal.pntd.0000389 (2009).

161 Sonthalia, N., Mukherjee, K., Saha, A. & Talukdar, A. Treatment of hypertrophic osteoarthropathy in the case of pulmonary metastasis secondary-to-nasopharyngeal carcinoma with zoledronic acid: an enlightening experience. *BMJ case reports* **2012**, doi:10.1136/bcr-2012-006759 (2012).

162 Soumahoro, M. K. *et al.* The Chikungunya epidemic on La Reunion Island in 2005-2006: a cost-of-illness study. *PLoS Negl Trop Dis* **5**, e1197, doi:10.1371/journal.pntd.0001197 (2011).

163 Suhrbier, A., Jaffar-Bandjee, M. C. & Gasque, P. Arthritogenic alphaviruses--an overview. *Nature reviews. Rheumatology* **8**, 420-429, doi:10.1038/nrrheum.2012.64 (2012).

164 Tanaka, S., Nakamura, K., Takahasi, N. & Suda, T. Role of RANKL in physiological and pathological bone resorption and therapeutics targeting the RANKL-RANK signaling system. *Immunological reviews* **208**, 30-49, doi:10.1111/j.0105-2896.2005.00327.x (2005).

165 Tarkowski, A. *et al.* Current status of pathogenetic mechanisms in staphylococcal arthritis. *FEMS microbiology letters* **217**, 125-132 (2002).

166 Tat, S. K., Pelletier, J. P., Velasco, C. R., Padrines, M. & Martel-Pelletier, J. New perspective in osteoarthritis: the OPG and RANKL system as a potential therapeutic target? *The Keio journal of medicine* **58**, 29-40 (2009).

167 Teo, T. H., Lum, F. M., Lee, W. W. & Ng, L. F. Mouse models for Chikungunya virus: deciphering immune mechanisms responsible for disease and pathology. *Immunologic research* **53**, 136-147, doi:10.1007/s12026-012-8266-x (2012).

168 Thiberville, S. D. *et al.* Chikungunya fever: epidemiology, clinical syndrome, pathogenesis and therapy. *Antiviral research* **99**, 345-370, doi:10.1016/j.antiviral.2013.06.009 (2013).

169 Treuting, P. & Dintzis, S. *Comparative anatomy and histology. [electronic resource] : a mouse and human atlas*. (Oxford : Academic, 2011., 2011).

170 Tsetsarkin, K. A., Chen, R., Sherman, M. B. & Weaver, S. C. Chikungunya virus: evolution and genetic determinants of emergence. *Current opinion in virology* **1**, 310-317, doi:10.1016/j.coviro.2011.07.004 (2011).

171 Tunyogi-Csapo, M. *et al.* Cytokine-controlled RANKL and osteoprotegerin expression by human and mouse synovial fibroblasts: fibroblast-mediated pathologic bone resorption. *Arthritis and rheumatism* **58**, 2397-2408, doi:10.1002/art.23653 (2008).

172 Turner, C. H. *et al.* Genetic regulation of cortical and trabecular bone strength and microstructure in inbred strains of mice. *J Bone Miner Res* **15**, 1126-1131, doi:10.1359/jbmr.2000.15.6.1126 (2000).

173 Tuuminen, T., Lounamo, K. & Leirisalo-Repo, M. A review of serological tests to assist diagnosis of reactive arthritis: critical appraisal on methodologies. *Frontiers in immunology* **4**, 418, doi:10.3389/fimmu.2013.00418 (2013).

174 Vijayakumar, K. *et al.* Economic impact of chikungunya epidemic: out-of-pocket health expenditures during the 2007 outbreak in Kerala, India. *The Southeast Asian journal of tropical medicine and public health* **44**, 54-61 (2013).

175 Villamil-Gomez, W. E., Gonzalez-Camargo, O., Rodriguez-Ayubi, J., Zapata-Serpa, D. & Rodriguez-Morales, A. J. Dengue, chikungunya and Zika co-infection in a patient from Colombia. *Journal of infection and public health*, doi:10.1016/j.jiph.2015.12.002 (2016).

176 Voide, R., van Lenthe, G. H. & Muller, R. Differential effects of bone structural and material properties on bone competence in C57BL/6 and C3H/He inbred strains of mice. *Calcified tissue international* **83**, 61-69, doi:10.1007/s00223-008-9120-y (2008).

177 Volk, S. M. *et al.* Genome-scale phylogenetic analyses of chikungunya virus reveal independent emergences of recent epidemics and various evolutionary rates. *Journal of virology* **84**, 6497-6504, doi:10.1128/jvi.01603-09 (2010).

178 Volpe, A. *et al.* Chikungunya outbreak--remember the arthropathy. *Rheumatology (Oxford)* **45**, 1449-1450, doi:10.1093/rheumatology/kel275 (2006).

179 Walsh, N. C. & Gravallese, E. M. Bone remodeling in rheumatic disease: a question of balance. *Immunological reviews* **233**, 301-312, doi:10.1111/j.0105-2896.2009.00857.x (2010).

180 Wauquier, N. *et al.* The acute phase of Chikungunya virus infection in humans is associated with strong innate immunity and T CD8 cell activation. *The Journal of infectious diseases* **204**, 115-123, doi:10.1093/infdis/jiq006 (2011).

181 Waymouth, H. E., Zoutman, D. E. & Towheed, T. E. Chikungunya-related arthritis: case report and review of the literature. *Seminars in arthritis and rheumatism* **43**, 273-278, doi:10.1016/j.semarthrit.2013.03.003 (2013).

182 WHO. *Neglected Tropical Diseases*, <http://www.who.int/neglected_diseases/diseases/en/> (2016).

183 Wikan, N., Sakoonwatanyoo, P., Ubol, S., Yoksan, S. & Smith, D. R. Chikungunya virus infection of cell lines: analysis of the East, Central and South African lineage. *PloS one* **7**, e31102, doi:10.1371/journal.pone.0031102 (2012).

184 Win, M. K., Chow, A., Dimatatac, F., Go, C. J. & Leo, Y. S. Chikungunya fever in Singapore: acute clinical and laboratory features, and factors associated with persistent arthralgia. *Journal of clinical virology : the official publication of the Pan American Society for Clinical Virology* **49**, 111-114, doi:10.1016/j.jcv.2010.07.004 (2010).

185 Yaseen, H. M., Simon, F., Deparis, X. & Marimoutou, C. Identification of initial severity determinants to predict arthritis after chikungunya infection in a cohort of French gendarmes. *BMC Musculoskelet Disord* **15**, 249, doi:10.1186/1471-2474-15-249 (2014).

186 Zachary, J. F. & McGavin, M. D. *Pathologic Basis of Veterinary Disease*. 5th edn, (Elsevier, 2012).

187 Zamli, Z. & Sharif, M. Chondrocyte apoptosis: a cause or consequence of osteoarthritis? *International journal of rheumatic diseases* **14**, 159-166, doi:10.1111/j.1756-185X.2011.01618.x (2011).

188 Zeana, C. *et al.* Post-chikungunya rheumatic disorders in travelers after return from the Caribbean. *Travel medicine and infectious disease* **14**, 21-25, doi:10.1016/j.tmaid.2016.01.009 (2016).

189 Zhang, Y. & Jordan, J. M. Epidemiology of osteoarthritis. *Clinics in geriatric medicine* **26**, 355-369, doi:10.1016/j.cger.2010.03.001 (2010).

APPENDIX: CONSENT FORM

PLOS ONE is a member of PLOS journals, which applies the Creative Commons Attribution license to all of their publications. This states that no permission is required to reuse or repurpose articles, as long as the original article is cited.

VITA

Brad Goupil was born in Camp Springs, Maryland and moved frequently through much of his life, living in the following additional locations: England, California, Ohio, Iowa, Mississippi, Connecticut, Minnesota, and finally moving to Pride, Louisiana in 2012. He received his Bachelor's of Science and Master's of Science degrees from the University of Connecticut in 2004 and 2005, respectively. He subsequently moved to Minnesota and received his Doctorate in Veterinary Medicine from the University of Minnesota (UMN) in 2010. He stayed on at the UMN to complete a residency in veterinary anatomic pathology. He then entered the graduate program in the Department of Pathobiological Sciences at Louisiana State University in 2013, under the mentorship of Dr. Christopher Mores, to further pursue his interests in emerging infectious disease research. During his time there, he passed his certifying exam in veterinary anatomic pathology in 2014. Brad anticipates graduating with his PhD in December 2016. After graduating, he will continue a career as an anatomic pathologist, including continuing to pursue his interests in bone and joint diseases and emerging infectious diseases.